Self-Healing Properties of Water Filtration Membranes Containing Amphiphilic Comb Polymer

by

Caitlin Albright Devereaux

B.S. Chemistry
Harvey Mudd College, 2002

Submitted to the Department of Materials Science and Engineering in Partial Fulfillment of the Requirements for the Degree of

Master of Science in Materials Science and Engineering

at the

Massachusetts Institute of Technology

September 2004

Signature of Author.....
Department of Materials Science and Engineering
July 21, 2004

Certified by.....
Anne M. Mayes
Toyota Professor of Materials Science and Engineering
Thesis Supervisor

Accepted by.....
Carl V. Thompson II
Stavros Salapatas Professor of Materials Science and Engineering
Chair, Departmental Committee on Graduate Students

Self-Healing Properties of Water Filtration Membranes Containing Amphiphilic Comb Polymer

by

Caitlin Albright Devereaux

Submitted to the Department of Materials Science and Engineering on
July 21, 2004 in Partial Fulfillment of the Requirement for the
Degree of Master of Science in Materials Science and Engineering

ABSTRACT

Freshwater shortages are a tremendous problem for certain areas of the world, and given projected world population increases, they will pose a problem for a rising number of people in the future. A variety of technologies are currently used to extract usable water from wastewater, including water filtration membranes. Membrane technologies are promising because they require little energy and are scalable. However, many membrane materials tend to foul quickly when exposed to the organic species in wastewater feed streams.

Approaches to preventing membrane fouling include surface grafting of hydrophilic polymers onto membranes and the use of hydrophilic polymers as the bulk material. The former approach works moderately well, but it requires an increased number of fabrication steps, and the surface treatments tend to lose their effectiveness over time. The use of hydrophilic bulk materials leads to loss of membrane strength and resistance to wastewater elements such as chlorine. Neither option provides membranes that can maintain fouling resistance for extended periods of time.

This thesis investigates an alternative method of fouling prevention, first described by Hester et al. This approach involves the fabrication of blend membranes containing poly(vinylidene fluoride) (PVDF) and roughly 10 wt% of a comb polymer additive, poly(methyl methacrylate-*r*-poly(oxyethylene methacrylate)) (P(MMA-*r*-POEM)). The additive self-segregates to the membrane surface during fabrication and imparts long-term fouling resistance to the membrane. Even after harsh cleaning, which degrades the PEO chains present at the surface, membrane performance can be partially restored with a simple 18-hour anneal in a 90°C water bath.

Membranes are subjected to both surface analysis and filtration experiments, as well as other characterization techniques. Surface analysis is accomplished via x-ray photoelectron spectroscopy (XPS). Membrane samples are cleaned (in hydrogen peroxide or chromic-sulfuric acid (Chromerge)) and/or annealed (in 90°C deionized water), and their elemental surface composition and specific carbon binding environments are determined by XPS. Filtration experiments are done by alternating feed solutions of deionized water and a foulant (either bovine serum albumin or an oil/water emulsion). The flux of the feed solution is measured before fouling, during

fouling, and after fouling, to determine the extent of fouling recovery. Also, the compositions of the permeates are analyzed via ultraviolet-visible spectroscopy to determine the rejection coefficient of the membrane.

The data presented in this thesis show that PVDF blend membranes containing P(MMA-*r*-POEM) are capable of generating a fresh surface layer of PEO multiple times, even after extended cleaning sessions using concentrated acid. Membranes of varying thickness are shown to exhibit PEO-regenerative abilities, but it appears that thicker membranes have better fouling recovery than thinner, filtration-series membranes. Also, it is found that a blend membrane stripped of all of its surface PEO (by a 24-hour-long exposure to Chromerge) is able to restore PEO to its surface with roughly 24 hours of annealing. However, the new surface density is not as high as the original surface density and does not increase with longer annealing periods, possibly because of surface equilibrium effects or kinetic limitations. It also does not regain all of its initial fouling resistance, possibly because of the presence of partially degraded PEO chains at its surface.

Additionally, poly(methyl acrylate-*r*-poly(oxyethylene methacrylate)) (P(MA-*r*-POEM)) is investigated as a substitute for P(MMA-*r*-POEM). This new comb formulation could impart improved wettability to PVDF membranes. To investigate the fouling resistance of this comb additive, blend membranes containing P(MA-*r*-POEM) and PVDF were manufactured by the Pall Corporation. However, the formulations studied prove not to resist fouling, likely due to water solubility of the comb additives. They do not impart long-term fouling resistance to filtration membranes, but they may be improved with further research or be appropriate for single-use applications.

Thesis Supervisor: Anne M. Mayes
Title: Toyota Professor of Materials Science and Engineering

Table of Contents

List of Figures

List of Tables

Acknowledgements

First, I am very grateful to Anne Mayes, my advisor, for being patient with me during my times of indecision and for guiding me through this project. She not only provided excellent academic insight when I needed it, but she also cared about my well-being on a personal level. I am continually amazed at how much she exceeds the requirements of her position, and I consider myself lucky to have chosen such a kind and understanding person as my advisor.

I am also indebted to the members of the Mayes group, an impressively friendly, intelligent, and outgoing group of people, who made my daily life much more enjoyable. Special thanks go to Ariya Akthakul, who taught me the basics of membrane research, and to Will Kuhlman, who generously helped me with my comb problems, taught me NMR, and did cell studies for me, despite his busy schedule. To everybody in the group, I am so thankful to have been able to share my time at MIT with you. You made me feel welcome, helped me innumerable times, and made research much more enjoyable.

Quality instrumentation was invaluable in collecting the data in this thesis. Libby Shaw (in the MIT Center for Materials Science and Engineering (CMSE)) spent numerous hours in front of the XPS with me, patiently teaching me the intricacies of data collection and analysis. Mike Frongillo, also in the CMSE, expertly taught me how to use the SEM and sputter coated all of my samples.

Financial support in the form of a generous fellowship was provided by the Department of Defense's National Defense Science and Engineering Graduate Fellowship program. Further support for the research itself was graciously extended by the US Office of Naval Research. Also, Pall Corporation provided a number of membranes and polymer samples for testing, which significantly reduced the amount of synthesis and fabrication I had to do.

Finally, I cannot express how much I value the support that my family and friends have given me during the past two years. My parents, Linda Albright and Robert Devereaux, have repeatedly impressed me with their insight and understanding, despite my deviation from my plans to get a PhD. Knowing that they'll support me no matter what I choose to do makes it much easier to leave the academic path that I have been following since high school and to try something completely different. Also, I could not have come this far without the love and emotional support provided by my fiancé, Patrick Vinograd. He supported my decision to move across the country and pursue exciting research opportunities at MIT, even though it meant being in a long-distance relationship for two years. I can't wait to see what the future holds for us!

Chapter 1. Introduction

At first glance, the earth has an abundance of water. The hydrosphere contains roughly 1370 million km^3 of water [1]. But, of this generous supply, only 2.5% is freshwater, and only one third of this freshwater is available in liquid form (the remainder is frozen in ice caps and glaciers). The amount of available freshwater is whittled down even further by geographic constraints. All told, the total stable renewable supply of freshwater is 12,500 km^3, which is 0.0009% of the total water on earth [2].

A recent study reports that approximately 35% of this renewable freshwater supply is currently in use in households and industry, with an additional 19% being used in-stream, to dilute pollutants, in fisheries, and for transportation purposes [2, 3]. Between 1950 and 1990, water use tripled [2]. If such use increases continue without a significant improvement in water purification technologies, by 2030 the world will face severe water shortages, and delicate freshwater ecosystems may be irreversibly damaged.

Solutions to this problem are currently being pursued by both government institutions and scientific researchers. In addition to conservation strategies, water purification technologies are necessary to address this impending crisis. With successful water purification techniques, wastewater, brackish water, and saltwater could be used for crop irrigation and other purposes, reducing the need for freshwater.

A variety of water purification techniques are available. Traditional approaches include distillation; coagulation and flocculation followed by sedimentation; sand filtration; and chlorine treatment [4]. Of these traditional approaches to water purification, the first requires a great deal of energy, and the rest require pretreatment of samples with chemicals to induce colloid aggregation [1]. Membrane filtration is a relatively new technology (having become commercially practical in only the last 40 years [5]), but it has many advantages over classic water purification techniques.

Membranes require little energy and no chemical additives. Also, they are compact and modular [6] and can be used at ambient temperature, which is favorable for biological and food and drug applications [7]. Unfortunately, membranes tend to foul easily, which

leads to high maintenance costs and short lifetimes. Additionally, they tend to have relatively low selectivity. Although these are both concerns, this thesis addresses the problem of fouling only.

The fouling-resistant membranes studied in this thesis could potentially be of widespread use in water filtration applications, especially in wastewater filtration and waste reduction. For instance, the volume of an oily waste solution can be reduced by 90% by treatment with an ultrafiltration (UF) membrane [6]. Currently, membranes used in industry are quickly fouled by proteins and fats in wastewater. This necessitates frequent cleanings and, eventually, replacement of the membrane. Moeckel reports that "cleaning and membrane replacement contribute up to 50% of the operating costs or 30% of the total costs of a typical UF membrane system" [8]. This is a costly problem, and the development of more fouling-resistant membranes would allow the water filtration industry to cut cleaning and replacement expenses.

Previous research has introduced a self-organizing, fouling-resistant membrane that, even after harsh cleaning, can "heal" itself and present a fresh, fouling-resistant surface with a simple heat treatment in water [9, 10]. The research described in this thesis is needed to determine if this new technology is appropriate for use in wastewater filtration, in which fouled membranes are cleaned with harsh chemicals. It also investigates the regenerative capacity of these membranes, i.e. how often the membrane surface can renew itself before its capacity is exhausted.

Chapter 2. Background

2.1. Membrane Basics

2.1.1. Overview

Membranes take a variety of forms (polymer or ceramic, neutral or charged), but generally, a synthetic membrane is a device that "separates two phases and restricts the transport of various chemical species in a rather specific manner" [7]*. Although membranes come in many different forms, this thesis will focus on polymer membranes used to treat aqueous feed solutions, yielding an aqueous permeate.

The goal for most membrane applications is to maximize permeate flux while retaining selectivity. A variety of driving forces exist that can affect flux through a membrane, including electric fields and concentration gradients [7], but hydrostatic pressure is the dominant force in membrane-based water purification [13].

Table 2.1. A partial list of synthetic membranes used in water filtration
Sources: [1], [6], [7], [14-17].

	Separation Process		
	Microfiltration	*Ultrafiltration*	*Reverse Osmosis*
Membrane Type	Symmetric microporous membrane, 0.1 to 10 micron pore radius	Asymmetric microporous membrane, 1 to 10 nm pore radius	Asymmetric "skin type" membrane
Important Feature	Controlled pore sizes and uniform distribution	Controlled pore sizes and uniform distribution	Consistent material properties
Common Materials	Poly(vinylidene fluoride) (PVDF), polysulfone	Cellulose acetate, PVDF, polysulfone, polypropylene	Cellulose acetate, polyamides
Driving Force	Hydrostatic pressure difference 0.1 to 1 bar	Hydrostatic pressure difference 0.5 to 5 bar	Hydrostatic pressure difference 20 to 100 bar
Method of Separation	Sieving mechanism due to pore radius and absorption	Sieving mechanism	Solution-diffusion mechanism
Sample Applications	Sterile filtration, clarification, suspensions, emulsions	Separation of macromolecular solutions, emulsions	Separation of salt and heavy metals from aqueous solutions

* General information on membranes is available in [5], [11], and [12].

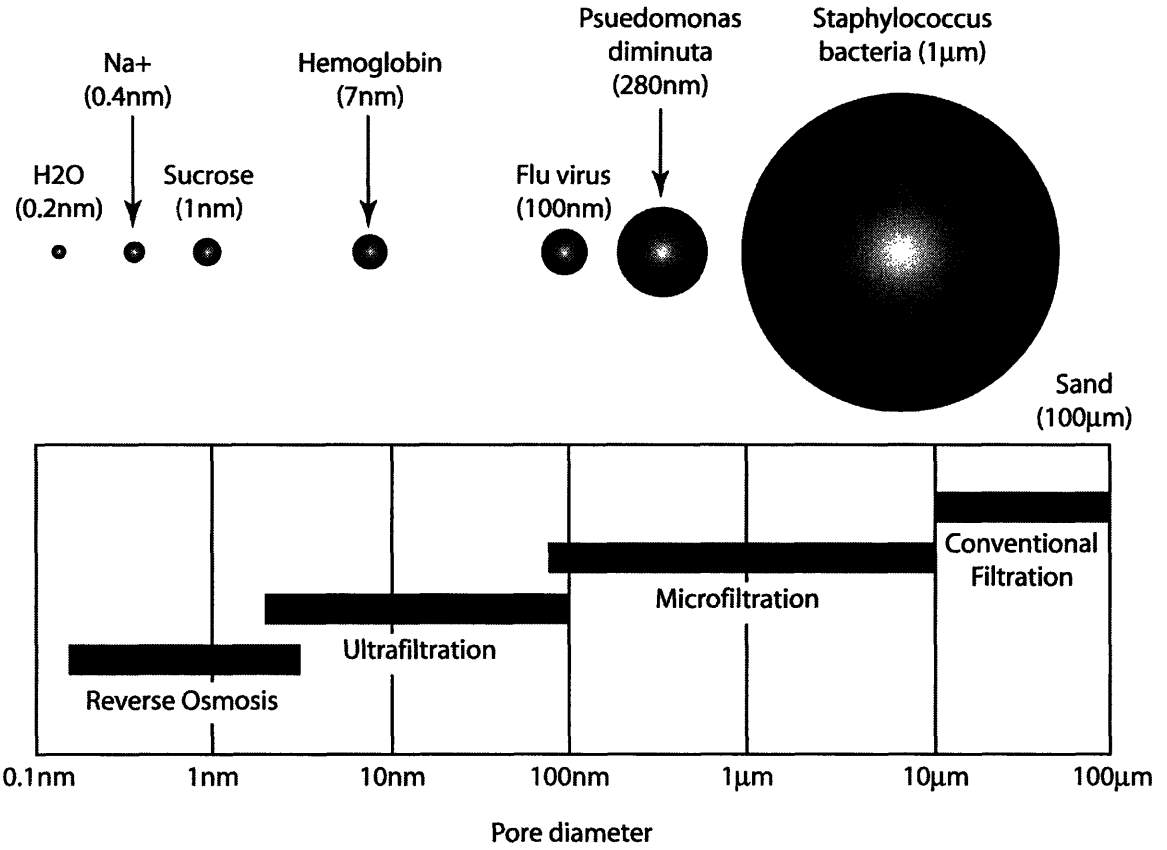

Figure 2.1. A comparison of particle size and membrane type
Adapted from [13].

Filtration membranes are classified based on their average pore size or the sizes of particles they allow through (Figure 2.1). The main membrane types are: *microfiltration* (MF), *ultrafiltration* (UF), and *reverse osmosis* (RO). Their characteristics are described in Table 2.1.

2.1.2. Membrane Transport Mechanisms

The rate of transport of a solute across a membrane is determined by two factors: *mobility* and *concentration* of the solute within the membrane. Mobility is determined by the size and physical traits of the solute, while its concentration in the membrane is decided by the affinity of the solute for the membrane material [7].

There are three types of membrane transport: *passive, facilitated,* and *active.* In all types of transport, there is a chemical potential gradient created by differences in hydrostatic

pressure, concentration, electrical potential, and temperature. Facilitated and active transport involve solute transport against the gradient, which requires energy input [7]. This research is concerned only with passive transport, where solutes move along a gradient created mainly by a difference in hydrostatic pressure.

Table 2.2. Selected applications for MF, UF, and RO
Sources: [6], [12], [33], [34].

Membrane Type	Applications
Microfiltration	*Water:* drinking water, municipal sewage and non-sewage waste treatment *Biotechnology:* cell harvesting, clarification of HPLC samples and viral solutions, sterilization of additives and DNA solutions, plasma separation and blood oxygenation *Industry:* surfactant recovery in carwashes, filtering latex paints, removal of heavy metal hydroxides, lignin and oil-water effluents in waste, hydrocarbon separations, coal liquids *Food/Beverage:* clarification of cheese whey, defatting of milk, clarification of wine, beer, juice, and vinegar, purification of dextrose from corn
Ultrafiltration	*Water:* high purity water, gray water (domestic water), small scale water reuse, drinking water, municipal sewage treatment *Biotechnology:* enzyme recovery, protein harvesting (algae/plankton) *Industry:* paint, dye and latex recovery from waste, concentration of oily emulsions to reduce pollution, pulp and paper mills, petroleum processing, abattoirs (recovery of blood fractions) *Food/Beverage:* fractionation of milk for cheese manufacture, fractionation of cheese whey and increased cheese yield, specialty milk products, fruit juice processing and clarification, concentration of gelatin, recovery of soy proteins in soybean processing
Reverse Osmosis	*Water:* desalination, ultrapure water, potable water, removal of environmental pollutants from water *Industry:* reuse and recovery of metals, dye recovery in textiles, water reuse in pulp and paper industry, boiler feedwater for power generation, treatment of percolation water, removal of heavy metals, treatment of industrial emulsions *Food/Beverage:* preconcentration of milk and whey, specialty milk products, fruit juice processing, concentration of sweeteners

2.1.3. Membrane Applications

In addition to being used in water purification [18, 19], membranes also have applications in the food industry [20-23], water softening [24], drug delivery [25, 26], and

fractionation of molecules [10, 22]. Additionally, many researchers are investigating pH-sensitive membranes [27-32]. Table 2.2 details more examples of membrane applications.

2.1.4. Membrane Architectures

Commercially-available membranes tend to be either *homogeneous* or *asymmetric* (Figure 2.2). Homogeneous membranes have pores that are roughly the same size throughout the membrane's thickness. This is not the case for asymmetric membranes, which are composed of two parts: (1) a thin film (0.1 to 1 micron thick) with small pores that control selectivity atop (2) a thick, highly porous supporting layer that provides mechanical strength and increased permeate flux. Asymmetric membranes are important in water purification processes and can be made of one material (*non-composite*) or a combination of materials (*composite*). Non-composite asymmetric membranes are made via immersion precipitation, as described below. Thin film composite membranes are generally made by interfacial polymerization of a selective polymer layer on top of a porous membrane, followed by cross-linking [7].

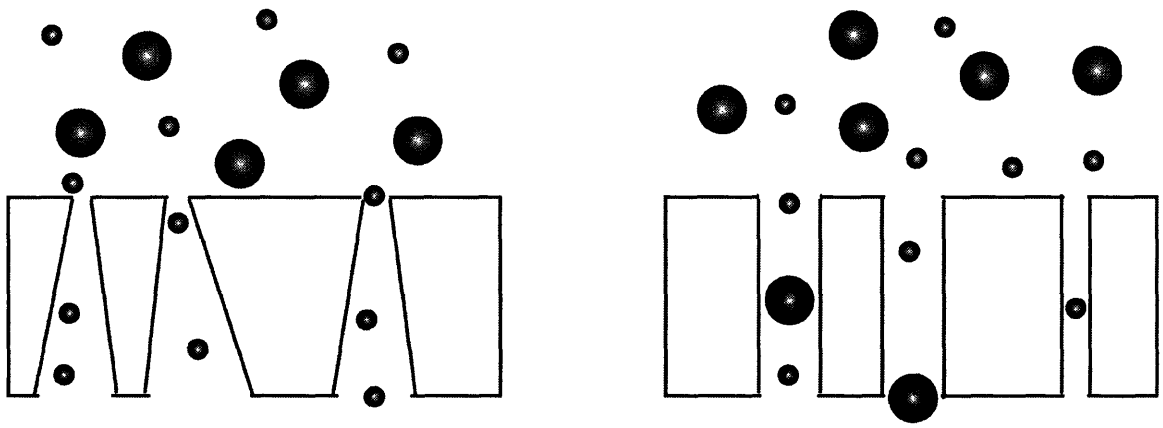

(a) Asymmetric Membrane (b) Symmetric Membrane

Figure 2.2. Filtration characteristics of asymmetric and symmetric membranes Symmetric membranes are also known as *homogeneous membranes*. Adapted from [7].

Porous membranes can be made in a variety of ways, including track etching, sintering, stretching, and phase inversion [5, 7]. Phase inversion by immersion precipitation is the most important fabrication method for polymer membranes and is also known as the

Loeb-Sourirajan process (Figure 2.3). It involves submerging a film (20 to 200 microns thick [7]) of polymer solution into a bath of nonsolvent. The nonsolvent invades the film, causing it to separate into a solid polymer phase and a liquid solvent phase, creating pores as the solvent leaves [5]. Immersion precipitation tends to yield membranes with asymmetric structures. Pore traits can be controlled by adding salts or additives such as glycerol to the initial polymer solution or by varying the temperature and composition of the casting bath [7, 35].

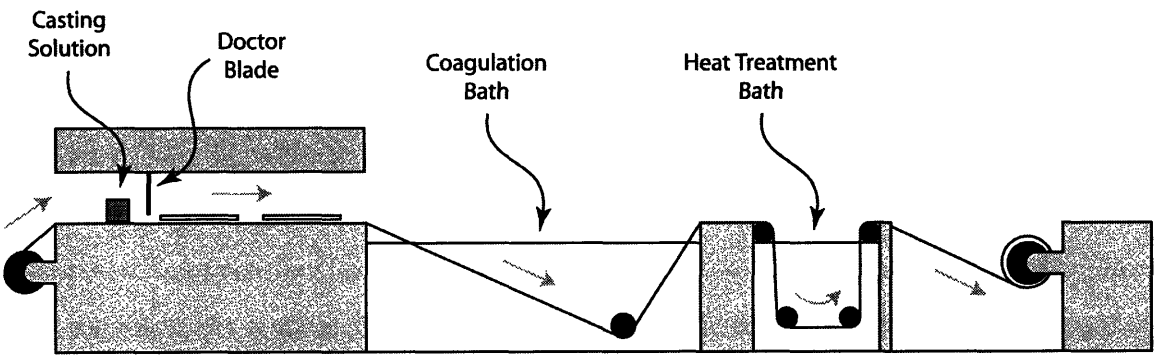

Figure 2.3. The immersion precipitation process
(1) A polymer solution is introduced to the apparatus, (2) Solution is cast onto a moving belt using a doctor blade, (3) Solvent evaporation occurs (optional), (4) Immersion of the film in a nonsolvent, causing polymer precipitation, (5) Heat treatment in another nonsolvent bath (optional), (6) Rinsing and rolling. Adapted from [9].

2.1.5. Membrane Modules

The main goal of a filtration apparatus is to expose the feed solution to as much membrane area as possible [13]. Cost and scalability are also concerns. In small laboratory situations, *dead-end filtration* tends to be used because of its simplicity. In this approach, the feed solution is forced through a membrane, with foulants being left behind in a cake on the surface of the membrane (Figure 2.4). Unfortunately, this leads to rapid fouling, so dead-end filtration is only feasible for small-scale experiments [33].

Industrial applications generally use *cross-flow filtration*. Cross-flow filtration is more complicated and expensive to set up, but it is less susceptible to fouling and gives greater permeate throughput. Types of cross-flow filtration modules include spiral wound, hollow fiber, plate and frame, capillary, and tubular [33].

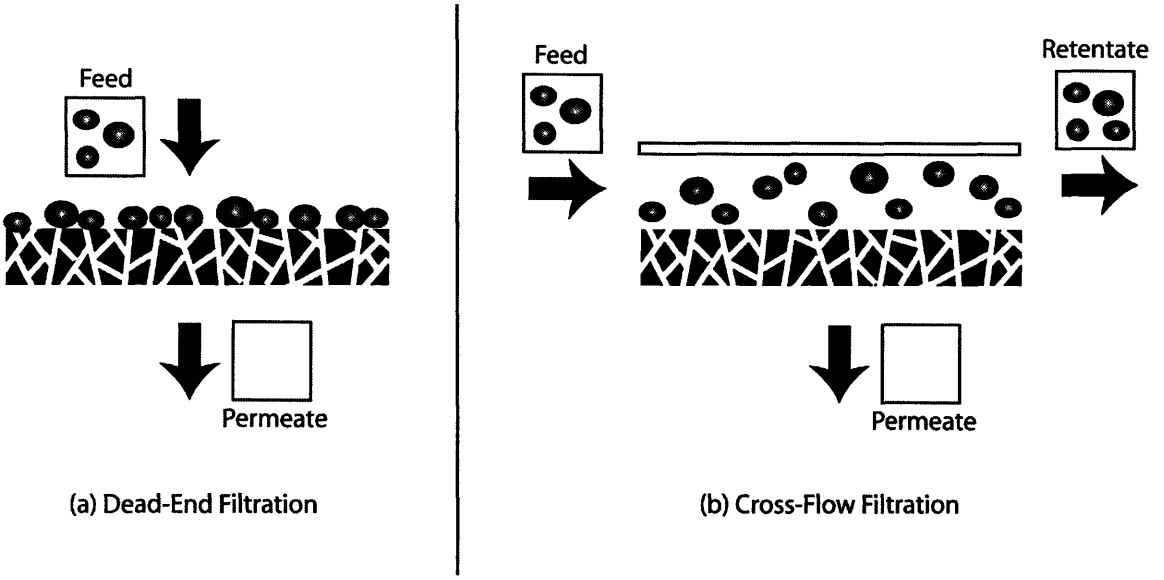

Figure 2.4. Diagrams of dead-end and cross-flow filtration
The diagrams show the tendency of dead-end filtration to foul rapidly. Adapted from [13].

Spiral wound modules (Figure 2.5) are the most popular because they are compact and inexpensive to manufacture and replace [13]. They were originally developed for RO but are now used in UF and MF as well. They consist of a series of membrane envelopes wrapped around a perforated tube, which carries the permeate out of the module [36]. *Hollow fiber* modules (Figure 2.6) are also popular, but because of their high fouling susceptibility, they are not used in many UF applications [36]. *Plate and frame* are among the oldest types of modules, and they are rarely used in UF or RO because of leaks and expense [36]. *Capillary* modules are mostly used for ultrapure water UF [13]. *Tubular* modules (Figure 2.7) are used most often for UF in industry due to their fouling resistance, but they are expensive compared to the other module types [36].

Although cross-flow filtration is preferable to dead-end filtration in industrial contexts, dead-end filtration is used in this research because of its simplicity and convenience. Because "dead-end filtration would be a worst-case operating condition" [13], it seems safe to assume that any filtration results in this research could only be improved in a cross-flow filtration context.

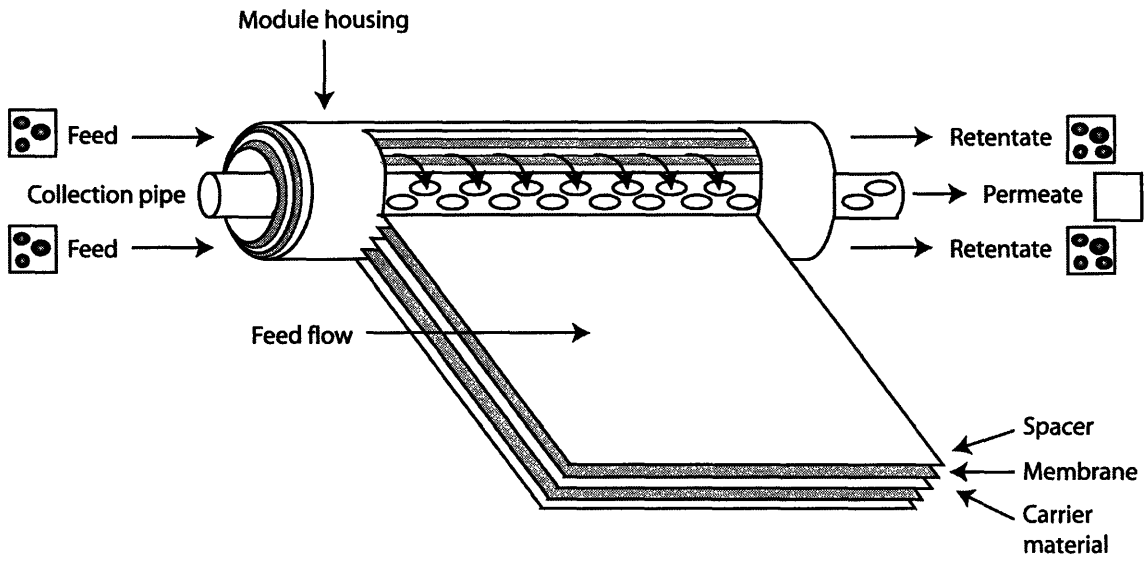

Figure 2.5. A spiral-wound membrane module
Adapted from [36].

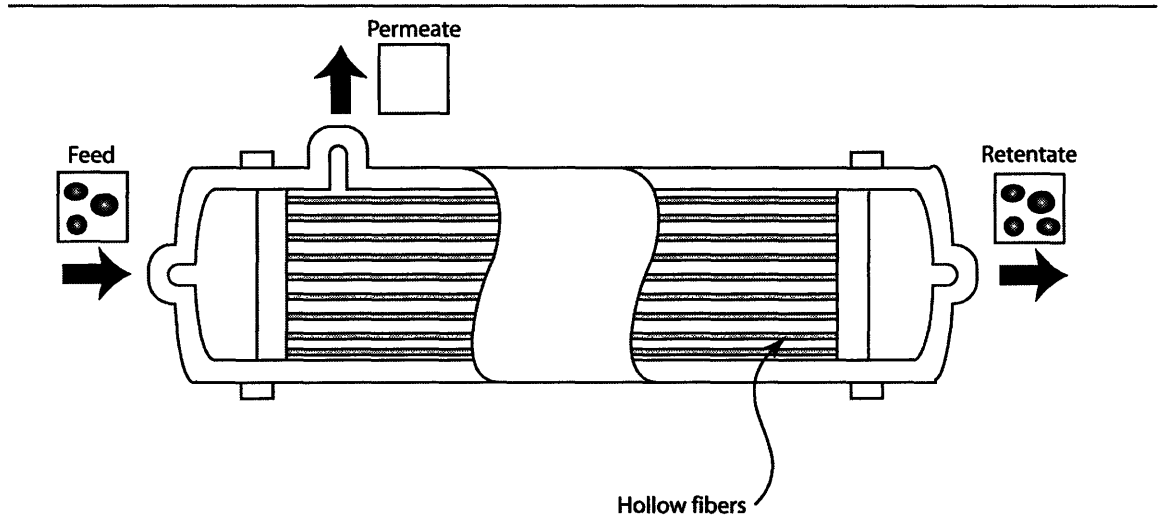

Figure 2.6. A hollow-fiber filtration module
Bore-side feed, used for pressures up to 150 psi. Adapted from [36].

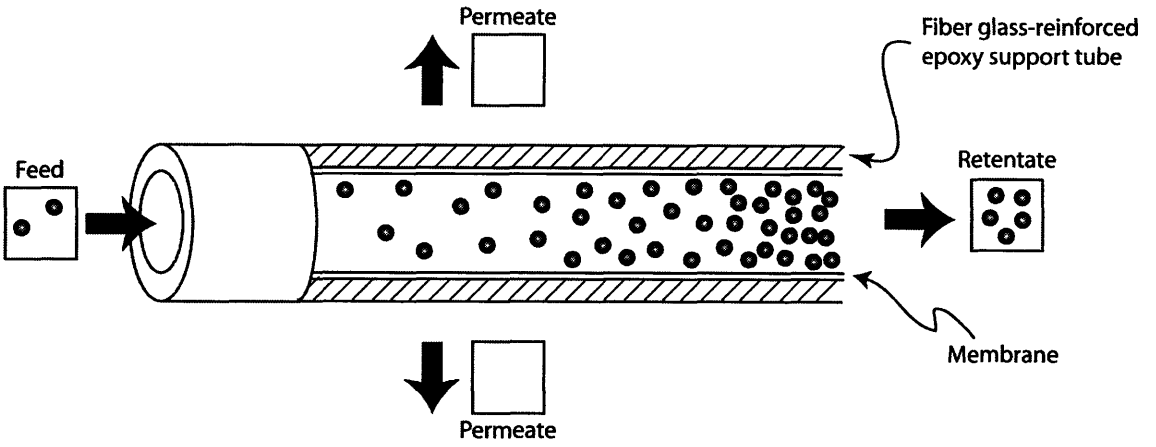

Figure 2.7. A tubular module
Diameters of 5-10 mm are common. Adapted from [36].

2.2. Fouling

2.2.1. Common Foulants

Foulants commonly encountered in wastewater include *particulates* (rocks, trash, small aquatic animals, sand, algae, bacteria, viruses), *colloids* (oil) that cause cloudiness, and *solutes* (ions, sugars, proteins, humic acids), which may impart color to the water [1, 37]. The macroscopic foulants can be removed by a simple sieving process, but the microscopic components tend to be attracted to membrane surfaces, which leads to clogging of pores and blocking of surfaces and eventually to a decrease in flux.

2.2.2. Fouling Theories

Fouling occurs due to a combination of many factors, and it is hard to determine exactly how each factor contributes to experimentally observed flux decline. According to Belfort, fouling is a combination of *concentration polarization* (the reversible buildup of a solute near the surface of a membrane, which is independent of membrane properties) and *adsorption* of the foulant onto the membrane surface and pores [33]. Some interpretations of fouling follow this simple definition and credit the flux decline to three sequential stages: (1) concentration polarization, (2) protein deposition, and (3) further

deposition and consolidation of the fouling layer [38, 39]. Figure 2.8 schematically depicts the flux decline profile explained by this theory.

Other theories are more complicated, as shown in Figure 2.9. But the general consensus is that fouling is due to a buildup of a solute (normally protein) at a membrane's surface and in its pores. In UF, the fouling tends to be mainly on the surface (although researchers have observed protein penetration into the membrane pores as well [40]), while in MF, fouling occurs in the pores as well as at the surface, which leads to a much faster incapacitation of the membrane [39]. Additionally, the morphology of the pores affects the rate of flux decline. Straight-through pores, such as those obtained by track etching, exhibit a faster decline in flux than interconnected pores because the latter allow the flow to redirect itself around a blockage [41]. A depiction of various types of fouling can be found in Figure 2.10.

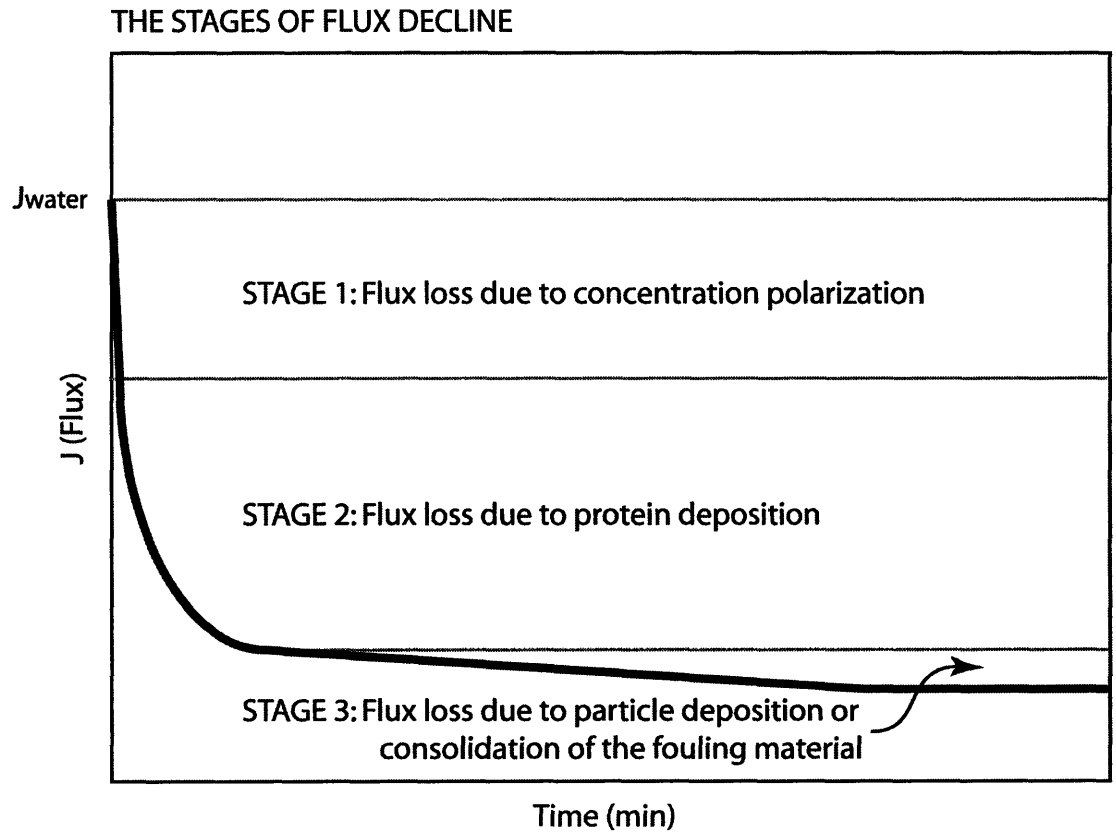

Figure 2.8. The three stages of flux decline
Adapted from [39].

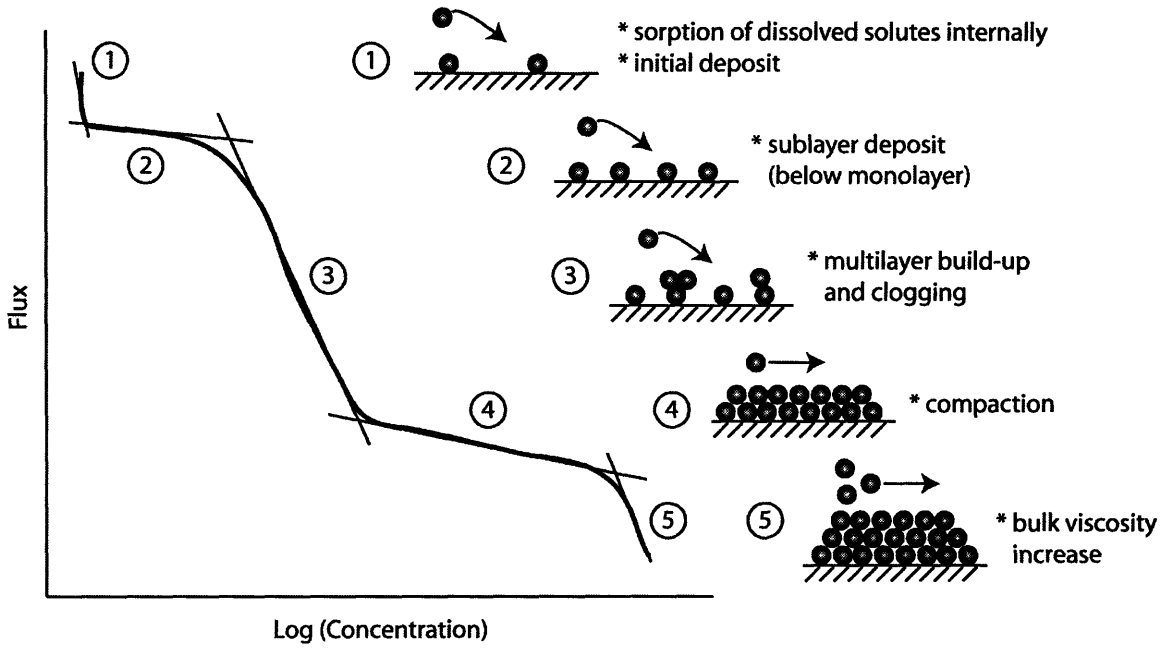

Figure 2.9. The stages of flux decline of the Belfort model
Adapted from [33].

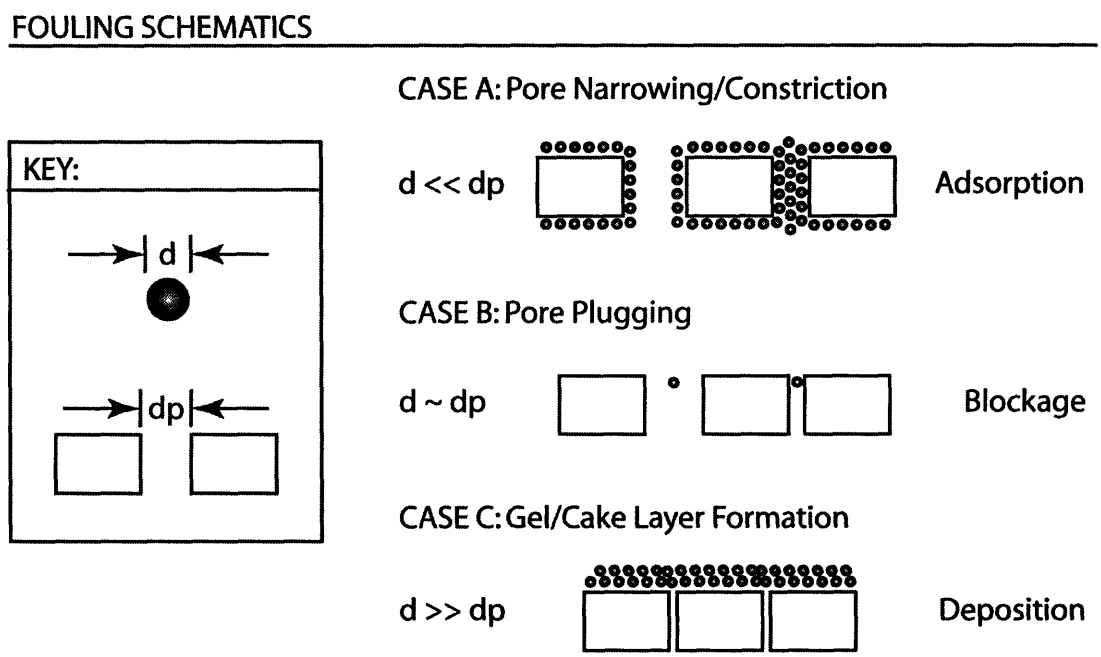

Figure 2.10. Types of fouling for different relative pore diameters
Adapted from [13].

It is important to note that an initial decline in flux for a newly-manufactured membrane may be due to compaction of the membrane's pore structure, so it is useful to run a pure

water feed through new membranes prior to fouling to rule out compaction as a factor in flux decline.

2.2.3. Solutions to the Fouling Problem

It has been established that hydrophilic surfaces foul less quickly than hydrophobic ones [42, 43]. However, hydrophilic membrane materials tend to be mechanically weak and undesirable for high-pressure applications such as UF. Therefore, it is desirable to impart hydrophilic characteristics to the surfaces of hydrophobic membranes (such as poly(vinylidene fluoride) (PVDF) and polysulfone), in order to combine the fouling resistance of a hydrophilic surface with the strength of a hydrophobic bulk material.

Techniques for increasing the surface hydrophilicity of hydrophobic membranes include:

- modification of the bulk membrane material [8, 44, 45]
- graft polymerization of the membrane surface [14, 27, 46-56]
- post-fabrication coatings [15, 57]
- adsorption of hydrophilic species onto the surface [42, 58]
- use of additives in the casting solution [15, 59]
- use of hydrophilic materials in the bulk, such as modified cellulose acetate [60]

These approaches, although effective, have a number of drawbacks. Most require additional fabrication steps, which increase the cost of membrane fabrication. Also, the effectiveness of the hydrophilic component diminishes over time, due to dissolution into the feed solution. Finally, all of these membranes foul eventually, and harsh cleaning can wear away any remaining surface treatments.

In addition to modifying membranes prior to filtration, approaches such as backwashing and cleaning can be used post-fouling to restore high flux. Shear flow has been investigated as a means of removing foulants from membranes, in the form of increased cross flow velocity and/or backwashes [23, 38]. Chemical cleaning approaches are also used and vary depending on the type of foulant. Oils and fats are treated with detergents,

proteins with enzymes and alkaline detergents, and inorganic salts with acids or bases [61]. It is also common to use harsh acid washes and scrubbing to remove foulants from membrane surfaces and pores. However, this causes increased deterioration of the membrane, which leads to higher replacement costs [19, 21, 33, 42].

No matter what the post-fouling approach, initial flux cannot be completely recovered. A small amount of irreversible fouling occurs over time, as shown in Figure 2.11.

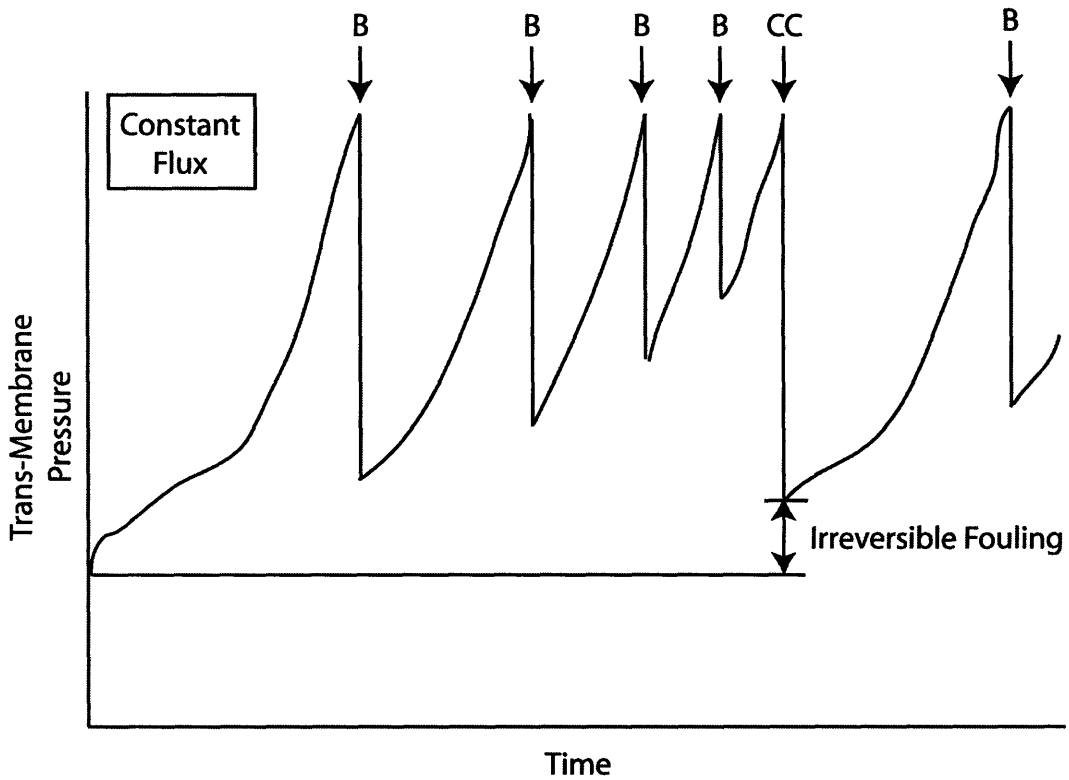

Figure 2.11. An example plot of pressure versus time for a UF device
B = backwash, CC = chemical cleaning. The time between backwashes is normally on the order of 30 minutes. As is shown, fouling occurs over time, and neither backwashing nor cleaning can completely reverse it. Adapted from [9].

Although a combination of pretreatment and cleaning can be effective against fouling, most hydrophilic surface treatments cannot withstand multiple cleanings. It is desirable to have a hydrophilic surface component that will not wash away over time and can recover from harsh cleaning treatments. Amphiphilic comb polymer additives may satisfy this need.

2.2.4. Comb Polymers and Fouling Prevention

Previous research in the Mayes group (upon which the current research is based) has used amphiphilic comb polymer additives to reduce membrane fouling. A small percentage of additive is mixed with the bulk casting solution. During immersion precipitation, the comb self-segregates to the membrane surface and internal pore surfaces, making them hydrophilic, thus preventing fouling. The comb is entangled with the bulk material and is water insoluble, so it does not leave the surface over time as some other hydrophilic treatments do. Additionally, if the comb at the surface is depleted because of harsh cleaning, a simple aqueous annealing step can be used to replenish the supply of functional comb at the surface [10].

2.3. Comb Polymers

2.3.1. Block Copolymers

A block copolymer is a macromolecule composed of two types of polymer chains. Block copolymers can be linear, branched or hyper-branched (stars/dendrimers). The research described in this thesis involves a random copolymer composed of a hydrophobic component (e.g. poly(methyl methacrylate) (PMMA) or poly(methyl acrylate) (PMA)) and a hydrophilic component (poly(oxyethylene methacrylate) (POEM)) to form a branched or comb-like structure, with the hydrophobic component forming the backbone and the hydrophilic side chains forming the "teeth" of the comb.

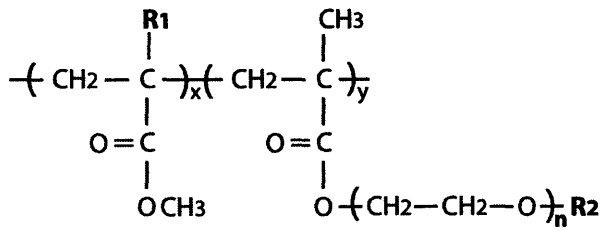

	PMMA-*r*-HPOEM	PMA-*r*-POEM
R1	—CH3	—H
R2	—H	—CH3
n	10	~9

Figure 2.12. Chemical structures of P(MMA-*r*-POEM) and P(MA-*r*-POEM)

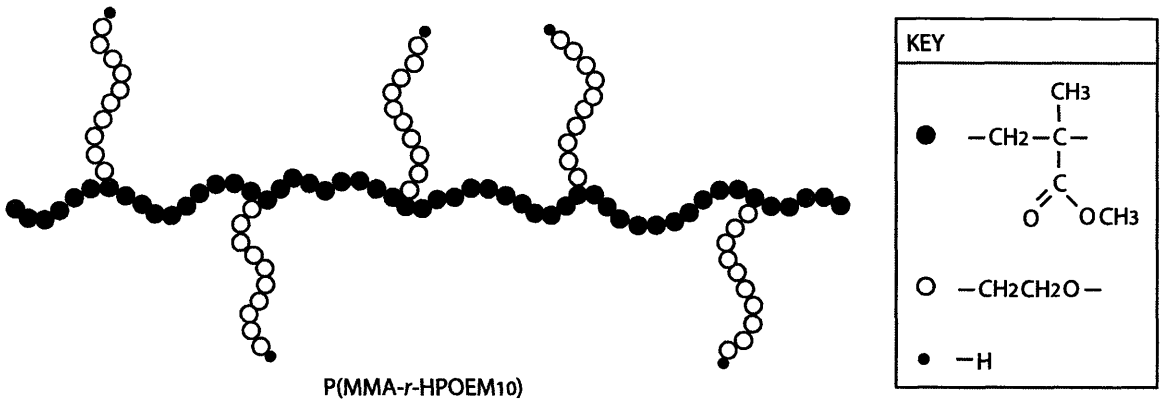

Figure 2.13. Cartoon of the relative length of comb teeth to backbone polymer Cartoon is for the P(MMA-*r*-POEM) used in this research (8.6 mol% POEM). Adapted from [9].

The chemical structure and relative block lengths of the combs used in this research are depicted in Figures 2.12 and 2.13.

2.3.2. Applications of Comb Polymers

Recently, amphiphilic comb polymers have been used in a variety of applications. They are particularly interesting in the biomaterials field, as they can impart a bio-inert PEO surface to a mechanically strong hydrophobic material, such as PVDF. Additionally, their side chains can be end-modified with peptide sequences to promote directed adhesion of cells to surfaces [62]. It is also possible to make membranes whose pore diameters vary with solution pH, using a comb with acrylic acid side chains [63]. And finally, as in this thesis, combs can be used to impart fouling-resistant surface chemistries to separation membranes [9, 64].

In these separation membranes, the comb polymer is mixed with the bulk component in solution prior to membrane fabrication. Because of its hydrophilic side chains, the comb migrates to the membrane surface during immersion precipitation in a water bath, to minimize surface energy. Thus, the comb imparts a high density of PEO chains to the membrane surface and pores without any extra fabrication steps (Figure 2.14).

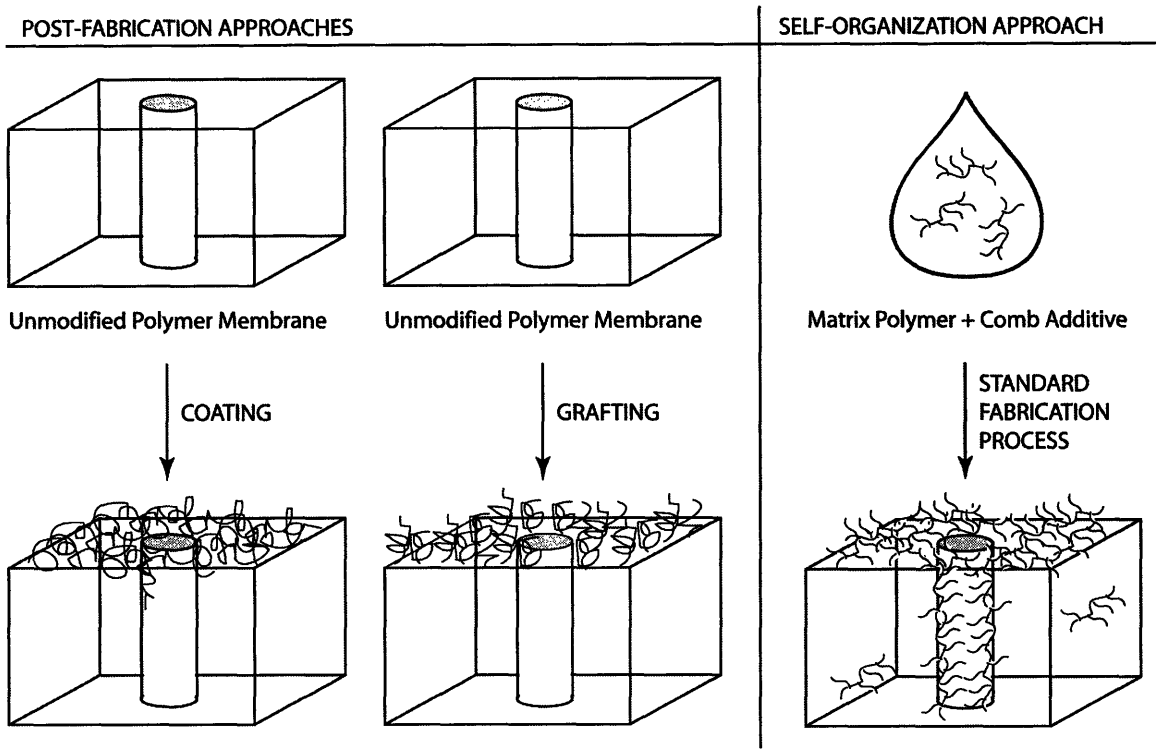

Figure 2.14. Comparison of coating, grafting, and self-organization
Adapted from [9].

2.3.3. Material Properties

The bulk material used in the membranes described in this thesis is poly(vinylidene fluoride) (PVDF), a hydrophobic polymer commonly used in industry [44]. It is used in membranes because of its good chemical, mechanical, and thermal properties, but its inherent hydrophobicity is a drawback [15]. Conveniently, P(MMA-*r*-POEM) comb can be used to impart hydrophilicity to PVDF membranes.

The POEM component is the key to the comb's hydrophilicity. Its side chain, poly(ethylene oxide) (PEO), has long attracted scientific interest because of its strong hydrophilic nature. It has hydrogen bonding capabilities, which make its surface bio-inert and protein-resistant. However, PEO is water soluble, so in order to be used in water filtration applications without dissolving, it must be combined with a hydrophobic block (in this case, PMMA).

Although it is the unusual properties of the PEO that make the comb so useful in preventing fouling, the PMMA backbone is necessary to prevent dissolution of the PEO and to entangle the comb with the PVDF matrix. Because PMMA is miscible with PVDF [59, 65], it is a natural choice for the hydrophobic component in the comb. Other hydrophobic components that are miscible with PVDF, such as PMA [65], also hold potential.

2.4. Research Goals

Previous research by Jonathan Hester in this laboratory showed that a PVDF membrane with 10 wt% P(MMA-*r*-POEM) comb additive was able to largely regain its comb surface coverage and fouling resistance after a harsh cleaning by simply annealing the membrane in 90°C water for 12 hours. The goal of this thesis research was to continue this line of investigation and determine the extent of the comb-modified membranes' regenerative properties, for PVDF membranes incorporating P(MMA-*r*-POEM) as well as P(MA-*r*-POEM).

Chapter 3. Experimental Methods: P(MMA-*r*-POEM)/PVDF Blend Membranes

3.1. Overview

The regenerative properties of blend membranes containing P(MMA-*r*-POEM) comb additive were evaluated using two different cleaning solutions. One was a heated solution of hydrogen peroxide, and the other was a much stronger concentrated acid bath. After each cleaning session, membranes were annealed in water to bring new comb to the surface. Samples were analyzed by x-ray photoelectron spectroscopy (XPS) to determine their surface compositions and susceptibility to fouling. Additionally, filtration membranes were fabricated and their flux measured using a simple dead-end cell setup, with pure water and BSA feed solutions.

3.2. Membrane Manufacture

3.2.1. Polymer Solutions

Blend membranes for regeneration experiments were made by immersion precipitation. Polymer casting solutions were made by combining appropriate amounts of poly(vinylidene fluoride) (PVDF) in solution, comb in solution, and any pore-forming agents necessary, then stirring until homogeneous. The P(MMA-*r*-POEM) comb additive was made via free radical synthesis by Daniel Pregibon in the Griffith Lab at MIT, and its properties are outlined in Table 3.1.

Table 3.1. Properties of the P(MMA-*r*-POEM) comb used in blend membranes
As reported by D. Pregibon. Molecular weight is based on polystyrene (PS) standards.

Sample Name	DCPLB003	M_w *(g/mol)*	30,000
Amt. MMA	67 wt%	*Amt. HPOEM*$_{526}$ *(n=10)*	33 wt%
Polydispersity	4.7	*Purity*	> 99%
Water solubility	Not soluble	*Units of PMMA:POEM*	10.7 : 1

Membranes were made from the same basic mixture of comb, PVDF, and solvent (either dimethyl formamide (DMF) or N-methyl pyrrolidone (NMP)), but a variety of casting solutions were used. Table 3.2 provides solution compositions.

Table 3.2. Casting solutions for P(MMA-*r*-POEM)/PVDF blend membranes
The same P(MMA-*r*-POEM) comb was used for all membranes (DCPLB003).

Casting Solution	Solution Composition (wt%)				Expected wt% comb in bulk ($\phi_{w,b}$)
	PVDF	*Comb*	*Glycerol*	*Solvent*	
1	10% $PVDF_{275k}$	1%	--	89% DMF	10
2	17% $PVDF_{275k}$	2%	2%	79% DMF	10
3	17% $PVDF_{534k}$	2%	2.5%	78.5% NMP	11

3.2.2. Filtration Membranes

The goal in fabricating filtration-quality (F-series) membranes was a defect-free asymmetric membrane structure. After a blend solution had been prepared, it was filtered through a 1 micron glass microfiber filter (Whatman 25mm GD/X, Clifton NJ) to remove any dust particles. The filtered solution was then degassed at 40-60°C for 2 or more hours to remove any bubbles that might cause defects. Next, the solution was poured onto a 3 3/8" x 5" first surface optical mirror (Edmund Scientific Co., Barrington, NJ). It was spread to a uniform thickness using a cylindrical casting bar (Ref. [9], Appendix E provides fabrication details) with an 8-mil (0.008") gate size. The mirror and polymer film were immediately immersed in a deionized water (dW, Millipore MilliQ, 18.2 MΩ cm) bath at 90°C. The membrane was left in the bath for 10 minutes after it had separated from the mirror surface, then immersed in a room temperature dW bath for 30 minutes, and finally allowed to air dry.

3.2.3. Surface Analysis Membranes

Surface analysis (S-series) membranes were analyzed by XPS only. Since they were never used for filtration, only the surface composition was considered important—the morphology of the membranes did not have to be carefully controlled. Because these membranes did not need to be defect-free, their fabrication process was less complicated than for filtration membranes. The blend solution was poured into a Teflon dish, allowed to level itself, then immersed in a 90°C dW bath to promote the segregation of comb to the surface. The dish and membrane were allowed to sit in the bath for roughly ten minutes, then they were removed and the membrane air-dried. For regeneration trials, the membrane was subsequently annealed at 90°C in dW for 24 hours to ensure a uniform

distribution of comb at the surface. Table 3.3 provides fabrication parameters for both types of membranes.

Table 3.3. Membrane fabrication parameters
F = filtration-quality membrane, S = surface analysis membrane.

Membrane	Solution	Bath Temp (degrees C)	Casting/Prep Details
S-040204	1	90	
F-040301	1	90	8-mil gate
F-040310	2	90	8-mil gate
F-040317 F-040324 F-040505	3	90	8-mil gate

3.3. Regeneration Experiments

Regenerative studies were done on blend membranes to gauge how well the membrane could recover from chemical cleaning, both strong and weak. Studies involved a number of rounds of cleaning, each followed by an annealing round. The cleaning round was expected to degrade the membrane surface and decrease fouling resistance, and the annealing round was expected to bring new comb to the surface and aid in recovery from fouling. After each cleaning or annealing step, a small sample was reserved for use in XPS and static fouling tests.

3.3.1. Cleaning

Separate studies involving two different cleaning solutions (one mild and one harsh) were conducted on P(MMA-*r*-POEM)/PVDF blend membranes. The cleaning procedures are as follows:

Mild Cleaning Conditions: The membrane sample was stirred for one hour in a 40°C solution of 10% hydrogen peroxide (30% H_2O_2, Baker) in dW.

Harsh Cleaning Conditions: The membrane sample was left to sit for 30 minutes (or longer, as indicated), unstirred, in a room temperature bath of concentrated chromic-sulfuric acid (Chromerge, VWR).

Following both types of cleaning, the samples were rinsed thoroughly with deionized water and allowed to air dry.

3.3.2. Annealing

Membranes designated as "annealed" in this thesis were processed by stirring gently in a dW bath at 90°C for a specified period, normally 18 hours. Annealing has been shown to bring more comb to the surface of the membrane [9], which would be expected to enhance fouling resistance.

3.3.3. Static BSA Fouling

All regeneration samples were tested to determine their relative fouling susceptibility. A small piece of each sample was submerged in a solution of approximately 2 mg/mL bovine serum albumin (BSA, Sigma-Aldrich A-7906) in phosphate-buffered saline solution (PBS, 1 packet/liter of house dW). The protein concentration was consistent within each trial, but it varied somewhat between trials. The sample was left to sit in the fouling solution for one hour, then rinsed twice with PBS, twice with house dW, and allowed to air dry. After this, the sample was analyzed by XPS to determine the amount of nitrogen present on the surface.

3.4. Characterization Methods

3.4.1. X-ray Photoelectron Spectroscopy

X-ray photoelectron spectroscopy (XPS, Kratos Analytical Axis Ultra, Manchester England) was used to determine the surface composition of the membranes (specifically

the amount of comb and PEO at the surface and the degree of fouling) with the beam normal to the sample surface. First, samples were pumped down to ultra-high vacuum, then X-rays from a monochromatic aluminum target (Al Kα, 1487 eV) bombarded the surface, and the resulting ejected core electrons were used to determine the elemental composition of the sample surface [66].

Survey runs (between electron binding energies of 0 and 1100 eV) were used to determine the range of elements present at a sample's surface. Typically, C, F, and O appeared in the spectra (Table 3.4 gives their typical binding energies). Nitrogen and other trace elements were also observed for fouled samples. Each survey was the average of at least two sweeps, to improve spectral resolution.

Table 3.4. Typical binding energies of element electrons in XPS
The energies can be shifted by charge buildup in the sample or by elemental binding environments.

Element/Orbital	Binding Energy (eV)
F 1s	686
O 1s	531
N 1s	398
C 1s	284
Si 2s	152

High-resolution C 1s spectra (between 279 and 302 eV) were obtained in order to determine the relative amount of comb and/or PEO at the surface of the membranes. These high-resolution spectra reveal the different types of carbon bonds that exist at the sample surface, as well as the relative amounts of these bond types. Each spectrum involved at least three sweeps, and in most cases, multiple spectra were taken at different locations on the sample and the results averaged together. The spectra were fitted using CasaXPS software. The method used to calculate comb content is outlined in Appendix A.

Example survey and high-resolution XPS spectra are shown in Figures 3.1 and 3.2.

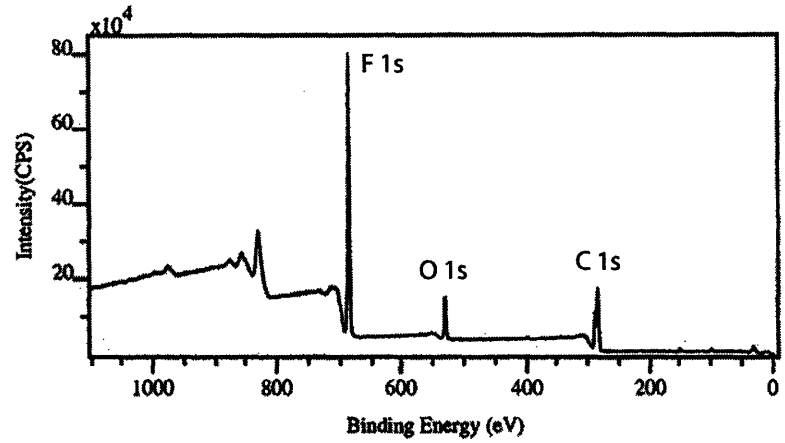

Figure 3.1. A typical XPS survey spectrum sample
Peaks are labeled with their element and electron shell.

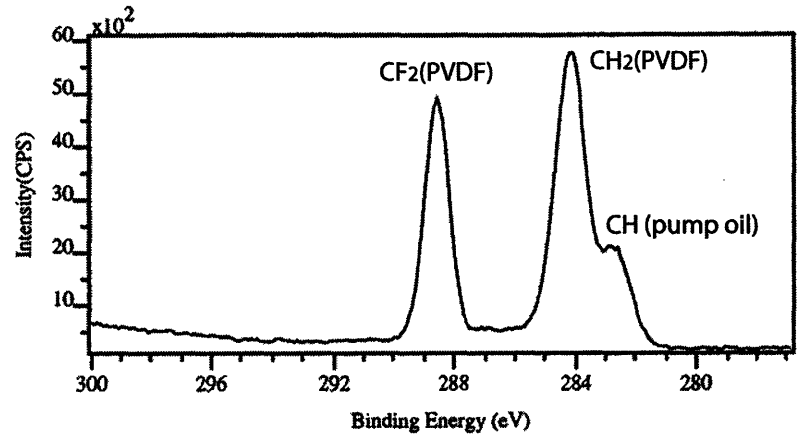

Figure 3.2. A typical C 1s high-resolution XPS spectrum sample
This spectrum is for PVDF. Peaks are caused by carbon in different chemical bonding environments. The two left-hand peaks are from the two bonding environments of carbon in PVDF. The rightmost peak (at 285 eV) is due to hydrocarbon fouling from the XPS pump oil and appears in most spectra.

3.4.2. Filtration Experiments

Flux Apparatus Setup

An Amicon 8010 dead-end filtration cell (Beverly, MA) was used for all flux experiments. It had a maximum pressure of 75 psi and a 10 mL capacity. The filtration setup is depicted in Figure 3.3. This filtration cell accommodated membrane discs of

diameter 25 mm (filtration area: 4.1 cm^2). A specially-made circular die was used to cut appropriately-sized pieces of membrane.

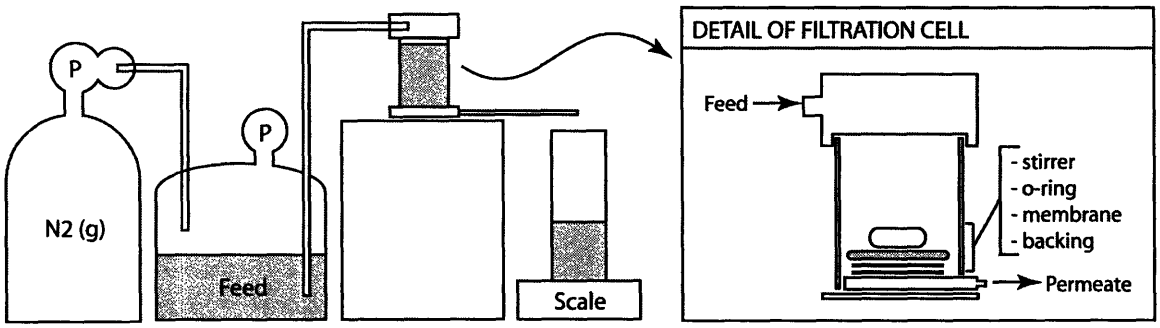

Figure 3.3. Low-pressure filtration setup
Includes a detail of the filtration cell.

In a typical filtration experiment, the membrane disc was pre-wet with dW for 10 minutes. Next, the filtration cell was assembled around the membrane and filled with pure deionized water. The assembled cell was then attached to a large pressurizable vessel, also holding dW. This vessel was manufactured by Millipore (Bedford, MA) (Cat # XX6700P10, maximum capacity 10L). A similar vessel (Cat # XX6700P01, maximum capacity 1 Gallon) was used for fouling solutions, so that it was easy to exchange feed solutions during an experiment.

Flux Calculations

Flux was calculated as the difference in collected permeate mass per unit time. The mass of permeate was monitored, as was the time elapsed since the initial application of pressure to the contents of the cell. Time-mass data points were collected roughly every minute during a filtration. Flux was plotted as a function of average time (i.e., the average of the two times used in the flux calculation described above). Flux was always normalized by pressure, and in some cases by initial flux (for comparison purposes).

Flux Linearity and Compaction

Before all flux experiments, the linearity of the flux response with respect to pressure for pure water was measured. Flux measurements were collected at three or more pressures, and these were then normalized by pressure and plotted, to ensure that the flux varied

linearly with applied pressure. Including the time required for these linearity experiments, pure water was run through the membranes for a total of at least 30 minutes prior to fouling experiments, to prevent flux decline due to membrane compaction from obscuring fouling effects on the flux data.

Fouling with BSA

Fouling experiments used bovine serum albumin (BSA, Sigma-Aldrich, A-7906). A concentration of 0.1 mg/mL BSA in PBS (in house dW) was used unless otherwise noted. Following the pure water linearity measurements and compaction outlined above, the flux of the BSA solution was measured. Specifically, the cell was filled with BSA solution, as were the smaller feed vessel and tubing. The same operating pressure was used for the compaction run and the fouling (this pressure was chosen based on the membrane's initial flux, and was normally between 10 and 50 psi), and flux was measured for 30 minutes or more. Also, 1 mL permeate aliquots were collected at 1, 5, 10, and 20 minutes after initial application of pressure and later characterized by ultraviolet (UV) spectroscopy to determine the amount of BSA allowed through the membrane.

Following BSA filtration, the cell, feed vessel, and tubing were once again filled with deionized water. Also, the cell was gently rinsed with dW to dislodge any weakly attached protein from the membrane surface. The apparatus was reassembled, and pure water flux was measured for at least 10 minutes.

BSA absorbs strongly at a wavelength of 279 nm, so UV spectroscopy was used to determine the concentration of BSA in the permeate. Concentration standards of either 1 mg/mL or 0.1 mg/mL (depending on the feed solution) and 0 mg/mL (pure deionized water) were used to determine permeate BSA concentrations (assuming a linear relationship between absorption and concentration). A Cary 5E UV/Vis spectrophotometer and disposable UV-transparent plastic cuvettes (Plastibrand Disposable UV Cuvettes, 1.5 mL capacity, VWR cat. No. 7591 50) were used in these experiments. At least three sets of data were collected for each sample and averaged.

3.4.3. SEM of Membranes

Scanning electron microscopy (SEM) was used to visualize membrane morphological features. Both the front (separation) surface and cross-section of each membrane were imaged using SEM. Cross-sectional samples were obtained via freeze fracture by liquid nitrogen (samples were immersed in liquid nitrogen for approximately 5 minutes, then manually broken in half to reveal a fresh cross-section for analysis). Both types of samples were mounted on a sample post using carbon tape, then coated with ~100 angstroms of Au/Pd prior to imaging to prevent charge buildup. The data were collected on a JEOL 6320 SEM with an accelerating voltage of 3 kV. Magnifications and scale bars are given for each image. Typically, the cross-sectional samples were viewed at 1000x magnification, while the surface samples were viewed at 20,000x magnification.

3.4.4. Gas Sorption Surface Area Analysis

Membrane surface area was determined by Quantachrome Instruments (Boynton Beach, FL) using gas sorption. The membrane sample (roughly 0.1 g) was allowed to outgas in a vacuum at room temperature overnight. Subsequently, it was cooled to 77K, and the surface area was determined using the multi-point Brunauer-Emmett-Teller (BET) method [67]. Nitrogen gas was used as the adsorbate.

Chapter 4. Experimental Methods: P(MA-*r*-POEM)/PVDF Blend Membranes

4.1. Overview

The flux and fouling resistance of P(MA-*r*-POEM) comb-enhanced PVDF membranes made by Pall Corporation were tested. P(MA-*r*-POEM) is of interest because it would be expected to yield membranes that wet better than those containing P(MMA-*r*-POEM). Flux was tested using pure water, BSA, and oil/water emulsions. Membranes were subsequently characterized via SEM and XPS and their rejection coefficients found using UV/Vis spectroscopy. Also, the comb itself was tested to determine its fouling resistance and water solubility.

4.2. Membrane Manufacture

All P(MA-*r*-POEM)/PVDF blend membranes were manufactured by Pall Corporation using a proprietary procedure. Membranes were made from a mixture of PVDF and one of two different compositions of P(MA-*r*-POEM) comb additive. The first membrane, referred to here as *Pall 1*, reportedly had pores roughly 0.1 μm in size and was made with a high molecular weight (MW) comb additive. The second membrane, *Pall 2*, was reported to have pores 0.02 μm in size and used a lower MW additive. Pall probably made these pore size estimates using size exclusion filtration. They also provided control membranes, including *ungrafted PVDF*, which was an unmodified PVDF membrane, and *grafted PVDF*, which was a PVDF membrane surface-grafted with a hydrophilic species, most likely hydroxy-ethyl methacrylate.

4.3. Characterization Methods: Comb

In addition to providing membranes for filtration tests, Pall provided samples of the comb polymers used in making the membranes. These combs were labeled AC403-5 ("low MW") and AC403-11c ("high MW") and were received dissolved in N,N-Dimethylacetamide (DMAc). Table 4.1 reports the information that accompanied each comb sample.

Table 4.1. Properties of Pall P(MA-*r*-POEM) comb solutions
As reported by Pall.

Name	% DMAc	Molecular Weight (g/mol)
AC403-5 ("low MW")	40	13,000
AC403-11c ("high MW")	50	50,000 – 60,000

In order to characterize the polymers, it was desirable to isolate the comb in powder form. This was accomplished by precipitating the comb from solution into cold diethyl ether (~0°C) twice (the second time using tetrahydrofuran (THF) as the polymer solvent). After the comb was isolated, it was subjected to the following analyses.

4.3.1. Gel Permeation Chromatography

Gel permeation chromatography (GPC) was used to verify the comb molecular weights. The comb samples were dissolved in THF to make ~5 mg/mL solutions. These solutions were then filtered through a 0.2 micron filter, and molecular weight data was collected on a Viscotek VE 2001 GPCmax. Molecular weights were determined based on polystyrene (PS) standards.

4.3.2. CyQuant Cell Study

The CyQuant assay (Molecular Probes, C-7026) was used to determine the affinity of cells for the pure comb polymers and was done by W. Kuhlman. First, a 10 mg/mL solution of each comb was made in toluene. Next, the solution was spin-coated onto silanized glass cover-slips and dried under vacuum overnight. The comb films were exposed to a cell solution (20,000 WTNR6 cells in MEM-alpha medium) and incubated for 24 hours. Samples were then washed with PBS and imaged via light microscopy. Following this, the samples were subjected to the CyQuant assay to determine the extent of cell proliferation.

4.3.3. X-ray Photoelectron Spectroscopy

Comb films were spin-coated onto glass slides, as for the CyQuant study. These films were then analyzed via XPS. For each sample, a survey and high-resolution C 1s spectrum were taken as described in Section 3.4.1. The spectra were analyzed to determine the types of carbon bonds present as well as the elements present at the film surface.

4.3.4. Nuclear Magnetic Resonance

Nuclear magnetic resonance (NMR) was used to verify the chemical compositions of the comb polymers. Comb was dissolved in *d*-$CHCl_3$ to give ~20 mg/mL solutions. W. Kuhlman performed the NMR data collection.

4.4. Characterization Methods: Membranes

4.4.1. Flux Experiments

Flux data were collected as for the P(MMA-*r*-POEM) membranes as described in Section 3.4.2, with additional oil/water fouling trials as described below. For the P(MA-*r*-POEM) membranes, the BSA trials were done using a solution of 1 mg/mL BSA in house dW, with no PBS added. The absence of PBS was not expected to have a large impact on the membrane fouling.

Fouling runs also were done using oil/water microemulsions containing 1000 ppm oleic acid and 1000 ppm triethanolamine in dW. The flux measurement process was the same as that described for BSA. Oil/water permeates were studied by acquiring UV/Vis absorption spectra between 300 and 800 nm and observing the relative intensities of the spectra in this range of wavelengths. A plot of concentration standards is included in Appendix F.

4.4.2. BCA Assay

A BCA (bicinchoninic acid) Assay (Pierce, 23235) was used to quantify protein affinity for each membrane. Equally-sized samples of Pall 1, Pall 2, and ungrafted PVDF membranes were incubated for 1 hour in a 1 mg/mL BSA/PBS solution. The samples were then rinsed five times with PBS and left to air-dry. Next, the samples were treated with BCA reagents, as were vials of BSA standards. Aliquots from each test tube were transferred to a plate reader and subjected to a spectroscopic reading at 562 nm. More information on this assay can be found in the Pierce Micro BCA Protein Assay Kit.

Chapter 5. Results: P(MMA-*r*-POEM)/PVDF Blend Membranes

5.1. Annealing Kinetics

Although previous research [9, 68] had shown that annealing increases the amount of comb at the surface of a blend membrane, the kinetics of comb segregation had not been studied methodically. To study these kinetics, multiple pieces of membrane S-040204 (bulk wt% comb ($\phi_{w,b}$) = 0.10, bulk vol% comb (ϕ_b) = 0.15) were annealed in 90°C dW for varying amounts of time. The volume fraction of comb at the surface of each sample (ϕ_s) was determined by XPS, and the results are shown in Figure 5.1.

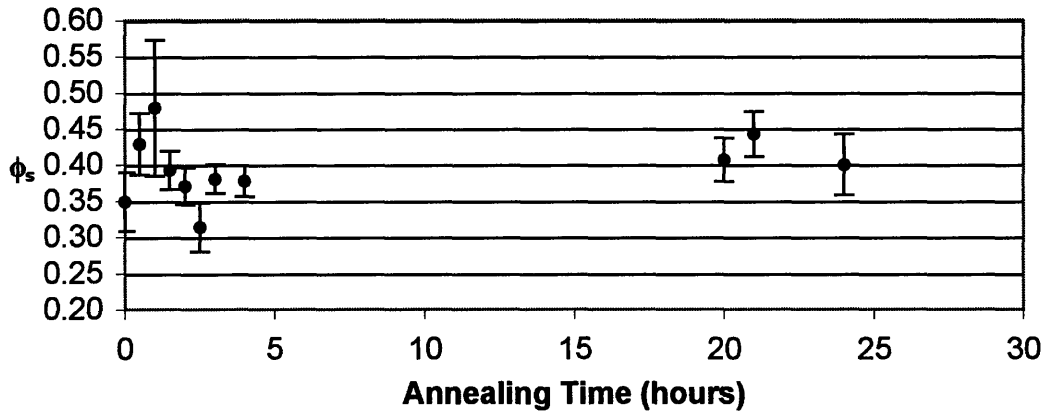

Figure 5.1. Annealing kinetics for P(MMA-*r*-POEM)/PVDF membrane
Plot of volume fraction of comb at the membrane surface (ϕ_s) versus the duration of annealing. Each data point represents XPS spectra of between 3 and 5 locations per sample.

The plot suggests that overnight annealing does not appreciably increase the comb density at the surface of a membrane that has been cast at 90°C, but it might cause the distribution of comb to become more uniform. It appears that 10 minutes of exposure to the 90°C water bath during casting is sufficient to achieve maximum comb density at the surface.

From this plot, the equilibrium near-surface comb fraction appears to be between ϕ_s = 0.35 and 0.45 for the 10 wt% comb P(MMA-*r*-HPOEM$_{10}$)/PVDF blend membrane. For a similar membrane containing 10 wt% P(MMA-*r*-POEM$_9$) and cast at 90°C, Hester found that ϕ_s = 0.54. Any number of factors could explain this difference. It could be due to

differences in casting solution compositions as well as differences in the combs used. The casting solution for Hester's membrane (F-10-9k2-90) contained glycerol and used NMP as a solvent, while S-040204 had no glycerol added and used DMF as its solvent. These differences could affect the morphology of the cast membranes, including the ratio of surface area to volume, leading to differences in surface coverage. Also, the two membranes were cast differently (Hester's used a 20-mil gate, while S-040204 was simply poured into a dish), although both were precipitated in a 90°C water bath.

Another possible explanation for the difference in comb coverage values is that the comb additive used for Hester's membrane was slightly different than that used in S-040204. Hester's comb used $POEM_9$ as its hydrophilic component, while the comb currently under inspection (DCPLB003) uses $HPOEM_{10}$. Also, the molecular weights and PEO content of the two combs differ—DCPLB003 has a molecular weight of roughly 30,000 g/mol (by PS standards) and 33 wt% PEO, while Hester's comb had a molecular weight of 63,300 g/mol and 51 wt% PEO. Thus, the comb used in Hester's investigation would be expected based on kinetic [10] and thermodynamic arguments to exhibit higher surface coverage.

Yet another possible contributor to the difference in comb coverage is that Hester's XPS data were collected at a takeoff angle of 45 degrees, while the data in this thesis were collected at an angle of 90 degrees. At a shallower takeoff angle, the X-rays don't penetrate the sample as deeply and so give readings nearer to the surface, so the 45 degree takeoff data would be expected to show more comb, assuming the comb preferentially segregates to the surface.

5.2. Regeneration Experiments

5.2.1. Hydrogen Peroxide Cleaning Studies

Hydrogen peroxide (H_2O_2) was used as a mild cleaning agent to test the regeneration properties of membrane S-040204. Samples were cleaned in a 40°C solution of hydrogen

peroxide for one hour, then annealed in dW at 90°C for 18 hours. Results are discussed below.

High-Resolution C 1s Spectra

High-resolution XPS C 1s spectra of PVDF, comb, and blend (S-040204) samples before and after cleaning with hydrogen peroxide are shown in Figure 5.2.

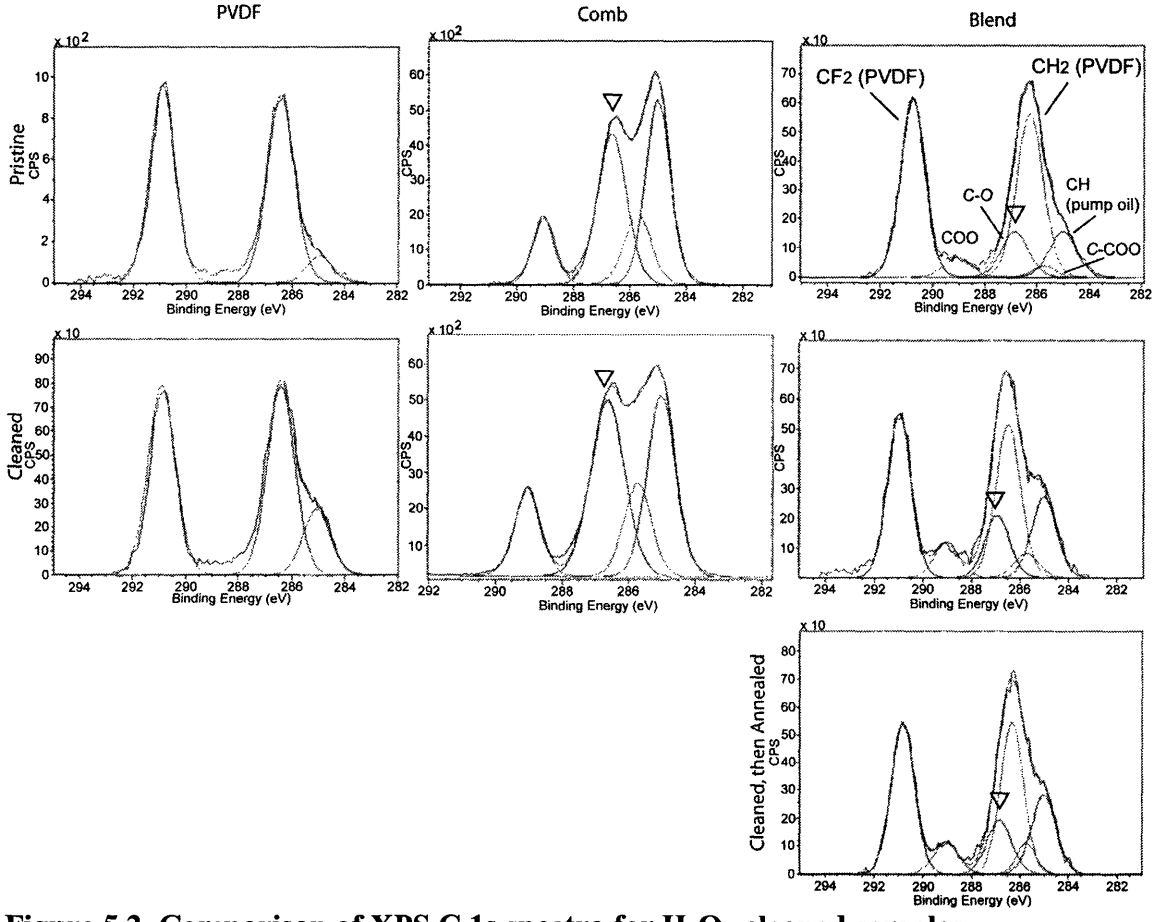

Figure 5.2. Comparison of XPS C 1s spectra for H_2O_2-cleaned samples
First row: pristine samples, *second row:* samples cleaned with H_2O_2, *third row:* samples cleaned with H_2O_2 and then annealed 18h in 90°C water. The PEO C-O peak is marked in the comb and blend spectra to show how it fluctuates with cleaning and annealing.

Ignoring the 285 eV hydrocarbon peak (which is affected by XPS pump oil fouling), the surface composition of PVDF does not change noticeably with cleaning. Similarly, for comb and blend membranes, the C-O peak (marked with an inverted triangle), which is related to the amount of PEO at the surface, does not change appreciably in relative area

before and after cleaning. In the comb spectra, the C-O peak comprises 56% of the peak area before cleaning and 55% after cleaning (this is again ignoring the hydrocarbon peak). Also, the ratio of the area of the C-O peak (a signal contributed solely by the PEO chains) to that of the COO peak (contributed by the comb backbone) remains virtually unchanged with cleaning and annealing, suggesting that the PEO chains are not being hydrolyzed by the hydrogen peroxide. For the blend, the C-O peak is 11.5% of the pristine sample, 15% of the cleaned sample, and 14% of the cleaned and annealed sample (Appendix B contains peak-fitting details for these samples). These compositions are nearly identical.

Based on the peak areas of the high-resolution C 1s spectra, it appears that exposure to hydrogen peroxide does not significantly reduce the amount of comb or PEO at the surface of a blend membrane. Thus, it would be expected that a regeneration experiment using hydrogen peroxide as the cleaning agent would not show any difference between cleaned and annealed samples, in terms of comb surface coverage. This is shown to be the case in the next section.

Comparison of Surface Fouling and PEO/Comb Coverage

A regeneration experiment was conducted in which pieces of membrane S-040204, which had previously been annealed for 24 hours to make the comb surface coverage more uniform, were subjected to rounds of cleaning and annealing. Each cleaning round involved exposure to 40°C hydrogen peroxide solution for 1 hour. During each annealing round, the membranes were exposed to 90°C dW for 18 hours. Samples were removed after each cleaning and annealing step and analyzed by XPS.

The naming convention for regeneration samples is as follows: "pristine" is the membrane before any cleaning or annealing (other than 24-hour pre-annealing), "clean 1" is a sample taken after the first round of cleaning, "anneal 1" is a sample that has been cleaned and then annealed once, "clean 2" is a sample that has been cleaned, annealed, and cleaned again, and so on. Results from an XPS analysis of the cleaned and annealed

samples (fouled and non-fouled) are given in Figure 5.3. Appendix A describes how the values in each plot were calculated from the XPS data.

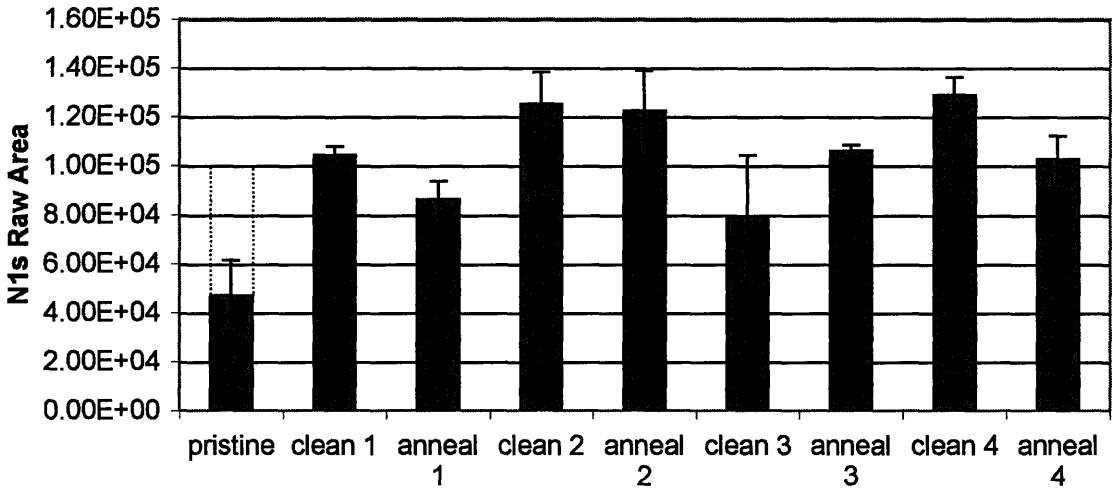

Figure 5.3a. Measure of surface fouling in H_2O_2 regeneration study
The plot shows the relative amount of nitrogen on the surface of BSA-fouled samples. The dotted line represents the expected pristine value. Each data point is an average of three readings (i.e., one specimen was analyzed at three different locations to obtain a given data point).

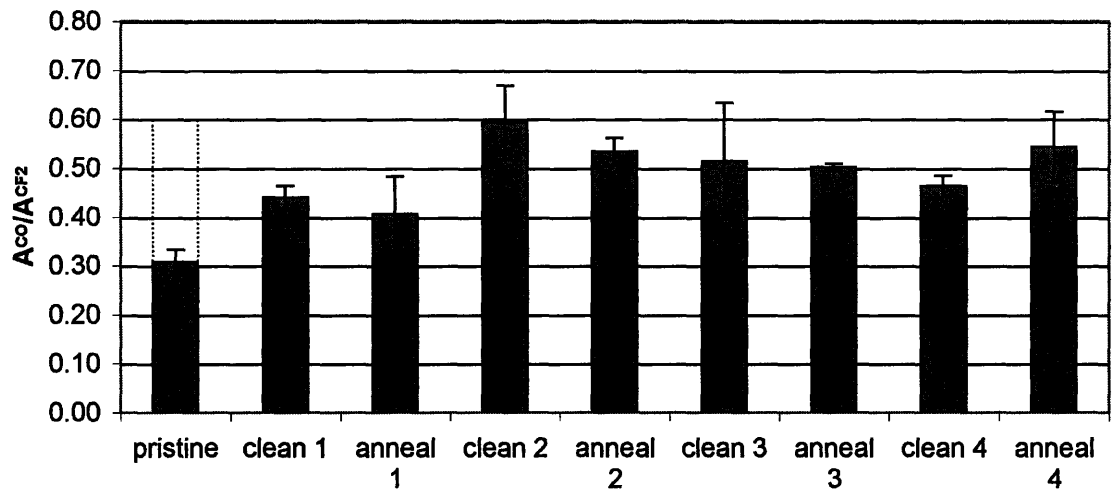

Figure 5.3b. Measure of PEO at surface in H_2O_2 regeneration study
The plot shows the change in the ratio of the C-O peak area to the CF_2 peak area, which is related to the amount of PEO exposed on the surface. Each data point is an average of three readings.

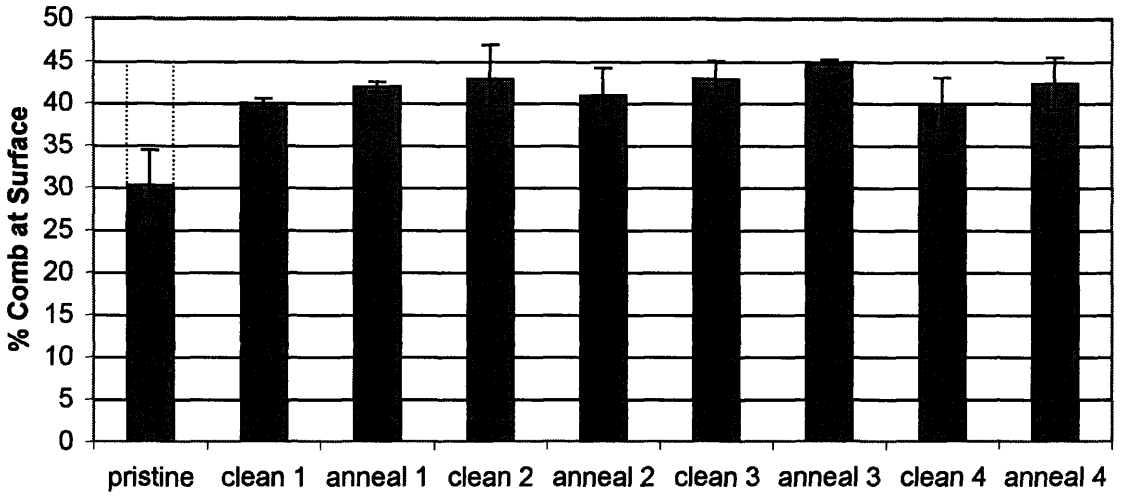

Figure 5.3c. Measure of comb at surface in H_2O_2 regeneration study
The plot shows the amount of P(MMA-*r*-POEM) comb on the surface. Each data point is an average of three readings.

First, it is useful to note that the pristine sample used in this study appears to deviate somewhat from other samples of S-040204 that were studied. Based on other samples, the expected pristine values for the plots in Figure 5.3 would be: nitrogen at surface ~ 100,000 CPS, $A_{CO}/A_{CF2} \sim 0.60$, comb at surface ~ 45%. These values are indicated on the plots with dotted lines. The deviance of the actual measured pristine values from these expected values is most likely due to non-uniformity in comb coverage across the membranes due to the hand-casting methods used.

Aside from the unusual results for the pristine sample, the remaining samples in this regeneration study behaved as expected, showing no statistical difference between cleaned and annealed samples. This agrees with the hypothesis that hydrogen peroxide does not affect the comb additive and so does not change the membrane surface characteristics upon cleaning.

It appears that hydrogen peroxide does not damage the PEO at the membrane surface appreciably or systematically. Although this data doesn't reveal much information about the membrane's regenerative properties, it suggests that the comb is resistant to mild

cleaning agents, which is promising for its use in applications that don't require harsh cleaning to maintain a high flux.

5.2.2. Chromerge Cleaning Studies

Concentrated chromic-sulfuric acid (Chromerge) was used to simulate long periods of harsh cleaning, which might be used for membranes fouled with proteins and oils. Chromerge is a mixture of chromic acid and concentrated sulfuric acid, and it is typically used to clean organic films off of glassware in laboratory settings. This treatment was previously shown by Hester to remove PEO from the surface of blend membranes and cause increased membrane fouling [10].

High-resolution C 1s Spectra

It is informative to look at the high-resolution C 1s XPS spectra for the blend membrane (S-040204) and its individual components before cleaning, after 30 minutes of cleaning in Chromerge, and after annealing. These spectra are shown in Figure 5.4.

The PVDF spectrum doesn't appear to change at all after cleaning (aside from a small decrease in the XPS pump oil fouling peak). This is to be expected, as Hester saw no change in the PVDF surface composition with acid cleaning either, and PVDF is a chemically resistant material. By contrast, the pure comb sample does change with cleaning. Again, the peak at 285 eV (the rightmost peak) is a combination of C-H from the comb backbone and fouling from the XPS pump oil, so it should not be considered when comparing spectra. Ignoring the 285 eV peak, it can be seen that the C-O peak (marked with an inverted triangle), arising from carbons in the PEO side chains, decreases after cleaning relative to the other peaks (from 74% of the pristine area to 42% of the cleaned area; Table B.3 gives more information). This is consistent with acid hydrolysis of the PEO side chains in the comb. It also agrees with a similar experiment done by Hester using pure P(MMA-*r*-POEM$_9$). In this experiment, he observed a decrease in the comb's C-O peak area (ignoring the hydrocarbon peak) from 67% to 62% after 30 minutes of cleaning with Chromerge. If the hydrocarbon peak is taken into

account, his observed change in area is 46% to 25%. Although Hester's observed C-O decrease was less dramatic than in this thesis, it reinforces the hypothesis that Chromerge damages PEO chains at the surface of a sample.

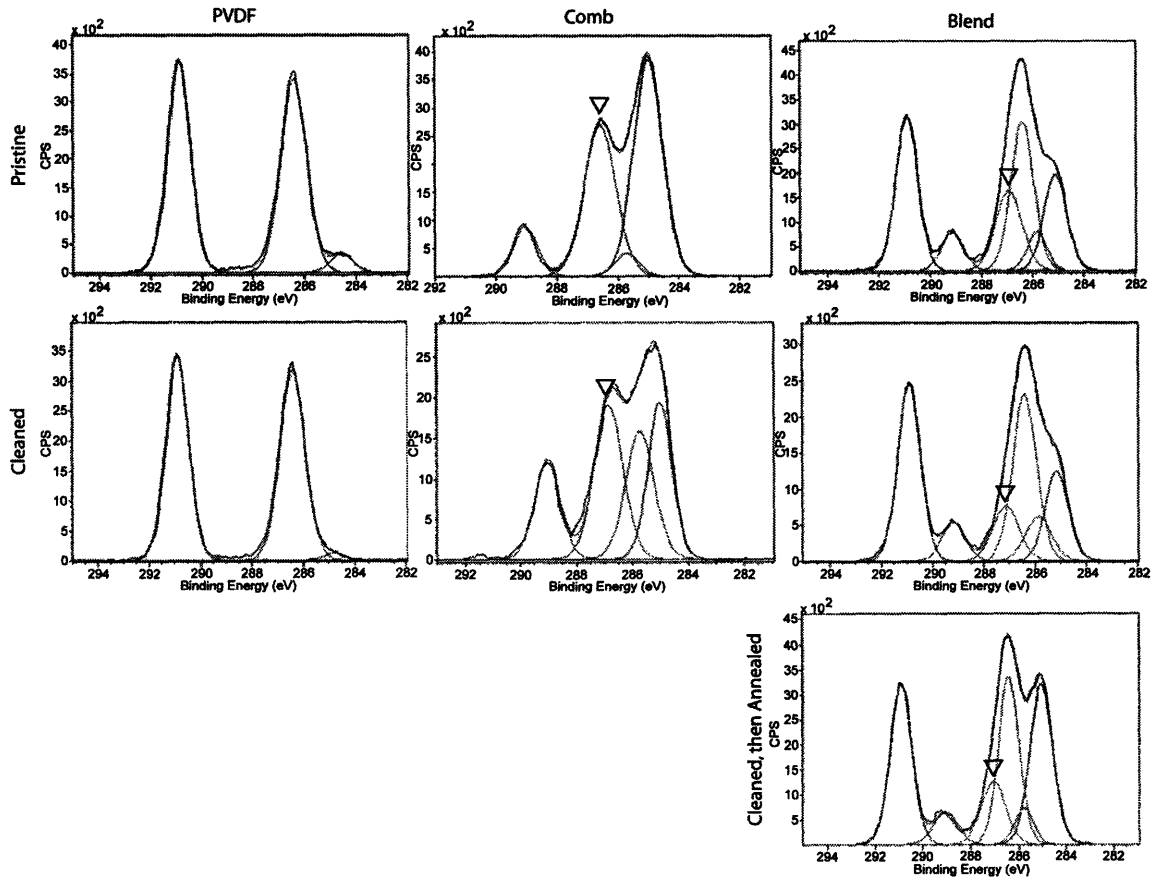

Figure 5.4. Comparison of XPS C 1s spectra for acid-cleaned samples
First row: pristine samples, *second row:* samples cleaned for 30 minutes with Chromerge, *third row:* samples cleaned and then annealed 18 hours in 90°C water. The PEO C-O peak is marked in the comb and blend spectra to show how it fluctuates with cleaning and annealing.

It is also worth noting that the ratio of the C-O peak to the COO peak (data provided in Section B.1) decreases greatly with 30-minute cleaning for the pure comb (A_{CO}/A_{COO} goes from 4.0 before cleaning to 1.8 after cleaning). The initial ratio is higher than expected (for a comb with 33 wt% of a POEM block containing 10 ethylene oxide repeat units, a ratio of roughly 3.3 would be expected), but this could be due to peak-fitting uncertainty or preferential location of the backbone at the surface under vacuum. Despite this slight inconsistency, the decrease in the ratio of C-O to COO is considerable,

suggesting that the acid is hydrolyzing the PEO side chains, leaving the COO-containing backbone intact.

Changes to the blend spectra can be explained by taking the pure PVDF and comb spectra into consideration. Again, the C-O peak (marked) decreases with cleaning. After annealing, it increases again, but not significantly. This is partially consistent with regeneration of the comb at the surface as seen by Hester (ignoring the 285 eV peak, for a 5 wt% blend membrane, he observed C-O peak areas of: 20% for the pristine sample; 10% after cleaning; and a return to 20% after annealing). In the current experiment, when the membrane is cleaned, the PEO is damaged, and the C-O signal decreases (from 20% to 13.5%), as expected. However, upon annealing, new comb does not appear to migrate to the surface (the area of the C-O peak does not increase appreciably, starting at 13.5% for the cleaned blend and only increasing to 14% for the annealed sample, which is not a statistically significant change). The failure of the PEO surface coverage to increase upon annealing is possibly due to the membrane having a low equilibrium surface coverage. Perhaps the pristine comb coverage was above that equilibrium, and so the membrane did not return to that coverage upon annealing. Also, it is possible that some comb PEO chains underwent only partial hydrolysis, remaining at the surface after annealing and preventing new comb from surfacing, but giving a reduced PEO signal. Or there could simply be insufficient comb density in the bulk to contribute to regeneration.

Another possibility is that a longer annealing period might be required to bring more comb to the surface, so an experiment was undertaken in which a membrane (F-040324) was cleaned for 30 minutes in Chromerge, then annealed for various lengths of time in 90°C water. The results are shown in Figure 5.5.

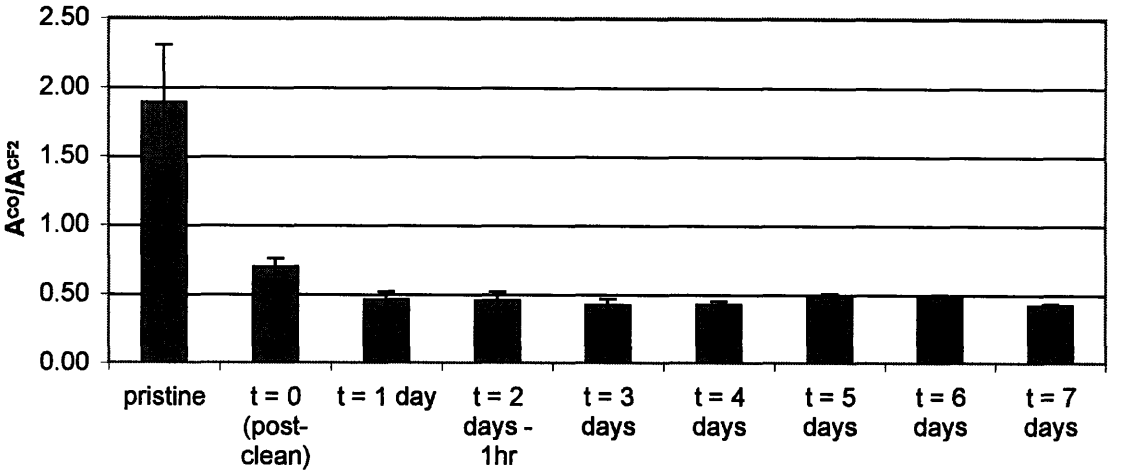

Figure 5.5. Amount of PEO at membrane surface vs. annealing time after cleaning A pristine membrane (F-040324) was cleaned in Chromerge for 30 minutes and subsequently annealed for the times indicated. Each data point is an average of three readings.

These results suggest that PEO coverage (and comb coverage, given in Appendix C) decreases with initial annealing, instead of increasing. This is probably because the initial coverage was higher than the equilibrium coverage. It was only with cleaning and annealing that the membrane could achieve its equilibrium coverage, which happened to be lower than the initial PEO surface coverage. This supports the explanation as to why a large increase in PEO coverage was not observed in the blend spectra in Figure 5.4 with annealing. It would be expected that a more dramatic difference between PEO coverage of cleaned and annealed samples would be observed in subsequent rounds of cleaning and annealing, once the equilibrium coverage had been attained.

Another possibility is that the hydroxy endgroups of the HPOEM chains cross-linked during annealing, preventing the damaged comb from leaving the surface and new comb from taking its place. However, the HPOEM comb itself was not observed to cross-link when heated in 90°C water overnight (it dissolved easily in DMF both before and after overnight heating), so this is probably not a contributing factor to the lack of comb regeneration.

It should be noted that membrane F-040324 was prepared differently than S-040204 (details are provided in Section 3.2)—most notably it was much thinner and so had less comb available in the bulk for regeneration. However, the general composition was the same, so the results are most likely applicable to the S-series membrane as well.

Acid Regeneration Trial 1

Based on the previous results, it would be interesting to investigate what would happen with multiple rounds of cleaning and annealing, once the comb surface coverage had equilibrated. To investigate this, pieces of membrane S-040204 were pre-annealed for 24 hours, then subjected to multiple rounds of 30-minute cleaning in Chromerge interspersed with 18-hour annealing in 90°C water. The results from XPS of the cleaned and annealed membranes are shown in Figure 5.6.

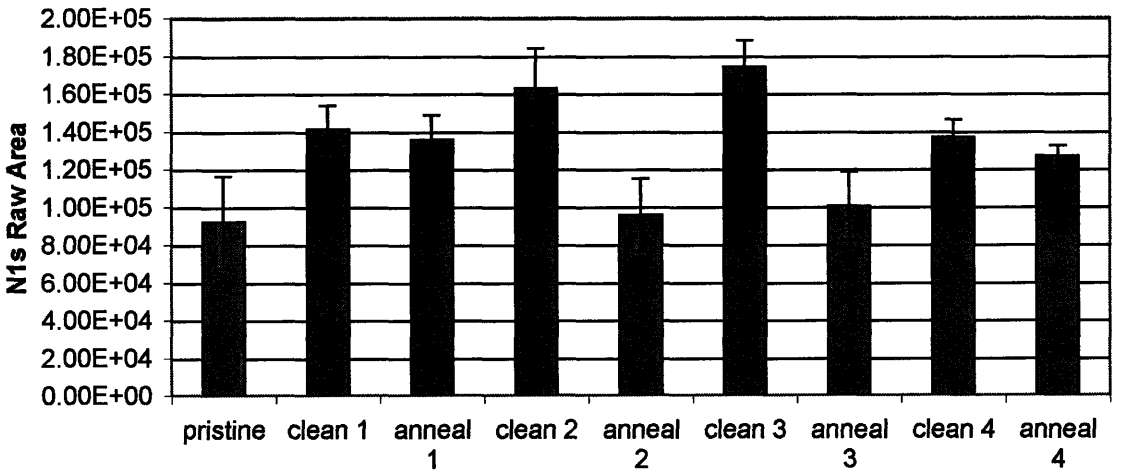

Figure 5.6a. Measure of surface fouling in acid regeneration trial 1
This plot shows the relative intensity of the N1s peak in an XPS survey of BSA-fouled samples. Each data point is an average of three readings.

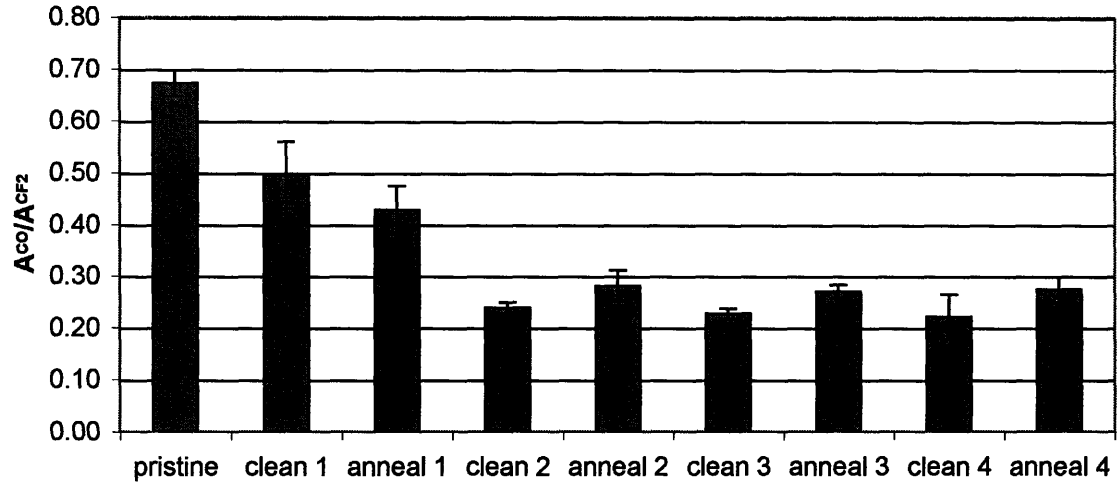

Figure 5.6b. Measure of PEO at surface in acid regeneration trial 1
This plot shows the change in the ratio of the C-O peak area to the CF_2 peak area, which is related to the amount of PEO exposed at the surface. Each data point is an average of three readings.

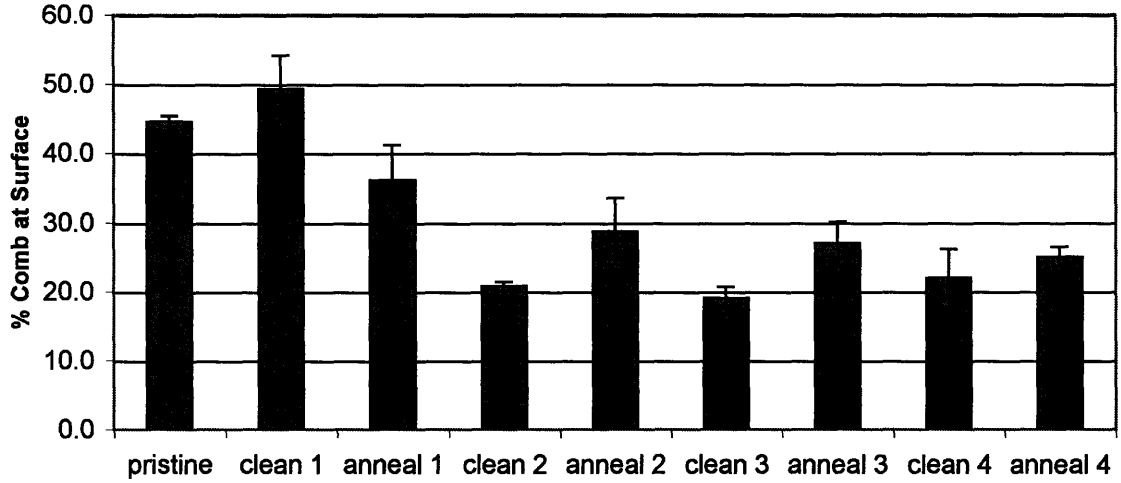

Figure 5.6c. Measure of comb at surface in acid regeneration trial 1
This plot shows the amount of P(MMA-*r*-POEM) comb on the surface of the samples. Each data point is an average of three readings.

Figure 5.6a shows the amount of nitrogen at the surface of BSA-fouled samples. Pristine and annealed samples (which are expected to have more intact PEO chains at their surface than cleaned samples do) were generally found to foul less than cleaned samples, even after four cleaning cycles. This can be explained by the degradation of PEO chains

at the surface of cleaned samples by the harsh acid treatment. Loss of PEO causes increased protein adsorption, leading to a higher N 1s signal for cleaned membranes.

Figure 5.6b compares the relative amounts of PEO at the membrane surface, as indicated by the ratio of the areas of the C-O peak (287 eV) and CF_2 (PVDF) peak (291 eV). The ratio of these two peak areas is related to the amount of PEO at the surface because the only components of the membrane contributing to the C-O peak are the PEO side chains, and the only component contributing to the CF_2 peak is the PVDF bulk material. As the amount of PEO at the surface increases, the ratio would be expected to increase. Figure 5.6b indicates that during the first round of cleaning and annealing, the amount of PEO at the surface radically decreases, as expected from prior experiments. After this, it appears that the annealed membranes have slightly more PEO at their surface than the cleaned membranes do. This is consistent with the hypothesis that the PEO chains at the surface reach an equilibrium coverage after the initial round of cleaning and annealing. Based on Figure 5.6a, this new equilibrium coverage is not so low as to affect the fouling resistance of the annealed membranes.

Figure 5.6c shows comb percentage values for each sample surface based on the comb backbone's COO peak (these values are equivalent to ϕ_s * 100%). There appears to be a slow decrease in the amount of comb at the surface of the membrane after each round of cleaning and annealing. This can be explained by a depletion in the supply of excess comb present in the bulk of the membrane. Also, the pattern observed in Figure 5.6c is similar to that of Figure 5.6b, where the amount of PEO at the surface tends to be greater for annealed membranes than for cleaned membranes.

A simple t-test comparing the cleaned and annealed samples for rounds 2-4 indicates that, for an alpha level of 0.05, the differences between annealed and cleaned samples are statistically significant for fouling, PEO, and comb values. For round 1, the differences between cleaned and annealed samples are not statistically significant.

Notably, the systematic decrease in comb in the annealed membranes is not directly reflected in the fouling data in Figure 5.6a. Based on the amount of comb present at the surface, the membrane after four annealing treatments would be expected to foul more than after one anneal, but this is not the case. It is possible that the amount of fouling is based not only on the amount of comb at the surface, but also on other unmeasured factors, such as PEO-stripped comb remaining at the surface. Also, Hester et al. found that a PVDF blend membrane containing 10 wt% of P(MMA-*r*-POEM) additive fouled more than one containing 5 wt% additive, after cleaning with Chromerge [10]. This suggests that the acid damages the comb, hydrolyzing the PEO chains, resulting in the loss of fouling resistance, since membranes with more comb foul more after acid treatment. If this is the case, it would explain why a membrane with more comb on its surface (such as the "anneal 1" sample) could still foul more if the comb were damaged.

The plots in Figure 5.6 show a definite pattern in fouling, amount of PEO, and amount of comb at the surface. Annealing improves fouling resistance and comb coverage after harsh cleaning, which would extend the lifetime of the membrane and reduce costs. Additionally, it appears that the membrane can maintain its fouling resistance after multiple rounds of cleaning and annealing. Given that treatments in industry are normally less harsh than the Chromerge treatment used here, the membrane should be able to maintain its fouling resistance for an extended amount of time, with periodic cleaning and annealing.

Acid Regeneration Trial 2

Since the membrane seemed to be able to regain its comb coverage following a brief cleaning in acid, a second regeneration experiment with longer cleaning intervals was performed to determine if the membrane could recover from this even harsher treatment. Samples of S-040204 (pre-annealed for 24 hours) were subjected to rounds of 18-hour cleaning in Chromerge, followed by 18-hour annealing. Results are shown in Figure 5.7.

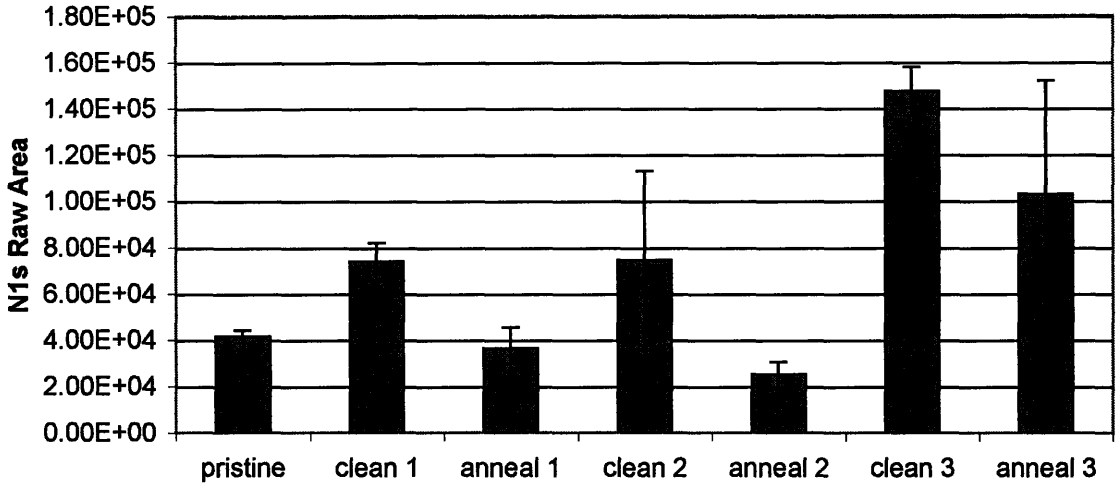

Figure 5.7a. Surface fouling for acid regeneration trial 2
The intensity of the N 1s peak is approximated by the raw area of the peak. Each data point is an average of three readings.

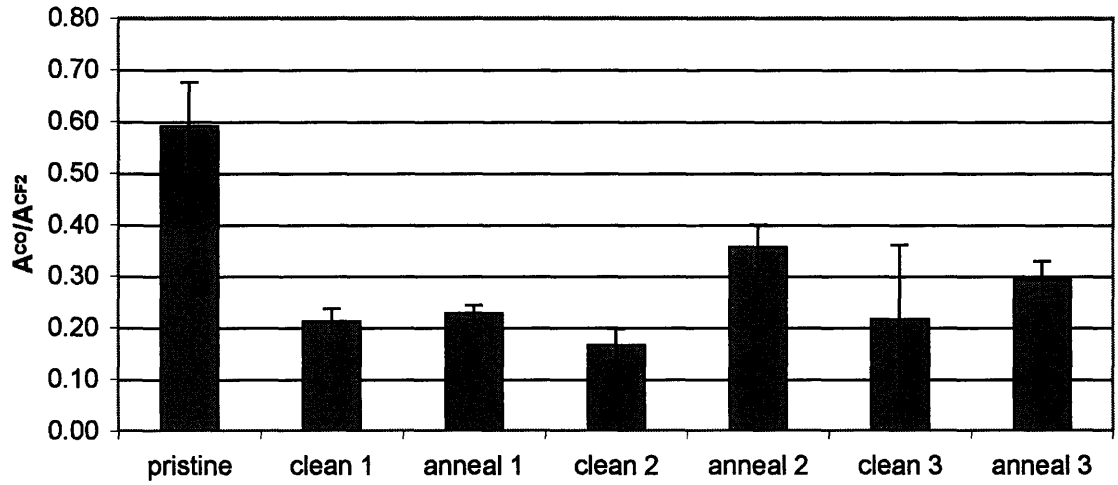

Figure 5.7b. PEO at sample surfaces for acid regeneration trial 2
The amount of PEO at the surface is related to the areas of the C-O and CF_2 peaks. Each data point is an average of three readings.

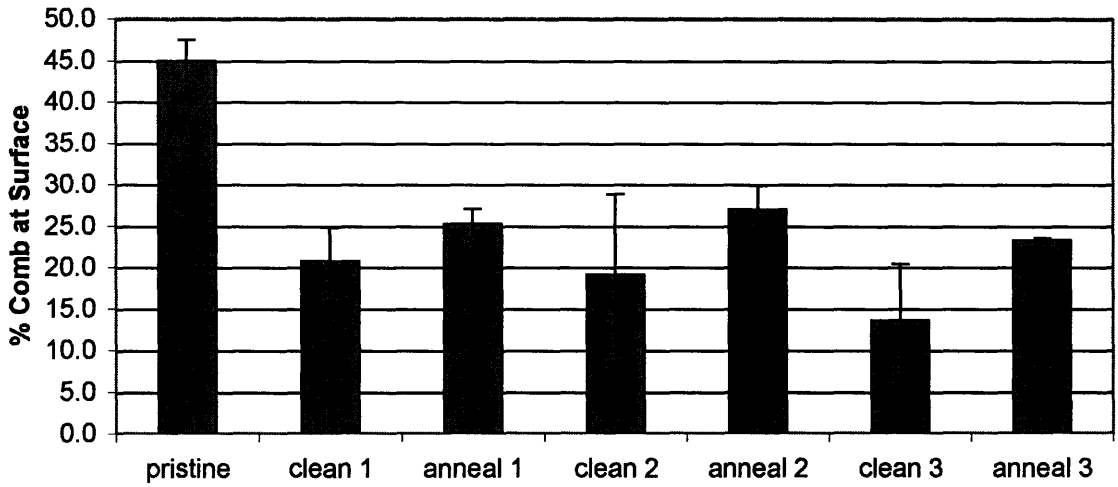

Figure 5.7c. Comb at the surface of samples from acid regeneration trial 2
The amount of comb at the surface is calculated using the area of the COO peak, as described in section A.3. Each data point is an average of three readings.

This harsher regeneration trial gave the same general pattern of behavior as that involving 30-minute Chromerge cleaning, but with more dramatic differences between cleaned and annealed samples. As can be seen from all three plots in Figure 5.7, cleaned samples tend to foul more and have less PEO and comb at their surfaces than annealed samples. Again, a t-test of all three plots indicates that the differences between cleaned and annealed samples (excluding the round 1 values for PEO) are statistically significant, for an alpha level of 0.05.

Although the differences between cleaned and annealed samples in both acid regeneration trials were statistically significant, it would be useful to demonstrate more decisively that annealing can cause new comb to come to the membrane surface after cleaning. To do this, it was necessary to determine how extensive a cleaning would be required to remove all the comb from the membrane surface and to find the amount of annealing required to reach maximum comb coverage following complete removal of comb from the surface. Once these two pieces of information had been obtained, a more definitive regeneration trial could be conducted. Also, for this new trial, filtration (F-series) membranes were used instead of the surface analysis (S-series) membrane, as the

F-series samples are more similar to the membranes used in industry and would be more useful to characterize.

Cleaning Kinetics Trial

First, it was necessary to determine how long an exposure to Chromerge would be needed in order to strip all of the PEO from a membrane's surface (membrane F-040310 was used). The results are shown in Figure 5.8 (additional results are provided in Appendix C).

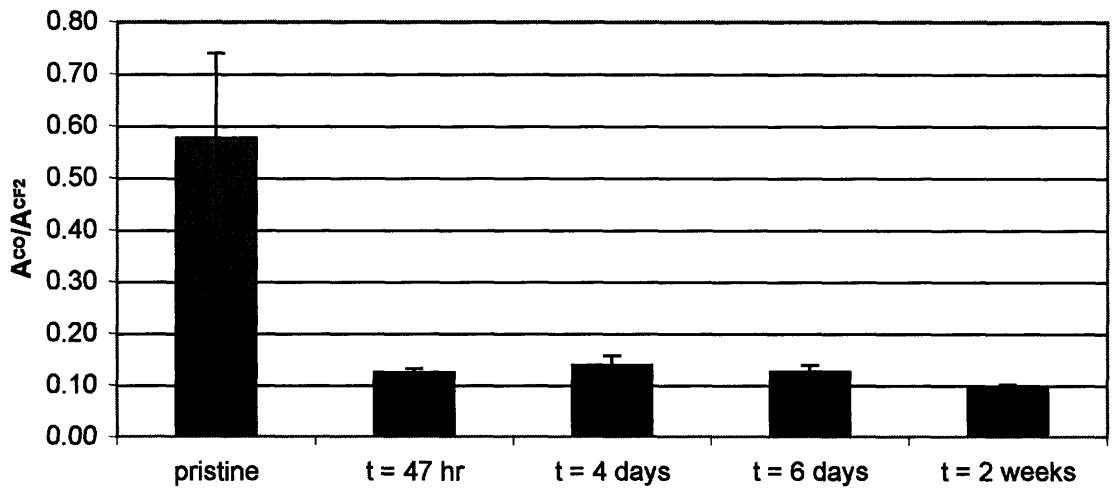

Figure 5.8. Amount of PEO at a membrane surface vs. cleaning duration
A pristine membrane (F-040310) was cleaned in Chromerge for varying lengths of time, as indicated on the plot, and the relative amount of PEO at its surface was determined. Each data point is an average of three readings.

The plot in Figure 5.8 is slightly misleading, as it suggests that PEO does not entirely disappear from the membrane's surface, even after two weeks of cleaning. This is due to noise in the XPS spectra as well as to peak-fitting uncertainties; because of these problems, C 1s high-resolution spectra can't be fit perfectly. This is illustrated in Figure 5.9. By comparing the cleaned blend spectrum in Figure 5.9b to the pure PVDF spectrum in Figure 5.9a, it is clear that after two weeks of cleaning, even though A_{CO}/A_{CF2} is not found to be zero by peak-fitting, there is no PEO left at the surface of the membrane. In fact, if a pure PVDF spectrum is fit using the same peaks as are used for blend membranes, it is determined to have $A_{CO}/A_{CF2} \sim 0.10$ and roughly 11% comb at the

surface. Clearly, neither of these results is accurate, as pure PVDF has no comb at its surface. This demonstrates that the processes of peak fitting and surface analysis have an inherent uncertainty. Because of this uncertainty, it is assumed that any values of A_{CO}/A_{CF2} near or below 0.10 and any comb coverage values of 10% or less are equivalent to zero PEO/comb at the surface.

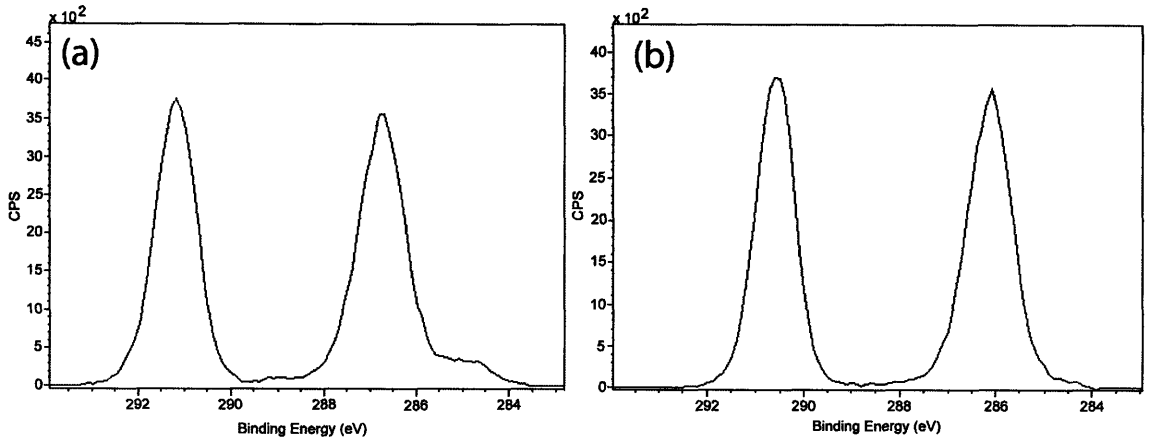

Figure 5.9. Comparison of pure PVDF and cleaned blend membrane
(a) pristine PVDF, (b) Membrane F-040310, cleaned in Chromerge for 14 days. Peak fitting incorrectly suggests that for (a) $A_{CO}/A_{CF2} = 0.08$ and %comb = 11, while for (b) $A_{CO}/A_{CF2} = 0.09$ and %comb = 5. In reality, both have $A_{CO}/A_{CF2} = 0$ and have 0% comb at their surfaces.

With this caveat in mind, it appears that all PEO has been removed from the membrane surface after only 47 hours of exposure to Chromerge. Since no samples were taken earlier than 47 hours, it is not known exactly when the last of the PEO is removed from the surface. Based on this and other cleaning experiments, the complete removal of PEO occurs somewhere between 18 hours of cleaning (when $A_{CO}/A_{CF2} \sim 0.20$) and 47 hours. It was decided that a cleaning duration of 24 hours would remove sufficient PEO (if not all, then almost all of it), and would be an acceptable cleaning cycle duration for the third regeneration trial.

Annealing Kinetics Trial

Once it had been decided that a cleaning duration of 24 hours would remove nearly all of the PEO from the membrane surface, the next step was to determine how much annealing

is necessary to attain the maximum amount of comb regeneration. A membrane (F-040324) was cleaned in Chromerge for 24 hours, then annealed in 90°C water for varying lengths of time. The results are shown in Figure 5.10 (Appendix C includes supplementary data).

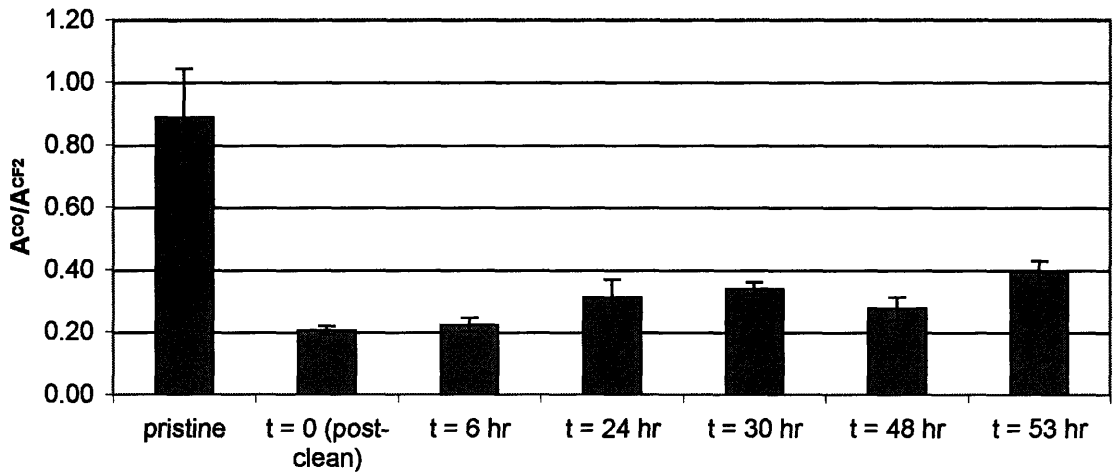

Figure 5.10. PEO coverage vs. annealing time following a 24-hour cleaning
The membrane sample was cleaned in Chromerge for 24 hours (this is the data point labeled t = 0), then annealed for varying lengths of time. Each data point is an average of three readings.

From this data, it appears that maximum PEO coverage is attained after approximately 30 hours of annealing, although it may increase slightly as time goes on. Based on this result, an annealing duration of 48 hours was used in the extended regeneration study, to be certain that the annealing time was long enough.

Acid Regeneration Trial 3

With the results of the cleaning and annealing kinetics trials in hand, a third regeneration study was conducted. A membrane (F-040505) was exposed to rounds of cleaning and annealing, consisting of 24 hours of cleaning with Chromerge followed by 48 hours of annealing in 90°C water. The results are shown in Figure 5.11.

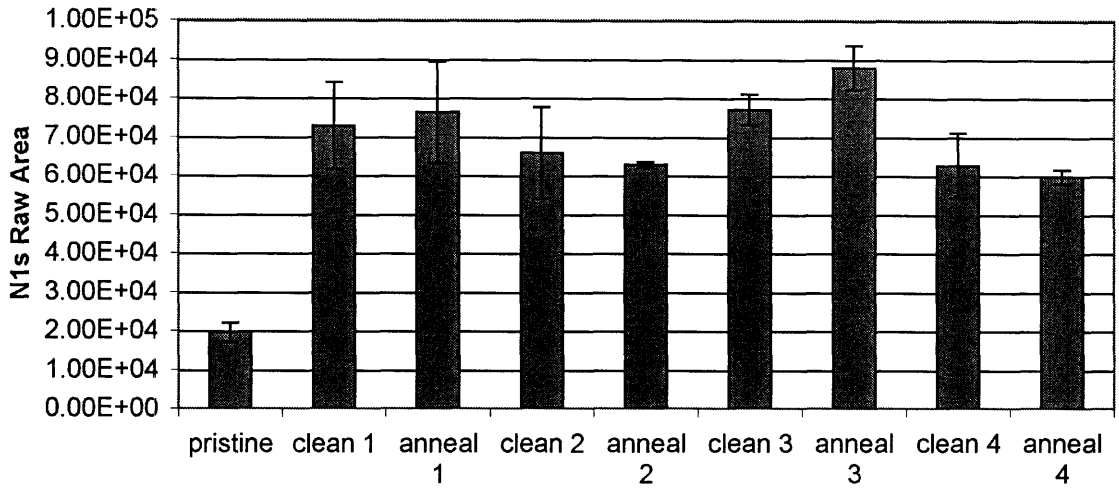

Figure 5.11a. Surface fouling for acid regeneration trial 3
The fouling is related to the area of the N 1s peak. Each data point is an average of three readings.

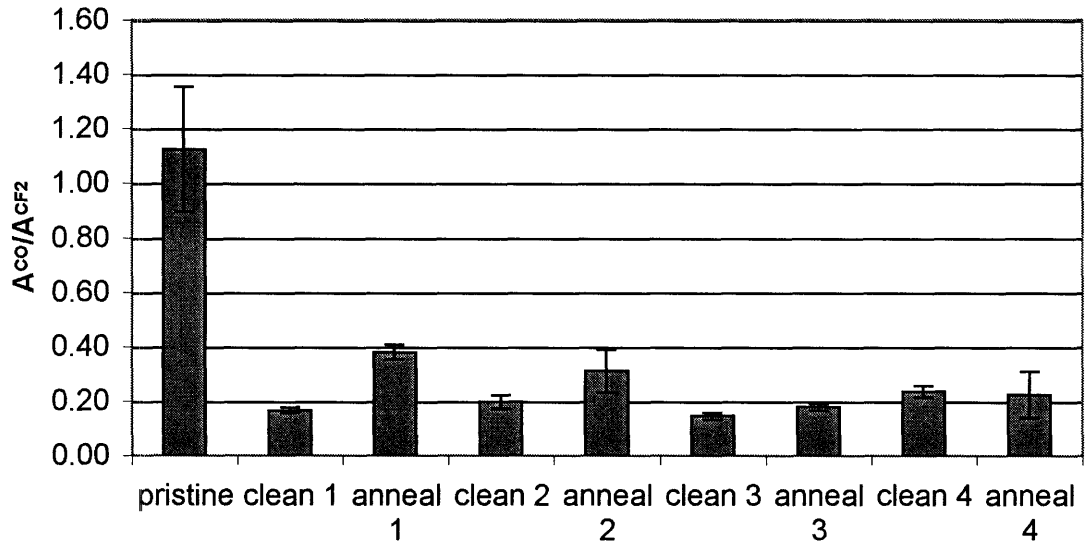

Figure 5.11b. PEO at surface for acid regeneration trial 3
The relative amount of PEO can be determined by a comparison of the areas of the C-O peak and the PVDF CF_2 peak. Each data point is an average of three readings.

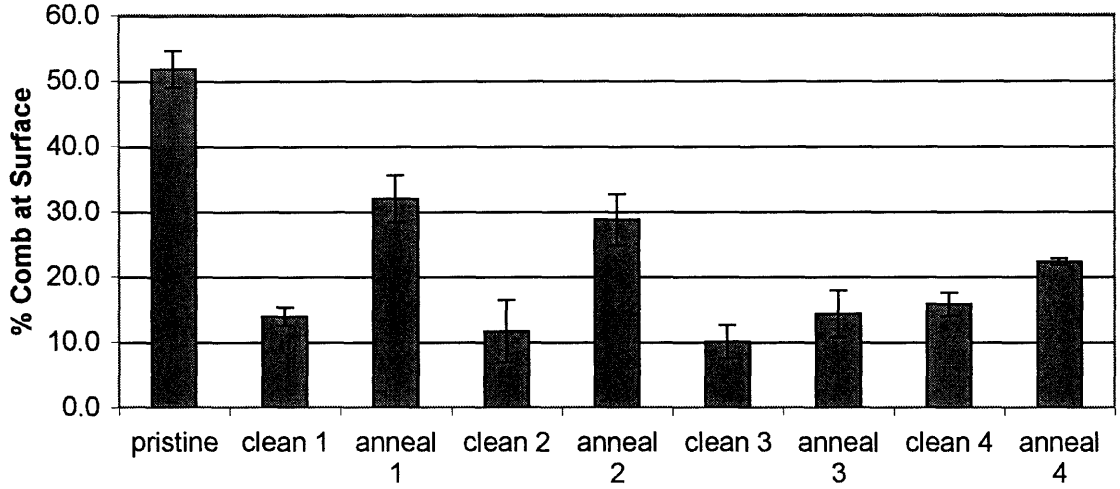

Figure 5.11c. Surface comb coverage for acid regeneration trial 3
The % comb value is based on the area of the COO peak, a signal that only comes from the comb backbone. Each data point is an average of three readings.

In this regeneration trial, cleaned samples are once again observed to have less comb and PEO coverage than annealed samples do. Strangely, the fouling does not seem to follow a given pattern, which is unexpected given the results from the previous regeneration trials. This will be discussed later.

Focusing on Figures 5.11b and 5.11c, it appears that nearly all of the comb and PEO are stripped from the surface with 24-hour cleaning. The "clean 3" sample appears to have zero comb remaining (based on the assumption made earlier that a sample with 10% comb or less actually had no comb at its surface), while the other cleaned samples might have some remnants of comb present. Samples "anneal 1" and "anneal 2" exhibit regeneration of both PEO and comb overall, with slightly less regeneration for "anneal 2". "Anneal 3" does not exhibit the same regeneration, which could be explained by the hypothesis that as surface comb is repeatedly removed, the bulk comb must travel farther to reach the surface. Longer annealing might be required following each subsequent cleaning round, to achieve the same degree of regeneration. This is consistent with the fact that the amount of comb at the surface seems to increase again with "anneal 4".

A simple t-test (alpha level of 0.05) comparing the cleaned and annealed samples in rounds 1-2 indicates that the differences between annealed and cleaned samples for the A_{CO}/A_{CF2} and comb values are statistically significant. This is not the case for the N 1s values, as noted above. Fluctuations in the N 1s intensity values are probably due to experimental error and not due to any actual difference in fouling susceptibility between samples. This lack of a fouling trend is unexpected, as previous trials demonstrated increased fouling for cleaned samples. Here, all samples other than pristine foul equally much.

Two possible explanations for this fouling behavior come to mind. First, it is possible that the amount of PEO at the surface of annealed samples is not sufficient to impart fouling resistance. Hester previously found that blend membranes with 30% or more comb coverage were fouling-resistant. Here, annealed samples have roughly 30% comb coverage, but the comb used has lower PEO content than that used by Hester. It is possible that the annealed samples simply didn't have quite enough PEO at their surfaces to convey fouling resistance to the membrane. However, in regeneration trials 1 and 2, fouling resistance was observed for annealed samples with less than 30% comb at their surfaces, so this hypothesis doesn't seem to bear out.

The second possibility is that the comb at the surface of annealed samples is damaged. Although an increased PEO signal is observed with annealing, perhaps the PEO chains are too short to resist fouling, or they may have been chemically altered by the acid environment. A plot of A_{CO}/A_{COO} for each sample in this trial (Appendix C) suggests that this is not the case, as the area ratio is the same for pristine and cleaned samples, meaning that there is the same ratio of PEO to backbone for the comb in both samples. Also, it is unclear why this problem wouldn't afflict the samples from Acid Regeneration Trial 2 as well, since those were exposed to acid for a similar length of time and exhibited the same unchanging A_{CO}/A_{COO} behavior. Perhaps the 24-hour cleaning leads to much more comb damage than the 18-hour cleaning.

Although the fouling behavior for Regeneration Trial 3 remains unexplained, it is clear from the PEO and comb analysis that more PEO does come to the surface with annealing. This can be seen especially well by examining the high-resolution C 1s XPS spectra for the pristine sample and first round of cleaning and annealing, in Figure 5.12.

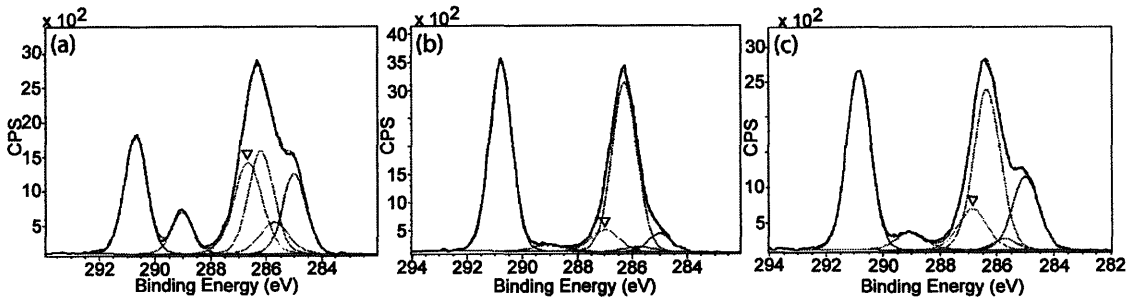

Figure 5.12. Comparison of C 1s XPS spectra for acid regeneration trial 3
(a) Pristine sample, (b) sample after 24 hours of cleaning, (c) cleaned sample following 48 hours of annealing. The C-O peak (which is related to surface PEO content) is marked with an inverted triangle.

The PEO C-O peak (marked) can be seen to decrease greatly upon cleaning (Figure 5.12b), as is the case for the comb backbone COO peak (289 eV). After annealing (Figure 5.12c), both peaks increase relative to the PVDF peaks (290.9 eV and 286.4 eV). It seems clear that comb returns to the membrane surface, as does PEO, even if the fouling data suggests that the PEO can no longer effectively impart fouling resistance.

It is also useful to compare the values of A_{CO}/A_{COO} for the "pristine" and "clean 1" samples in Acid Regeneration Trials 1 and 3 (plots are given in Section C.4). The ratio of the area of the C-O peak (which comes solely from the PEO chains) to that of the COO peak (which comes solely from the comb backbone) would be expected to relate to the amount of PEO still attached to the comb backbone. A lower ratio would mean that less PEO was attached to the comb backbone. For Acid Regeneration Trial 1, the ratio decreases from the pristine to the cleaned sample. For Trial 3, it remains unchanged with cleaning. This suggests that for short periods of cleaning (30 minutes), the PEO is more susceptible to degradation than the backbone. But with longer exposure to the acid (24 hours), the backbone degrades as much as the PEO does.

Calculation of Regeneration Capabilities Based on Surface Area

It is instructive to calculate how many regeneration cycles (full removal of comb followed by full restoration of comb) a filtration membrane would be expected to be capable of, in order to determine if lack of comb in the bulk might be contributing to the observed annealing behavior in Trials 1-3. Values needed for the calculation include:

- **Surface area of a typical filtration membrane**

  The surface area of membrane F-040324 was found to be 4.29 m^2/g using the BET gas sorption method described in Section 3.4.4. It was also experimentally determined that membrane F-040324 has a conversion factor of 0.0033 g/frontal cm^2. This yields a surface area of 0.014 m^2/frontal cm^2.

- **Typical comb surface coverage**

  XPS surface analysis of membranes F-040317, F-040324, and F-040505 (all cast using the same method and solution composition) suggests that they have roughly 50% comb surface coverage after casting. So it can be assumed that each time the comb surface layer regenerates, it would ideally cover 50% of the total surface area.

- **Height of a comb monolayer**

  This value is hard to estimate theoretically, so an experimental value is used instead. Walton et al. studied blends of P(MMA-*r*-POEM) (M_n = 40,700 g/mol) and PMMA using neutron reflectivity [69]. It was found that a thin PEO-rich layer formed at both surfaces of a thin film of the blend, and that this layer was ~0.05L thick, where L = 76 nm. From this data, it is estimated that a monolayer of comb is approximately 3.8 nm thick. Since the comb used by Walton et al. had a slightly higher molecular weight than the comb investigated in this thesis, the actual value is probably slightly below 3.8 nm. An estimated monolayer height of 3.5 nm will be used in this calculation.

Since the membrane is approximately 0.09 mm thick (estimated from the cross-sectional SEM in Figure 5.13c), a 1 cm^2 piece would have a volume of 0.009 cm^3. The amount of comb used in the polymer casting solution was approximately 11 wt%, or ~16 vol% (Table 3.2). This means that there is roughly 0.0014 cm^3 of comb in the membrane bulk. Dividing this by the thickness of a monolayer of comb (3.5 nm), there is **~0.4 m^2 of comb in the bulk** per 1 frontal cm^2 of membrane upon casting. The total membrane surface area was determined to be 0.014 m^2/frontal cm^2, as described above. If 50% of this surface is covered by comb, there would be **0.007 m^2 of comb exposed at the surface** per 1 frontal cm^2 of membrane after each regeneration. Using these estimates, it would be possible to have roughly **60 rounds of full regeneration** before the comb supply in the bulk would be exhausted. However, kinetic and thermodynamic considerations might strongly affect that observed behavior.

For instance, in Acid Regeneration Trial 3 (Figure 5.11), after two rounds of regeneration, the rate of return of comb to the surface with annealing is observed to decrease. The membrane requires two rounds of annealing to bring comb to the surface, probably because the comb has to migrate farther in order to get to the surface. "Anneal 3" exhibits very little comb regeneration, while "anneal 4" exhibits more (the intermediate cleaning stage is not expected to affect the surface coverage greatly, as the acid cannot penetrate into the membrane bulk, and there is very little comb present at the surface prior to "clean 4"). This suggests that although the membrane might be capable of 60 rounds of regeneration, it might take an unreasonably long annealing duration to bring comb to the surface as the number of regeneration rounds increases.

Despite these potential regeneration issues, this calculation is useful because it shows that there is ample comb in the bulk of F-040324 (as well as the other membranes, most likely). Based on this calculation, it seems that the poor comb recovery observed with annealing in Figures 5.4 and 5.5 is not due to any lack of comb in the bulk, but most likely due to a low surface coverage equilibrium, as previously supposed.

Comparison of Measured Surface Area to Literature Values

It is useful to compare the surface area measured for F-040324 with other values reported in the literature for polymer membranes made by immersion precipitation. Selected data are given in Table 5.1.

Table 5.1. Comparison of selected BET surface area values
All membranes were prepared by immersion precipitation; fabrication details can be found in the referenced articles.

Membrane Description	Thickness (μm)	BET Surface Area (m^2/g)
F-040324	90	4
Sulfonated polysulfone and cellulose acetate with poly(ethylene glycol) pore former [70]	90-110[†]	16-18
Cellulose acetate and polyethyleneimine, crosslinked by polyisocyanate [71]	180	12-24
Ethylene vinyl alcohol copolymer [72]	200-300[‡]	8-10

[†] Estimated using the fact that the reported gate size was 0.25 mm. For a 0.5 mm gate, Chen obtained a thickness of 180 μm, and in this thesis, membranes cast using a 0.20 mm (8-mil) gate were approximately 90 μm thick.
[‡] Estimated from SEM images of membranes cast using the same technique (no gate size specified) in [73].

Normalizing by membrane thickness, the range of surface areas reported by these authors is 0.03 – 0.2 $m^2/g \cdot \mu m$. Membrane F-040324 has a normalized surface area of 0.045 $m^2/g \cdot \mu m$, which is consistent with the range of values found in the literature, although slightly lower than what is normally observed. If the regeneration calculation is done using the range of normalized surface area values specified above, it is found that anywhere from 10 to 90 regenerations could ideally be expected from a typical 90 μm-thick blend membrane made by immersion precipitation, with higher surface area leading to fewer regenerations.

5.3. Filtration Experiments

5.3.1. Filtration Membranes

Three blend solutions of P(MMA-*r*-POEM) comb and PVDF were used to make filtration membranes (Tables 3.2 and 3.3 give details). These membranes were imaged via SEM, and the resulting micrographs are shown in Figure 5.13.

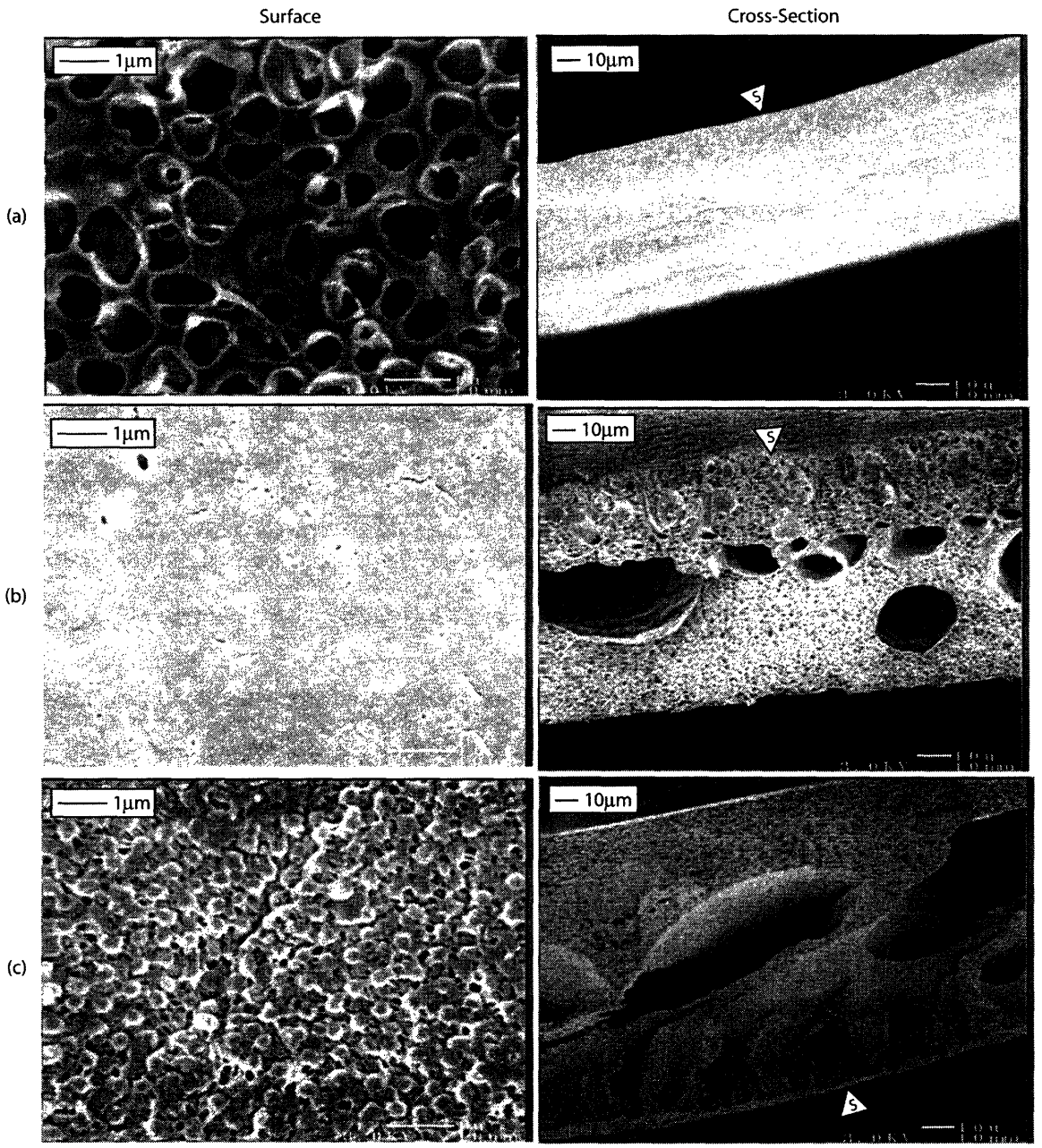

Figure 5.13. SEM micrographs of P(MMA-*r*-POEM)/PVDF membranes
(a) Membrane F-040301 (casting solution: P(MMA-*r*-POEM), PVDF, DMF), (b) Membrane F-040310 (casting solution: P(MMA-*r*-POEM), PVDF, glycerol, DMF), (c) Membrane F-040317 (casting solution: P(MMA-*r*-POEM), PVDF, glycerol, NMP). Surface images are at 20,000x and cross-sections at 1000x magnification. Separation surfaces are marked. Left-hand scale bars are 1 micron, right-hand scale bars are 10 microns.

The first membrane (Figure 5.13a) gave very low flux (~0.005 g/min•psi) because of its uniform density. The membrane was not acceptable for filtration experiments, both because of this low flux and due to its symmetric structure. The second membrane (Figure 5.13b) was cast from a solution containing glycerol, a pore former. Although pores can be seen in the membrane cross-section, the surface was very dense, and it did not have the defined asymmetric structure desired. It also gave a very low flux (~0.001 g/min•psi), much like the first membrane.

As can be seen in Figure 5.13c, the third membrane (F-040317) had a much better structure for filtration purposes. It had a porous surface and an asymmetric structure, due to the use of NMP as the solvent. This resulted in a separation surface with reasonably-sized pores and a defined separation layer. Additionally, the glycerol created large voids in the bulk of the membrane, increasing flux and throughput without sacrificing rejection capabilities. The flux properties of this membrane are described below (it is used interchangeably with membranes F-040324 and F-040505, as they were cast from the same polymer solution using the same method).

5.3.2. Flux Results

Regeneration Filtration Trial 1

An experiment was undertaken in which the same membrane disc (taken from membrane F-040324) was subjected to three different flux experiments:

- Pristine: The pristine membrane was tested
- Cleaned: The tested membrane was cleaned in Chromerge for 30 minutes and tested again
- Clean/Anneal: The tested membrane was cleaned in Chromerge for 30 minutes, annealed in 90°C water for 18 hours, then tested a third time.

Each experiment consisted of three stages during which flux was measured:

- Water before BSA: Pure dW was used as the feed solution for 10 minutes (prior to this, pure water was run through at a variety of pressures to ensure flux

linearity and to reduce the effects of compaction, but this data is not included in the flux plots). The flux values plotted in Figure 5.14 and others were taken immediately before the feed solution was changed to BSA.

- BSA, 1 hour: The feed solution was switched to BSA (1 mg/mL, in this case), and flux was measured for 1 hour. Permeate samples were taken and analyzed at various intervals. Flux values used in plots were taken after one hour of BSA flux.
- Water after BSA: The feed solution was changed back to dW and run for 15 minutes. Flux values used in plots were taken after 15 minutes of pure water flux following BSA exposure.

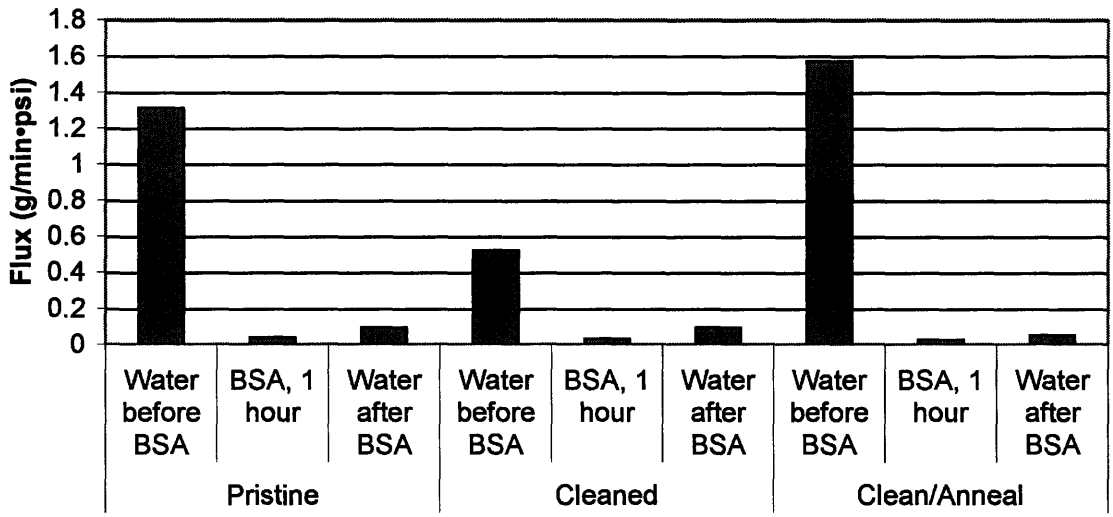

Figure 5.14. Flux behavior for Regeneration Filtration Trial 1
The BSA fouling solution was 1 mg/mL in PBS. Blend membrane F-040324 was used. Raw flux data is given in Figure D.1. The membrane had a filtration area of 4.1 cm^2.

The flux results are shown in Figure 5.14. The initial flux for each experiment ("Water before BSA") varied unpredictably. This is probably because each time the membrane was placed in the filtration cell, it was aligned differently, and so the flux changed. However, the "BSA, 1 hour" and "Water after BSA" flux values seem relatively consistent between experiments. For all membrane treatments, the flux recovers slightly after water is restored as the feed solution, but it does not increase to anywhere near the original (pre-BSA) flux value. It appears that the BSA feed solution was too

concentrated (1 mg/mL) to allow for good fouling recovery, so a second experiment was undertaken in which a more dilute fouling solution was used.

Regeneration Filtration Trials 2 and 3

An experiment very similar to Trial 1 was conducted, the only difference being that the BSA fouling solution had a concentration of 0.1 mg/mL instead of 1 mg/mL. This experiment was Regeneration Filtration Trial 2. The results are given in Figure 5.15. Also pictured are the results of Trial 3. This trial was intended to reproduce the results observed in Trial 2 (it used a different piece cut from the same membrane used in Trial 2). Additionally, two further rounds of 30-minute cleaning followed by 18 hour annealing were conducted for Trial 3 to view the effects of comb loss from the surface. Figure 5.15 also includes PVDF control data, also using a 0.1 mg/mL BSA fouling solution (data was only taken for the Pristine, Cleaned, and Clean/Anneal rounds for the PVDF control and Trial 2).

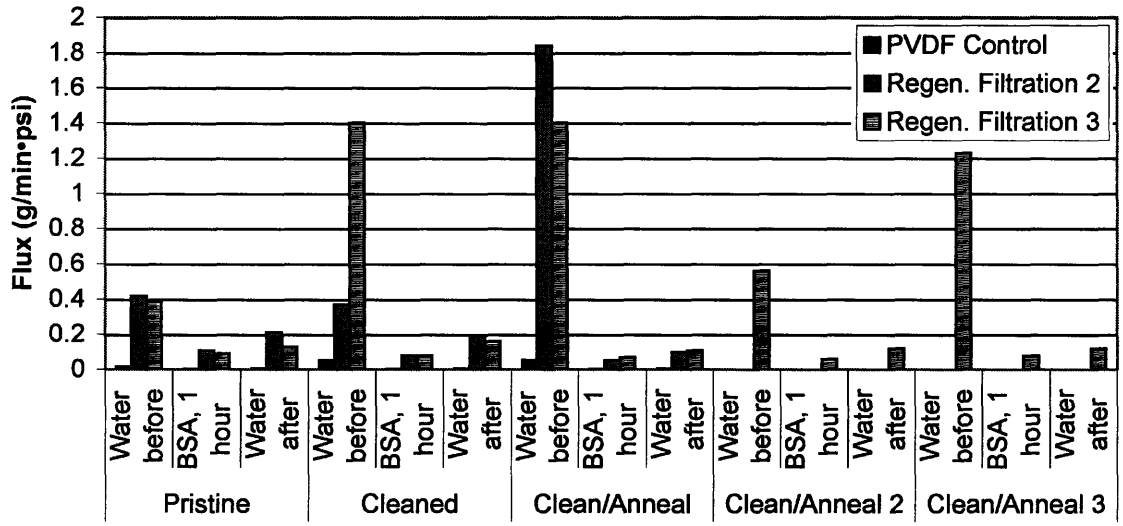

Figure 5.15. Flux behavior for Regeneration Filtration Trials 2 and 3
A comparison of the flux results of trials 2 and 3, as well as a PVDF control. The BSA fouling solution was 0.1 mg/mL in PBS. Different pieces of blend membrane F-040324 were used for the two trials. Raw flux data is given in Figures D.2, D.3, and D.5. The PVDF Control and Regen. Filtration 2 samples were not involved in the Clean/Anneal 2 and 3 experiments, so no data is listed for those. The membranes had a filtration area of 4.1 cm^2.

The blend membranes appear to be far superior to the PVDF in terms of absolute flux, giving roughly 25 times as much throughput as the PVDF control. However, this comparison is not entirely trustworthy, as the PVDF was not pre-wet with methanol, but with water, so its initial permeability was far less than that of the blend. When another piece of the PVDF control was pre-wet with methanol instead of water, the initial flux was ~0.1 g/min•psi after 10 minutes of pure water flux, a roughly six-fold increase in flux. Unfortunately, the membrane appeared to rupture following this measurement, so a full flux profile could not be obtained.

Despite the pre-wetting issue, it appears that the blend membranes still exhibit better initial flux than the PVDF control. Another reason for this improved flux could be that the use of comb additives in the blend membrane has been shown to increase membrane porosity [10], so the blend membrane was probably more porous and permeable than the PVDF control. Also, there is the previously-observed variability in initial flux depending on the exact positioning of the membrane in the filtration cell (Figure 5.14). And the rejection coefficients (given in Appendix D) are not equivalent for the three membranes, so this would prevent an accurate comparison. Because of these issues, it is difficult to compare the absolute fluxes of the PVDF and blend membranes.

Comparing the two blend membrane trials (which should have yielded the same results), it appears that the initial flux is indeed highly variable, as it changes unpredictably between experiments and trials. However, the blend membranes seem to behave similarly during and after fouling, recovering slightly when the feed solution is switched back to water, but still at a much lower flux than initially observed. It is encouraging that the membranes continue to show recovery after many cycles of cleaning and annealing, but they do not appear to recover any more than the PVDF control does, relatively speaking (Appendix D has detailed flux plots for a more accurate comparison of flux recovery between the two types of membranes).

The Clean/Anneal 2 and 3 data for Trial 3 might be expected to show improved fouling resistance recovery, as this type of behavior was observed in Acid Regeneration Trial 1

(Figure 5.6). In Acid Regeneration Trial 1, the amount of comb present at the surface decreased with the first round of cleaning and annealing but then increased with subsequent annealing steps. However, this improvement in fouling resistance was not observed in Filtration Trial 3, as the fouling recovery stayed roughly the same for three rounds of cleaning and annealing (Figure 5.15).

It appears that the blend membranes do not experience improved fouling resistance with annealing, compared to the PVDF control. Perhaps a thicker filtration membrane (similar to the S-series membrane from Regeneration Trials 1 and 2) would give better fouling recovery. Alternatively, using a comb additive with a different molecular weight and/or PEO block size might aid in the fouling recovery.

Regeneration Filtration Trial 4

A final set of experiments was conducted to study the filtration behavior of a membrane subjected to overnight cleaning. The trial was conducted similarly to Trial 2, except the membrane was cleaned for 18 hours instead of 30 minutes. The results are shown in Figure 5.16.

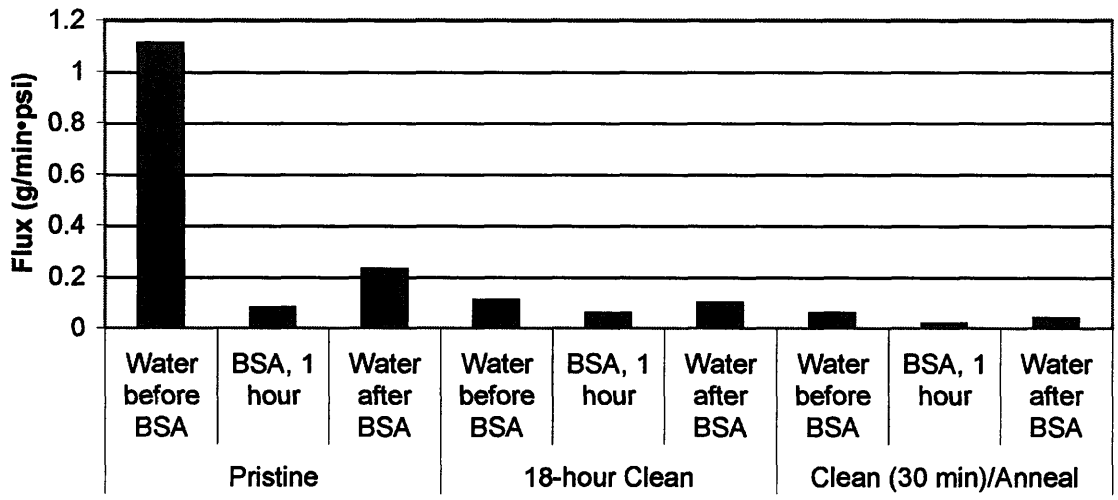

Figure 5.16. Flux behavior for Regeneration Filtration Trial 4
Similar to prior regeneration filtration trials, but in this trial, the "Clean" sample was exposed to Chromerge for 18 hours instead of 30 minutes. The BSA fouling solution was 0.1 mg/mL in PBS. Blend membrane F-040324 was used. Raw flux data is given in Figure D.4. The membrane had a filtration area of 4.1 cm^2.

It appears that the fouling recovery worsens slightly after 18 hour cleaning (which has previously been found to strip almost all the comb from the membrane surface), but it is still comparable to the recovery behavior of the PVDF control and of blend membranes cleaned for only 30 minutes in acid. Generally, the presence or absence of comb at the membrane surface does not appear to affect the fouling behavior of PVDF blend membranes. It is unclear why this is; more trials will be necessary to understand this behavior.

5.4. Summary

Overall, the results for the P(MMA-*r*-POEM)/PVDF blend membranes are encouraging. The amount of comb at the surface of a 10 wt% blend membrane is maximized during casting at elevated temperatures, and it is unnecessary to anneal longer to achieve maximal comb coverage, thus saving time during fabrication.

Also, the comb is resistant to damage by a weak cleaning agent (hydrogen peroxide), and it regenerates multiple times after cleaning with a harsh agent (Chromerge), even after extended periods of cleaning. Blend membranes can be expected to maintain their comb surface coverage after many rounds of routine cleaning and annealing in industry since most industrial cleaning solutions are milder than the concentrated Chromerge solution employed here.

In simple BSA adsorption experiments, pristine and annealed membranes generally showed better fouling resistance than cleaned membranes. However, preliminary filtration data does not indicate improved fouling resistance in flux trials, as compared to a PVDF control. It appears that blend membranes have improved flux, although it is not possible to directly compare the fluxes of the PVDF control and the blend membranes for a variety of reasons (different rejection coefficients, pre-wetting problems). It seems that more work will be needed to assess filtration performance.

Chapter 6. Results: P(MA-*r*-POEM)/PVDF Blend Membranes

6.1. Comb Properties

6.1.1. Gel Permeation Chromatography

The molecular weights obtained by GPC for the Pall P(MA-*r*-POEM) combs were somewhat consistent with those reported by Pall. Table 6.1 gives molecular weights based on PS standards.

Table 6.1. GPC Results for Pall P(MA-*r*-POEM) comb polymers
Molecular weights are based on PS standards.

Sample	M_w (g/mol, found by GPC)	M_w (g/mol, as reported by Pall)	PDI
Low MW comb	17,000	13,000	1.9
High MW comb	51,000	50,000 – 60,000	2.0

6.1.2. CyQuant

During the cell affinity testing, the comb samples were compared to two standards: tissue culture polystyrene (TCPS), for which cells have a high affinity, and P(MMA-*r*-POEM) (DCPLB003), for which cells have a very low affinity. The results are shown in Table 6.2.

Table 6.2. CyQuant results for P(MA-*r*-POEM) combs and controls
Three samples were prepared for each sample type, and three runs were done per sample, giving a total of nine data points per sample type.

Sample Type	DNA Quantification (μg/mL DNA)
P(MMA-*r*-POEM) (negative control)	-0.006 ± 0.001
High MW P(MA-*r*-POEM) comb	0.062 ± 0.005
Low MW P(MA-*r*-POEM) comb	0.10 ± 0.02
TCPS (positive control)	0.15 ± 0.04

It seemed odd that the combs were almost as attractive to cells as the positive control (TCPS) was. One possible explanation is that the comb films dissolved in the cell medium (PBS) overnight. To test this hypothesis, comb films similar to those used in the CyQuant assay (roughly 10 nm thick, cast on silicon instead of glass) were soaked in PBS for ~18 hours, then compared via microscopy to films that had not been soaked. The results are shown in Figure 6.1.

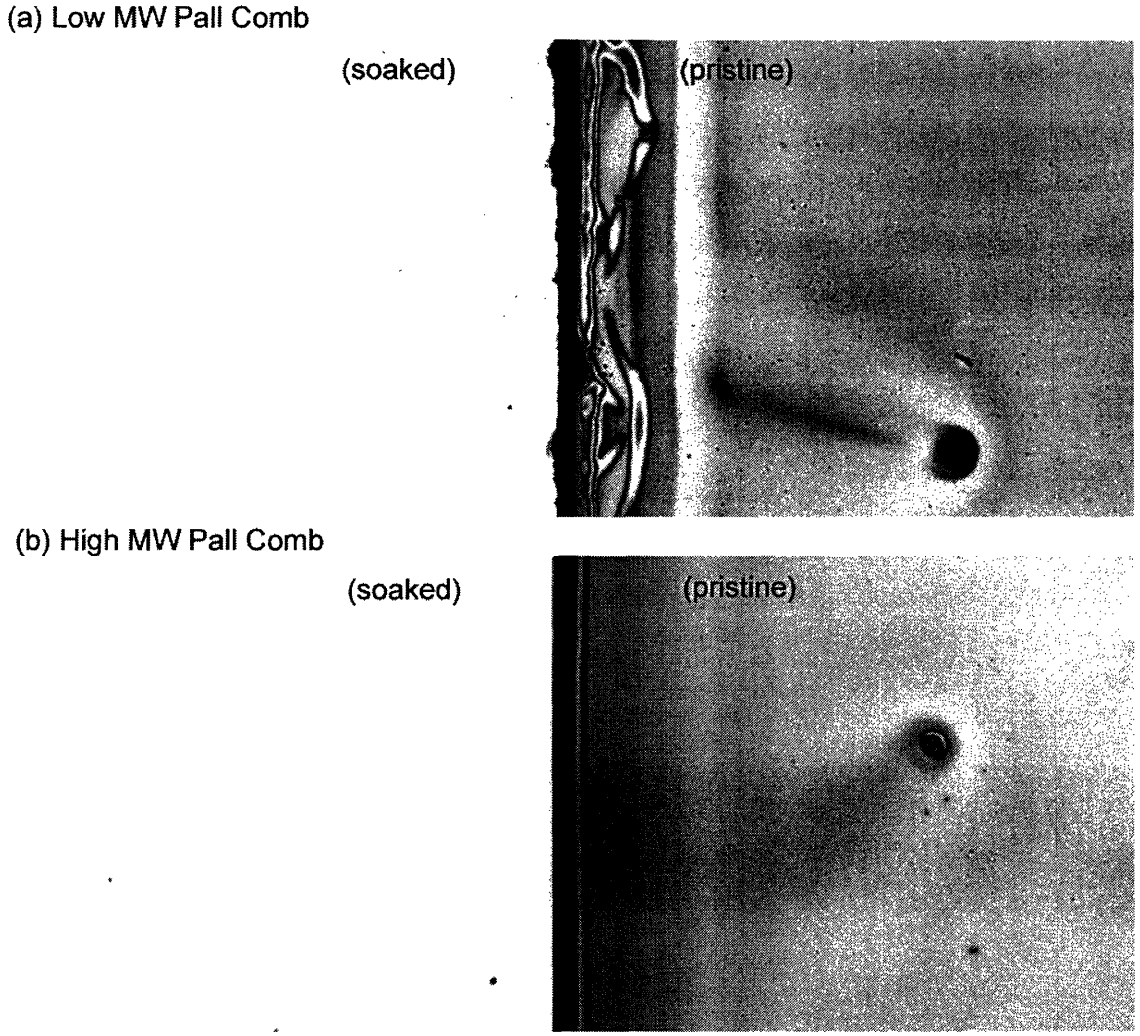

Figure 6.1. Comparison of soaked and pristine Pall comb films
(a) Low molecular weight Pall comb, (b) high molecular weight Pall comb. The images on the left are of the films after being soaked in PBS for approximately 18 hours. The images on the right are of the films as cast, without any treatment.

The left-hand images in Figure 6.1 (soaked films) appear to be bare silicon, while the right-hand images (pristine films) show common attributes of polymer films (dust "comets," color, and interference fringes at their edges). It appears that the comb films do indeed dissolve in PBS, and so the CyQuant results are not reliable, as the films did not stay intact during the assay.

6.1.3. X-ray Photoelectron Spectroscopy

The XPS spectra for the combs (details provided in Appendix E) look similar to each other and to the P(MMA-*r*-POEM) mentioned above. They both have a large C-O peak (from the PEO side chains) and smaller COO and C-COO peaks. Based on the values in Table E.1, there appear to be more PEO chains exposed at the surface of the high MW comb than the low MW comb, and/or more PEO in the high MW comb.

6.1.4. Nuclear Magnetic Resonance

The NMR spectra for the combs (reproduced in Appendix E) suggest that both combs are indeed P(MA-*r*-POEM), and that both were made with a POEM block with n = 9. The low MW comb polymer has 39 wt% POEM, and the high MW comb has 33.5 wt% POEM. Both of these values should be high enough to impart fouling resistance, according to Hester (his data suggest that combs with as little as 28 wt% POEM can achieve a surface coverage of 40% comb upon annealing and can maintain fouling resistance [9]).

6.1.5. Water solubility

The P(MA-*r*-POEM) swelled strongly when left in dW overnight and appeared to be moderately water soluble. A separate synthesis of P(MA-*r*-POEM) containing ~40 wt% POEM (by W. Kuhlman) also yielded a water-soluble polymer. It appears that substituting PMA for PMMA as the hydrophobic block causes a large change in the comb's water solubility, unfortunately. This reinforces the observation made in section 6.1.2 that the comb films dissolved in PBS solution overnight.

6.2. General Membrane Characteristics

Although analysis of the comb itself yielded unpromising results, it was still worthwhile to test the blend membranes. The membranes were characterized via high-resolution C

1s XPS to determine the amount of comb present at the surface before and after annealing in water at 90°C for 18 hours. The results are given in Table 6.3.

Table 6.3. Volume fraction of near-surface comb for Pall membranes

	Volume fraction of comb at surface (ϕ_s)	
Membrane	*Pristine*	*Annealed*
Pall 1	0.30	0.35
Pall 2	0.17	0.24

Previous research [9] has found that membranes with $\phi_s \geq 0.3$ should be protein-resistant. However, since the combs were found to be water soluble, it might be expected that a membrane with more comb surface coverage would have that comb more quickly washed away in solution, leading to increased fouling. Based on this hypothesis, Pall 1 might be expected to foul more than Pall 2, which was indeed found to be the case in filtration experiments (Section 6.3). It is also interesting to note that for both membranes, annealing brought slightly more comb to the surface, but instead of performing better, annealed membranes fouled more than the pristine membranes. This is also consistent with the hypothesis that a membrane with more comb at its surface would have that comb washed away more quickly and would foul more.

6.3. Dead-End Fouling of Membranes

Filtration trials were conducted for both Pall membranes. As can be seen from SEM images of their surfaces and cross-sections (Figure 6.2), they had a rather dense, symmetric structure throughout, but their surfaces had pores of acceptable size and morphology for filtration. SEM images are also given for the control membranes provided by Pall (Figure 6.3). *Ungrafted PVDF* was a plain PVDF membrane, and *grafted PVDF* was a PVDF membrane surface-grafted with a hydroxy ethyl methacrylate polymer.

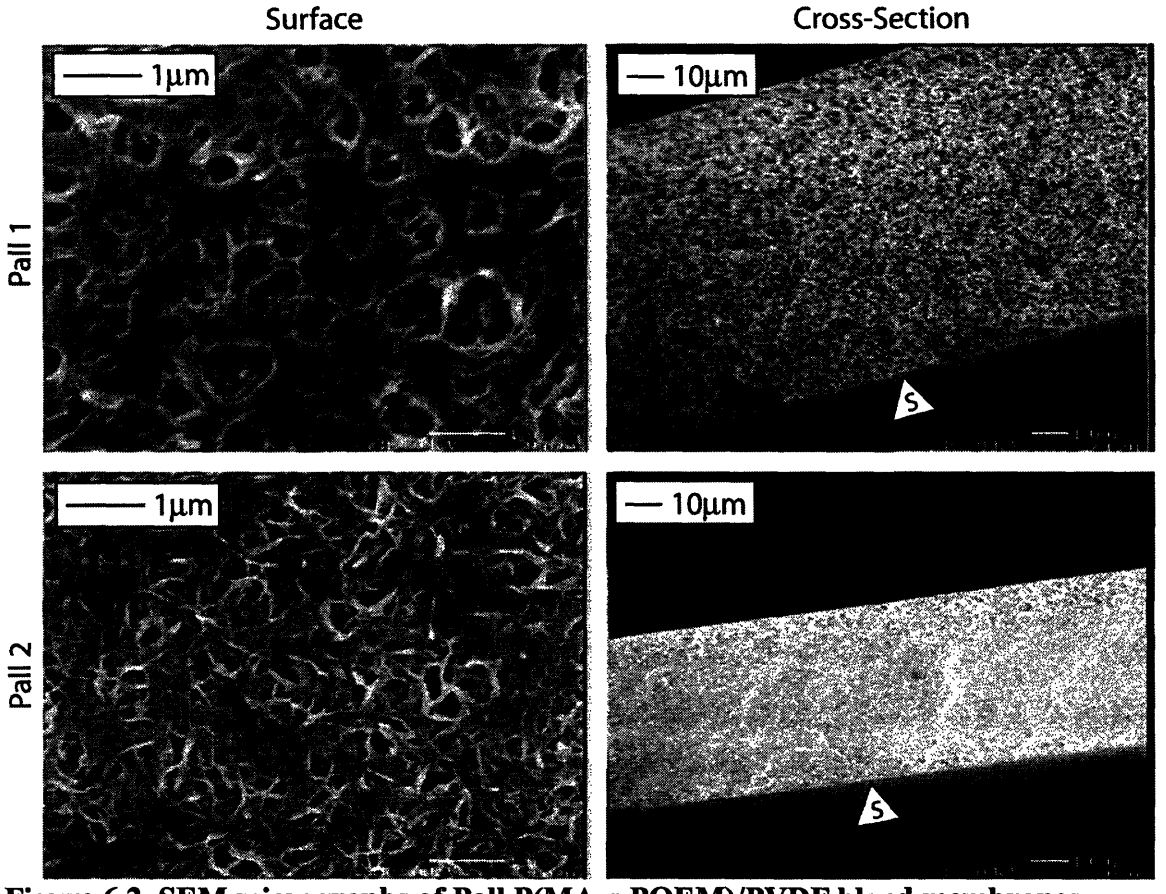

Figure 6.2. SEM micrographs of Pall P(MA-*r*-POEM)/PVDF blend membranes
Surface images are at 20,000x, and cross-section images are at 1000x magnification. The separation surface is marked in the cross-section micrographs. The left-hand scale bars are 1 micron, and the right-hand scale bars are 10 microns.

Typically, PVDF membranes have a lower surface porosity than that of Pall 1, but the ungrafted PVDF provided by Pall appears to have equal or greater surface porosity than Pall 1. However, the cross-sections of both PVDF controls show that the membrane interiors are less porous than that of Pall 1 (this is probably due to the porosity imparted by the comb additive during casting for the blend membranes). Based on the SEM micrographs of the Pall blend and control membranes, it seems that both controls would be acceptable for comparison to Pall 1. Pall 2, however, has smaller pores and is thinner, so it would be expected to behave differently than the controls.

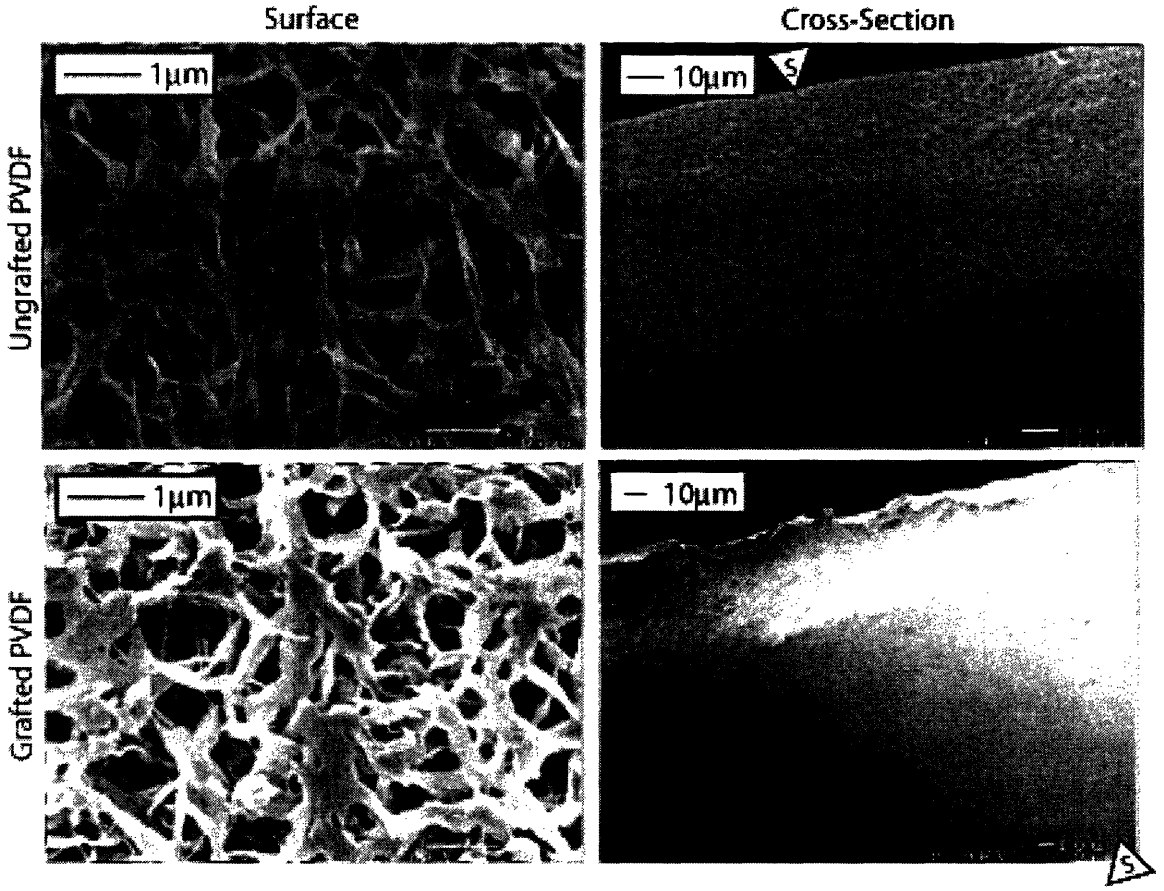

Figure 6.3. SEM micrographs of Pall control membranes
Surface images are at 20,000x, and cross-section images are at 1000x magnification (ungrafted PVDF) and 450x magnification (grafted PVDF). The ungrafted PVDF membrane's separation surface is marked in the cross-section image. The grafted membrane's separation surface is not shown in its micrograph, but the general location is marked. Left-hand scale bars are 1 micron; right-hand scale bars are 10 microns.

6.3.1. Flux Behavior

Filtration experiments were conducted as described in sections 3.4.2 and 4.4.1, using BSA and oil/water fouling solutions separately. The results are shown in Figures 6.4 and 6.5. Pall 2 membranes had much lower fluxes than Pall 1 membranes, probably because of the former's small pores and dense structure. This is not due to any pre-wetting problems, as Pall 2 gave the same initial flux when pre-wet with methanol instead of water.

(a) Pall 1, Pristine

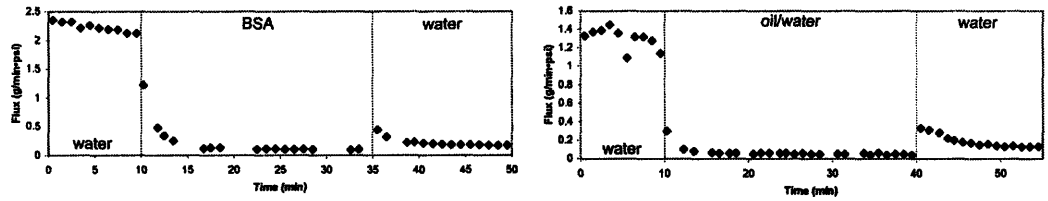

(b) Pall 1, Annealed

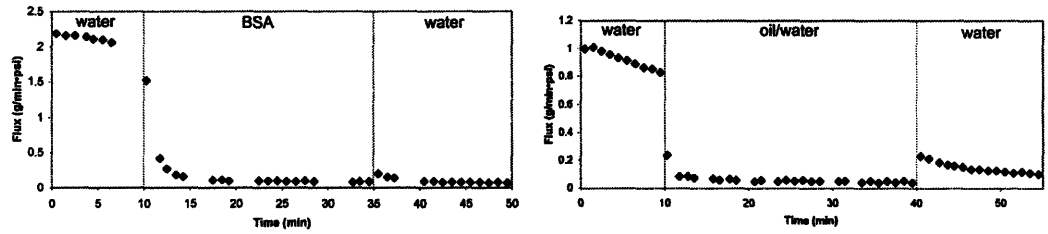

(c) Ungrafted PVDF

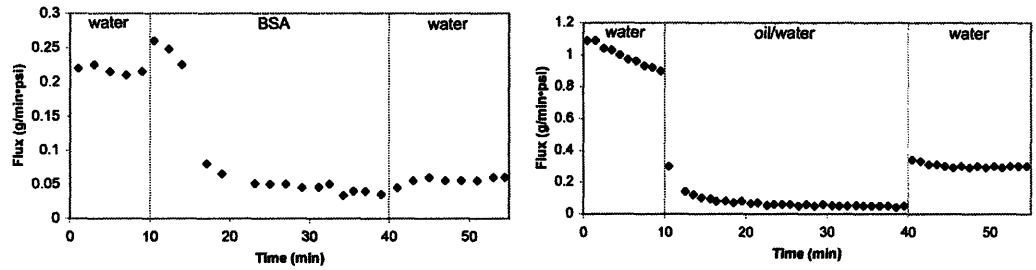

(d) Grafted PVDF

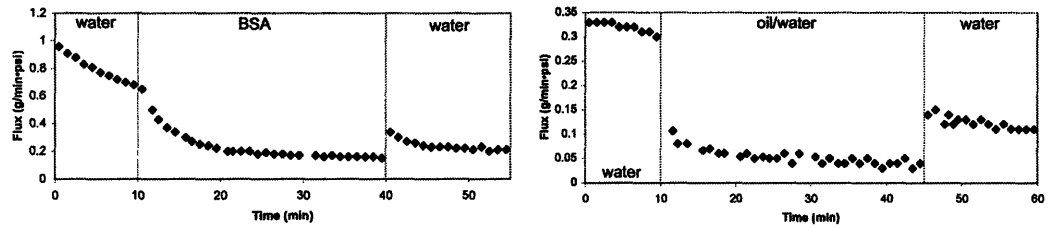

Figure 6.4. Flux data for Pall 1 and control membranes
(a) Pristine Pall 1, (b) Annealed Pall 1, (c) Ungrafted PVDF, (d) Grafted PVDF. Left-hand plots are for fouling with 1 mg/mL BSA, and right-hand plots are for fouling with oil/water. All data was collected at 10 psi. Pall 1 and grafted PVDF membranes were pre-wet with water, and ungrafted PVDF was pre-wet with methanol. The membranes had a filtration area of 4.1 cm^2.

(a) Pall 2, Pristine

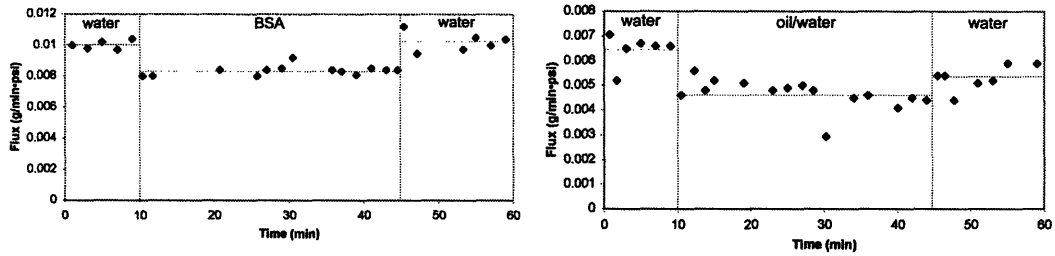

(b) Pall 2, Annealed

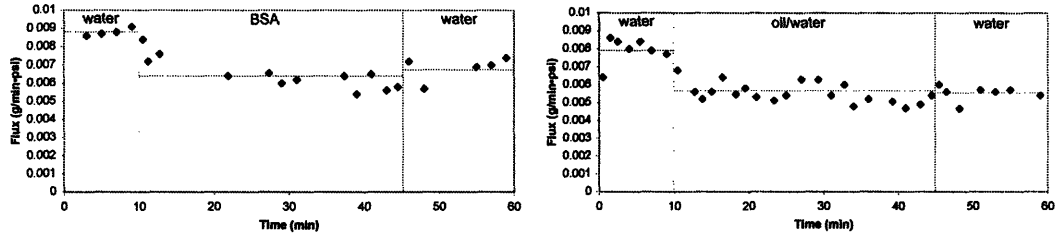

Figure 6.5. Flux data for Pall 2 membranes
(a) Pristine Pall 2, (b) Annealed Pall 2. Average flux values are marked with horizontal lines. Left-hand plots are for fouling with 1 mg/mL BSA, and right-hand plots are for fouling with oil/water. Data was collected at 50 psi. The membranes had a filtration area of 4.1 cm^2.

For both fouling solutions (BSA and oil/water), Pall 1 exhibited a significant decrease in flux and poor fouling recovery. The annealed sample of Pall 1 (annealed for 18 hours in 90°C water) had even worse fouling recovery. Pall 2 showed some flux decline, but near complete recovery. In fact, the small decrease in flux with the introduction of the fouling solution for pristine Pall 2 could have been due to a change in solution viscosity or to concentration polarization, instead of actual adsorption of foulant to the membrane surface and pores. Much like the annealed Pall 1 sample, the annealed Pall 2 sample exhibited incomplete fouling recovery. As noted in Section 6.2, it appears that the more comb a membrane has at its surface, the less it is able to recover from fouling.

If the filtration properties of Pall 1 are compared to the control membranes provided by Pall (ungrafted PVDF and grafted PVDF), it appears that the grafted PVDF membrane has better fouling recovery. In oil/water experiments, for example, the grafted PVDF returns to 31% of its initial flux with reintroduction of water as the feed solution, whereas Pall 1 only returns to 25% of its initial flux. Ungrafted PVDF has different fouling recovery abilities depending on the foulant used. For both foulants, the grafted PVDF

outperforms the ungrafted PVDF and blend membranes. But this is understandable, as it appears that the comb does not remain at the surface of the blend membranes but washes away during filtration.

As a supplement to the flux data given in Figures 6.4 and 6.5, XPS was done on fouled Pall 1 and 2 membranes. Table 6.4 compares the percentage of nitrogen at the membrane surfaces before and after running BSA through the membranes.

Table 6.4. Extent of BSA fouling for annealed and pristine Pall membranes

	% Nitrogen via XPS			
	Pristine		*Annealed*	
Membrane	**Before fouling**	**After fouling**	**Before fouling**	**After fouling**
Pall 1	0	5.8	0	7.1
Pall 2	0	0.8	0	2.6

As expected, prior to fouling with BSA, no nitrogen is detected on the membrane surfaces. After BSA filtration, it appears that Pall 1 fouled significantly more than Pall 2, and annealed membranes fouled more than pristine. These results agree with the flux behavior shown in Figures 6.4 and 6.5. This again supports the observation that fouling increases with the amount of comb present at the membrane surface.

6.3.2 Permeate Composition

Membrane rejection coefficients are given in Table 6.5. Rejection coefficients are calculated as follows (where $C_{foulant}$ is the concentration of the foulant):

$$R_{foulant} = 1 - \frac{C_{foulant}^{permeate}}{C_{foulant}^{feed}} \tag{6.1}$$

For both types of fouling solutions, Pall 2 exhibited higher rejection than Pall 1. This is most likely due to Pall 2's smaller pores. Additionally, the annealed membranes rejected more foulant (BSA or oil) than non-annealed. The best rejection was obtained using an annealed Pall 2 membrane, which rejected at least 99.5% of the oil in the feed solution and 90% of BSA, but which had very low flux.

Table 6.5. Rejection coefficients for Pall membranes
Determined using concentration values for the permeate sample collected after 20 minutes. A rejection coefficient of 1.0 is desirable, as it means that no foulant passes through the membrane.

	Rejection Coefficient (R)	
Sample	*BSA*	*Oil/Water*
Pall 1, Pristine	0.3	~ 0.987
Pall 1, Annealed	0.4	> 0.992
Ungrafted PVDF	1.0	> 0.992
Grafted PVDF	0.0	> 0.992
Pall 2, Pristine	0.55	> 0.992
Pall 2, Annealed	0.9	> 0.995

6.4. BCA Assay (Protein Affinity)

The data obtained from the BCA assay on Pall 1, Pall 2, and the ungrafted PVDF membrane are given in Table 6.6. As expected, Pall 1 and Pall 2 are no more protein-resistant than normal PVDF is, and the P(MA-*r*-POEM) blend membranes may even have more protein affinity than normal PVDF does. Due to variations in membrane surface area, these results cannot be compared directly to each other, but they support the data found in the CyQuant comb trial, which suggested that the combs dissolve during experiments involving aqueous media, leaving plain PVDF behind.

Table 6.6. BCA assay results for Pall membranes and PVDF control
Nine runs were conducted for each sample and the results averaged.

Sample Type	Protein Stain Concentration (μg/mL)
Pall 1	6 ± 1
Pall 2	6.1 ± 0.2
Ungrafted PVDF	4 ± 1

6.5. Summary

It appears that the P(MA-*r*-POEM) combs used in the experimental Pall blend membranes were water soluble and dissolved during aqueous filtration experiments and other characterization attempts. This is shown by the fact that comb films dissolve in PBS, as well as by the lack of fouling resistance observed for the membranes. The P(MA-*r*-POEM) provided by Pall is water-soluble, so it is unsuitable for use as an additive in water filtration membranes that need to be used repeatedly or for extended periods. If a water insoluble P(MA-*r*-POEM) additive could be synthesized, it could be used to impart lasting wettability and fouling resistance to PVDF membranes.

The combs imparted improved wettability to the PVDF membranes, despite their water solubility. The reduced manufacturing cost obtained by using comb additives would be desirable for manufacturing membranes for single-use applications, where water stability of the combs is less of a concern.

Chapter 7. Conclusions and Future Work

7.1. Regeneration of P(MMA-*r*-POEM)/PVDF Blend Membranes

Membranes containing roughly 10 wt% of P(MMA-*r*-POEM) blended with PVDF show promise for industrial application. They attain maximal comb surface coverage upon casting at elevated temperature. These blend membranes do not seem to be adversely affected by cleaning with warm hydrogen peroxide. Additionally, the self-segregating PEO comb surface layer provides fouling resistance and can be regenerated by a simple annealing step following harsh acid cleaning with Chromerge. Multiple regenerations were observed for filtration-series blend membranes whose surfaces were completely stripped of comb after each cleaning step. The amount of comb restored to the surface decreased each time, but this is probably due to the fact that after each cleaning step, comb has to travel farther to reach the surface, so longer annealing times are required. It was found that there is enough comb in the membrane bulk to give nearly 60 rounds of regeneration, so the gradual decrease in comb coverage over time is not due to lack of comb in the bulk. Despite the limitations to full recovery after multiple rounds of cleaning and annealing, the results suggest that blend membranes made with P(MMA-*r*-POEM) additive can maintain a higher throughput and be used for longer periods of time than other hydrophilically-modified filtration membranes.

Although both types of membranes exhibited comb and PEO surface regeneration, the S-series membrane (which was thicker than the F-series membranes) gave better fouling recovery than the F-series membranes. It would be useful to fabricate and study F-series membranes that are either cast thicker than 8 mils or contain a comb additive with a different molecular weight and/or composition. This might lead to filtration membranes that not only have improved flux but can also recover from fouling better than PVDF alone.

7.2. Properties of P(MA-*r*-POEM)/PVDF Blend Membranes

P(MA-*r*-POEM) was examined as a more wettable alternative to P(MMA-*r*-POEM). The P(MA-*r*-POEM) appeared to be water soluble and consequently did not impart fouling resistance to membranes--behavior which is not desirable in a comb additive. Lack of fouling resistance for Pall 1 and annealed membranes appeared linked to comb dissolution into the surrounding aqueous medium. It is believed that membranes with more comb at their surface are more prone to comb dissolution into solution, giving less fouling resistance. This would explain why the pristine Pall 2 membrane (which had the least comb surface coverage) exhibited complete fouling recovery in a BSA filtration and considerable recovery when fouled with an oil/water solution. On the other hand, Pall 1 and annealed membranes, which had more comb at their surfaces, had poor fouling recovery. It is worthwhile to note that all PVDF blend membranes had high porosity and wettability, as well as excellent rejection coefficients. These properties make them promising for single-use applications.

Since P(MA-*r*-POEM) was observed to make blend membranes more wettable than PVDF alone, it could certainly be useful. Once a water insoluble version of this additive is synthesized, it could lead to membranes that are both highly wettable and fouling-resistant, which could be used for applications requiring long-term operation. More research is needed to determine the ideal composition for this additive.

List of Symbols and Acronyms

BCA.....Bicinchoninic Acid

BET.....Brunauer-Emmett-Teller

BSA.....Bovine Serum Albumin

CSA/Chromerge.....Chromic-Sulfuric Acid

d-$CHCl_3$.....Deuterated Chloroform

DMAc.....N,N Dimethylacetamide

DMF.....Dimethyl Formamide

dW.....Deionized Water

GPC.....Gel Permeation Chromatography

MF.....Microfiltration

NMP.....N-Methyl Pyrrolidone

NMR.....Nuclear Magnetic Resonance

PBS.....Phosphate-Buffered Saline

PDI.....Polydispersity Index

PEO.....Poly (ethylene oxide)

POEM.....Poly (oxyethylene methacrylate)

PMA.....Poly (methyl acrylate)

PMMA.....Poly (methyl methacrylate)

PS.....Poly (styrene)

PVDF.....Poly (vinylidene fluoride)

RO.....Reverse Osmosis

SEM.....Scanning Electron Microscopy

TCPS.....Tissue Culture Polystyrene

THF.....Tetrahydrofuran

UF.....Ultrafiltration

UV.....Ultraviolet

XPS.....X-Ray Photoelectron Spectroscopy

Bibliography

1. Aptel, P.; "Membrane Pressure Driven Processes in Water Treatment;" *Membrane Processes in Separation and Purification*; J.G. Crespo and K.W. Boddeker, Ed.; Kluwer Academic Publishers: Dordrecht, The Netherlands, 1994, pp 263 - 281.
2. Postel, S.; "Dividing the Water;" *Technology Review* **1997**, *4*, 54-62.
3. Postel, S.L.; Daily, G.C.; Ehrlich, P.R.; "Human Appropriation of Renewable Fresh Water;" *Science* **1996**, *271*, 785-788.
4. Brennan, Mairin B.; "Waterworks;" *Chemical and Engineering News* **2001**, *79*, 32-38.
5. Baker, R.W.; "Membrane Technology;" *Encyclopedia of Separation Technology vol. 2*; D.M. Ruthven, Ed.; Wiley: New York, 1997, pp 1212-1270.
6. Caetano, A.T.; "Existing Industrial Membrane Applications;" *Membrane Technology: Applications to Industrial Wastewater Treatment*; A.T. Caetano, M.N. DePinho, E. Drioli, and H. Muntau, Ed.; Kluwer Academic Publishers: Dordrecht, The Netherlands, 1995, pp 47-62.
7. Strathmann, H.; "Synthetic Membranes and their Preparation;" *Synthetic Membranes: Science, Engineering, and Applications*; P.M. Bungay, H.K. Lonsdale, and M.N. de Pinho, Eds.; Kluwer Academic Publishers: Dordrecht; Boston, 1983, pp 1-37.
8. Moeckel, D.; Staude, E.; and M.D. Guiver; "Static Protein Adsorption, Ultrafiltration Behavior, and Cleanability of Hydrophilized Polysulfone Membranes;" *Journal of Membrane Science* **1999**, *158*, 63-75.
9. Hester, J.F.; *Surface Modification of Polymer Membranes by Self-Organization*, MIT Thesis, Cambridge, 2001.
10. Hester, J.F.; Banerjee, P.; and A.M. Mayes; "Preparation of Protein-Resistant Surfaces on Poly(vinylidene fluoride) Membranes via Surface Segregation;" *Macromolecules* **1999**, *32*, 1643-1650.
11. Kesting, R.E.; *Synthetic Polymer Membranes*; McGraw-Hill Book Company: New York, 1971.
12. Mulder, M.; *Basic Principles of Membrane Technology*; Kluwer Academic Publishers: Dordrecht; Boston, 1996.
13. Eykamp, W.; "Microfiltration and Ultrafiltration;" *Membrane Separations Technology, Principles and Applications*; R.D. Noble and S.A. Stern Eds.; Elsevier: Amsterdam; New York, 1995, pp 1-43.
14. Belfer, S.; Purinson, Y.; and O. Kedem; "Surface Modification of Commercial Polyamide Reverse Osmosis Membranes by Radical Grafting: an ATR-FTIR Study;" *Acta Polymerica* **1998**, *49*, 574-582.

15. Stengaard, F.F.; "Preparation of Asymmetric Microfiltration Membranes and Modification of their Properties by Chemical Treatment;" *Journal of Membrane Science* **1988**, *36*, 257-275.

16. Brandt, D.C.; Leitner, G.F.; and W.E. Leitner; "Reverse Osmosis Membranes State of the Art;" *Reverse Osmosis: Membrane Technology, Water Chemistry, and Industrial Applications*; Z. Amjad, Ed.; Van Nostrand Reinhold: New York, 1992, pp 1-35.

17. Mulder, M.; "The Use of Membrane Processes in Environmental Problems;" *Membrane Processes in Separation and Purification*; J.G. Crespo and K.W. Boddeker, Ed.; Kluwer Academic Publishers: Dordrecht, The Netherlands, 1994, pp 229-262.

18. Klie, J. and J. Daly; "Advanced wastewater treatment for marine vessels;" *Filtration and Separation* **2002**, *39*, 32-35.

19. Zhang, G.J. and Z.Z. Liu; "Membrane Fouling and Cleaning in Ultrafiltration of Wastewater from Banknote Printing Works;" *Journal of Membrane Science* **2003**, *211*, 235-249.

20. de Bruijn J.; Venegas A.; and R. Borquez; "Influence of crossflow ultrafiltration on membrane fouling and apple juice quality;" *Desalination* **2002**, *148*, 131-136.

21. Mohammadi, T.; Madaeni, S.S.; and M.K. Moghadam; "Investigation of Membrane Fouling;" *Desalination* **2003**, *153*, 155-160.

22. Osada, Y. and Y. Takeuchi; "Protein and Sugar Separation by Mechanochemical Membrane Having Chemical Valve Function;" *Polymer Journal* **1983**, *15*, 279-284.

23. Van Der Horst, H.C. and J.H. Hanemaaijer; "Cross Flow Microfiltration in the Food Industry: State of the Art;" *Desalination* **1990**, *77*, 235-258.

24. Mika, A.M.; Childs, R.F.; and J.M. Dickson; "Salt separation and hydrodynamic permeability of a porous membrane filled with pH-sensitive gel;" *Journal of Membrane Science* **2002**, *206*, 19-30.

25. Ishihara, K.; Kobayashi, M.; Ishimaru, N.; and I. Shinohara; "Glucose Induced Permeation Control of Insulin through a Complex Membrane Consisting of Immobilized Glucose Oxidase and a Polyamine;" *Polymer Journal* **1984**, *16*, 625-631.

26. Okahata, Y.; Noguchi, H.; and T. Seki; "Functional Capsule Membranes: Part 26. Permeability Control of Polymer-grafted Capsule Membranes Responding to Ambient pH Changes;" *Macromolecules* **1987**, *20*, 15-21.

27. Hautojarvi, J.; Kontturi, K.; Nasman, J.H.; Svarfvar, B.L.; Viinikka, P.; and M. Vuoristo; "Characterization of Graft-modified Porous Polymer Membranes;" *Industrial and Engineering Chemistry* **1996**, *35*, 450-457.

28. Ito, Y.; Ochiai, Y.; Park, Y.S.; and Y. Imanishi; "pH-sensitive Gating by Conformational Change of a Polypeptide Brush Grafted onto a Porous Polymer Membrane;" *Journal of American Chemical Society* **1997**, *119*, 1619-1623.

29. Iwata, H.; Hirata, I.; and Y. Ikada; "Atomic Force Microscopic Analysis of a Porous Membrane with pH-sensitive Molecular Valves;" *Macromolecules* **1998**, *31*, 3671-3678.

30. Mika, A.M.; Childs, R.F.; and J.M. Dickson; "Chemical Valves Based on Poly(4-vinylpyridine)-filled Microporous Membranes;" *Journal of Membrane Science* **1999**, *153*, 45-56.

31. Okahata, Y.; Ozaki, K.; and T. Seki; "pH-Sensitive Permeability Control of Polymer-grafted Nylon Capsule Membranes;" *Journal of the Chemical Society, Chemical Communications* **1984**, *8*, 519-521.

32. Ying, L.; Wang, P.; Kang, E.T.; and K.G. Neoh; "Synthesis and Characterization of Poly(acrylic acid)-graft-poly(vinylidene fluoride) Copolymers and pH-Sensitive Membranes;" *Macromolecules* **2002**, *35*, 673-679.

33. Belfort, G.; Davis, R.H.; and A.L. Zydney; "The Behavior of Suspensions and Macromolecular Solutions in Crossflow Microfiltration;" *Journal of Membrane Science* **1994**, *96*, 1-58.

34. Cheryan, M. and J.R. Alvarez; "Food and Beverage Industry Applications;" *Membrane Separations Technology : Principles and Applications*; R.D. Noble and S.A. Stern Eds.; Elsevier: Amsterdam; New York, 1995.

35. Strathmann, H. and K. Kock; "The Formation Mechanism of Phase Inversion Membranes;" *Desalination* **1977**, *21*, 241-255.

36. Baker, R.W. *Membrane Technology and Applications*; McGraw-Hill: New York, 2000.

37. Howe, K.J. and M.M. Clark; "Fouling of Microfiltration and Ultrafiltration Membranes by Natural Waters;" *Environmental Science and Technology* **2002**, *36*, 3571-3576.

38. Fane, A.G. and C.J.D. Fell; "A Review of Fouling and Fouling Control in Ultrafiltration;" *Desalination* **1987**, *62*, 117-136.

39. Marshall, A.D.; Munro, P.A.; and G. Tragardh; "The Effect of Protein Fouling in Microfiltration and Ultrafiltration on Permeate Flux, Protein Retention, and Selectivity: A Literature Review;" *Desalination* **1993**, *91*, 65-108.

40. Sheldon, J.M.; Reed, I.M.; and C.R. Hawes; "The Fine-Structure of Ultrafiltration Membranes. II. Protein Fouled Membranes;" *Journal of Membrane Science* **1991**, *62*, 87-102.

41. Ho, C.C. and A.L. Zydney; "Effect of Membrane Morphology on the Initial Rate of Protein Fouling During Microfiltration;" *Journal of Membrane Science* **1999**, *155*, 261-275.

42. Fane, A.G.; Fell, C.J.D.; and K.J. Kim; "The Effect of Surfactant Pretreatment on the Ultrafiltration of Proteins;" *Desalination* **1985**, *53*, 37-55.

43. Koehler, J.A.; Ulbricht, M.; and G. Belfort; "Intermolecular Forces between a Protein and a Hydrophilic Modified Polysulfone Film with Relevance to Filtration;" *Langmuir* **2000**, *16*, 10419-10427.

44. Munari, S.; Bottino, A.; and G. Capannelli; "Casting and Performance of PVDF Based Membranes;" *Journal of Membrane Science* **1983**, *16*, 181-193.

45. Nabe, A.; Staude, E.; and G. Belfort; "Surface Modification of Polysulfone Membranes and Fouling by BSA Solutions;" *Journal of Membrane Science* **1997**, *133*, 57-72.

46. Akhtar, S.; Hawes, C.; Dudley, L.; Reed, I.; and P. Stratford; "Coatings Reduce the Fouling of Microfiltration Membranes;" *Journal of Membrane Science* **1995**, *107*, 209-218.

47. Chen, H. and G. Belfort; "Surface Modification of Poly(ether sulfone) Ultrafiltration Membranes by Low-Temperature Plasma-Induced Graft Polymerization;" *Journal of Applied Polymer Science* **1999**, *72*, 1699-1711.

48. Ellinghorst, G.; Niemoeller, A.; and D. Vierkotten; "Radiation Initiated Grafting of Polymer Films - An Alternative Technique to Prepare Membranes for Various Separation Problems;" *Radiation Physics and Chemistry* **1983**, *22*, 635-642.

49. Iwata, H.; Ivanchenko, M.; and Y. Miyaki; "Preparation of Anti-Oil Stained Membrane by Grafting Polyethylene Glycol Macromer onto Polysulfone Membrane;" *Journal of Applied Polymer Science* **1994**, *54*, 125-128.

50. Kanamori, T.; Sakai, K.; Fukuda, M.; and Y. Yamashita; "Preferable Structure of Poly(ethylene glycol) for Grafting onto a Cellulosic Membrane to Increase Hemocompatibility Without Reduction in Solute Permeability of the Membrane;" *Journal of Applied Polymer Science* **1995**, *55*, 1601-1605.

51. Kramer, P.W.; Yeh, Y.-S.; and H. Yasuda; "Low Temperature Plasma for the Preparation of Separation Membranes;" *Journal of Membrane Science* **1989**, *46*, 1-28.

52. Mok, S.; Worsfold, D.J.; Fouda, A.; and T. Matsuura; "Surface Modification of Polyethersulfone Hollow-Fiber Membranes by Gamma-Ray Irradiation;" *Journal of Applied Polymer Science* **1994**, *51*, 193-199.

53. Nie, F.-Q.; Xu, Z.-K.; Huang, X.-J.; Ye, P.; and J. Wu; "Acrylonitrile-based copolymer membranes containing reactive groups: Surface modification by the immobilization of poly(ethylene glycol) for improving antifouling property and biocompatibility;" *Langmuir* **2003**, *19*, 9889-9895.

54. Pieracci, J.; Crivello, J.V.; and G. Belfort; "Photochemical Modification of 10 kDa Polyethersulfone Ultrafiltration Membranes for Reduction of Biofouling;" *Journal of Membrane Science* **1999**, *156*, 223-240.

55. Ulbricht, M.; Matuschewski, H.; Oechel, A.; and H.G. Hicke; "Photo-induced Graft Polymerization Surface Modifications for the Preparation of Hydrophilic Low-Protein-Adsorbing Ultrafiltration Membranes;" *Journal of Membrane Science* **1996**, *115*, 31-47.

56. Yamagishi, H.; Crivello, J.V.; and J. Belfort; "Development of a Novel Photochemical Technique for Modifying Poly(arylsulfone) Ultrafiltration Membranes;" *Journal of Membrane Science* **1995**, *105*, 237-247.

57. Nunes, S.P.; Sforca, M.L.; and K.V. Peinemann; "Dense Hydrophilic Composite Membranes for Ultrafiltration;" *Journal of Membrane Science* **1995**, *106*, 49-56.

58. Brink, L.E.S.; Elbers, S.J.G.; Robbertsen, T.; and P. Both; "The Anti-Fouling Action of Polymers Preadsorbed on Ultrafiltration and Microfiltration Membranes;" *Journal of Membrane Science* **1993**, *76*, 281-291.

59. Nunes, S.P. and K.V. Peinemann; "Ultrafiltration Membranes from PVDF/PMMA Blends;" *Journal of Membrane Science* **1992**, *73*, 25-35.

60. Ye, S.H.; Watanabe, J.; Iwasaki, Y.; and K. Ishihara; "Antifouling Blood Purification Membrane Composed of Cellulose Acetate and Phospholipid Polymer;" *Biomaterials* **2003**, *24*, 4143-4152.

61. Klinkowski, P.R.; "Ultrafiltration;" *Encyclopedia of Separation Technology vol. 2*; D.M. Ruthven, Ed.; Wiley: New York, 1997, pp 1570-1591.

62. Irvine, D.J.; Ruzette, A.V.G.; Mayes, A.M.; and L.G. Griffith; "Nanoscale Clustering of RGD Peptides at Surfaces using Comb Polymers. Part 2: Surface Segregation of Comb Polymers in Polylactide;" *Biomacromolecules* **2001**, *2*, 545-556.

63. Hester, J.F.; Olugebefola, S.C.; and A.M. Mayes; "Preparation of pH-responsive Polymer Membranes by Self-Organization;" *Journal of Membrane Science* **2002**, *208*, 375-388.

64. Akthakul, A.; *Design of Chemistry and Morphology of Polymer Filtration Membranes*, MIT Thesis, Cambridge, 2003.

65. Bernstein, R.E.; Cruz, C.A.; Paul, D.R.; and J.W. Barlow; "LCST Behavior in Polymer Blends;" *Macromolecules* **1977**, *10*, 681-686.

66. Chan, C.-M.; "X-Ray Photoelectron Spectroscopy;" *Polymer Surface Modification and Characterization*; Hanser Publishers: Munich, Germany, 1994, pp 77-152.

67. Sing, K.; "The Use of Nitrogen Adsorption for the Characterization of Porous Materials;" *Colloid Surface A* **2001**, *187*, 3-9.

68. Hester, J.F.; A.M. Mayes; "Design and Performance of Foul-Resistant Poly(vinylidene fluoride) Membranes Prepared in a Single-Step by Surface Segregation;" *Journal of Membrane Science* **2002**, *202*, 119-135.

69. Walton, D.G.; Soo, P.P.; Mayes, A.M.; Sofia Allgor, S.J.; Fujii, J.T.; Griffith, L.G.; Ankner, J.F.; Kaiser, H.; Johansson, J.; Smith, G.D.; Barker, J.G. and S.K. Satija; "Creation of Stable Poly(ethylene oxide) Surfaces on Poly(methyl methacrylate) Using Blends of Branched and Linear Polymers;" *Macromolecules* **1997**, *30*, 6947-6956.

70. Ramamoorthy, M. and M. Ulbricht; "Molecular Imprinting of Cellulose Acetate-Sulfonated Polysulfone Blend Membranes for Rhodamine B by Phase Inversion Technique;" *Journal of Membrane Science* **2003**, *217*, 207-214.

71. Chen, Z.A.; Deng, M.C.; Yong C.; He, G.H.; Ming, W. and J.D. Wang; "Preparation and Performance of Cellulose Acetate/Polyethyleneimine Blend Microfiltration Membranes and their Applications;" *Journal of Membrane Science* **2004**, *235*, 73-86.

72. Avramescu, M.E.; Sager, W.F.C. and M. Wessling; "Functionalised Ethylene Vinyl Alcohol Copolymer (EVAL) Membranes for Affinity Protein Separation;" *Journal of Membrane Science* **2003**, *216*, 177-193.

73. Avramescu, M.E.; Sager, W.F.C.; Mulder, M.H.V. and M. Wessling; "Preparation of Ethylene Vinylacohol Copolymer Membranes Suitable for Ligand Coupling in Affinity Separation;" *Journal of Membrane Science* **2002**, *210*, 155-173.

Appendix A: General Approach to Analysis of XPS Spectra

A.1. Data Collection

For all samples, unless otherwise noted, at least two types of XPS spectra were collected: (1) an elemental survey, (2) a high-resolution carbon 1s spectrum. Examples of these are shown in Figures 3.1 and 3.2.

A.2. Peak-Fitting

The survey spectra were fitted using the software on the XPS itself, and the raw area of the nitrogen peak was determined. The high-resolution spectra were deconvoluted using CasaXPS fitting software. The comb C 1s spectrum has four peaks, and the PVDF has two peaks, constrained as described below.

Table A.1. Constraints imposed on comb/PVDF constituent peaks during fitting
All peaks were constrained to a full width at half maximum (FWHM) between 0.9 and 1.2.

Peak ID	Species	Position	Area
A	COO (comb)	Unconstrained	Unconstrained
B	C-O (comb)	Between A-2.2 and A-2.6	Unconstrained
C	C-COO (comb)	A-3.3	Unconstrained
D	CH (comb/pump oil)	A-4.0	Unconstrained
E	CF_2 (PVDF)	Unconstrained	Unconstrained
F	CH_2 (PVDF)	E-4.5	E*1

The peaks, as defined above, were moved to approximately the correct position in the spectrum, and the Fit Components button was used until the fit no longer changed appreciably. The position was then calibrated, using the CH peak as a reference, set to 285 eV. For PVDF spectra alone, the position was calibrated using the CF_2 peak (which has a position of 290.9 eV for pure PVDF).

A.3. Determination of Fraction of Comb at Surface

A sample calculation for determining the volume fraction of comb at the surface is given below (A_X is the area of peak X). The percentage of comb at the surface is just the volume fraction multiplied by 100%.

1. *Mole fraction of comb near surface (n_s):* $$n_s = \frac{A_{COO}}{A_{CF_2} + A_{COO}} \quad \text{(A.1)}$$

2. *Repeat unit molar volume of comb (v_o^{comb}):* $$v_o^{comb} = \frac{\overline{M}_o^{comb}}{\overline{\rho}^{comb}} \quad \text{(A.2)}$$

Table A.2. Useful data for calculating molar volume values
Obtained from Aldrich.

Species	M_o (g/mol)	ρ (g/cm^3)
$POEM_9$	475	1.08
$HPOEM_{10}$	526	1.08
PMMA	100	1.19
PMA	86	1.22
PVDF	64	1.74

The $\overline{M}_o^{comb}$ and $\overline{\rho}^{comb}$ values are weighted combinations of the individual component values (shown in Table A.2). For instance, if a comb had 40 wt% $POEM_9$ and 60 wt% PMMA, that would translate into 12.3 mol% $POEM_9$ and 87.7 mol% PMMA. These are example calculations for that comb composition:

$$\overline{M}_o^{comb} = 0.123*475 + 0.877*100 = 146.1 \text{ g/mol}$$

$$\overline{\rho}^{comb} = 0.123*1.08 + 0.877*1.19 = 1.17 \text{ g/cm}^3$$

$$v_o^{comb} = \frac{146.1}{1.17} = 124.9 \text{ cm}^3/\text{mol}$$

For the P(MMA-*r*-POEM) comb used in this paper, v_o^{comb} = 115.6 cm^3/mol, and for PVDF, v_o^{PVDF} = 36.8 cm^3/mol.

3. *Volume fraction of comb near surface (ϕ_s):* $$\phi_s = \frac{n_s v_o^{comb}}{n_s v_o^{comb} + (1-n_s) v_o^{PVDF}} \quad \text{(A.3)}$$

A.4. Determination of Nitrogen (Extent of Fouling) at Surface

The amount of nitrogen on a fouled sample's surface can be directly related to the extent of fouling, since there is no nitrogen in the non-fouled samples, leaving BSA as the sole source of the signal. The amount of nitrogen at the surface of BSA-fouled samples was determined using an XPS survey. The raw area of the N 1s peak was used in all plots in this thesis as a representation of the extent of fouling.

Unfortunately, values of raw area for the N 1s peak cannot be compared between trials, as the XPS results tend to change in intensity from day to day, especially after maintenance. So fouling values can only be directly compared within a trial.

A.5. Determination of Relative Amount of PEO at Surface

Because the C-O peak should derive solely from the presence of PEO on the surface of nonfouled samples, the ratio of A_{CO} and A_{CF2} (a signal that comes only from the PVDF in the sample) can be used to determine the relative amount of PEO at the surface.

Appendix B: XPS Peak Breakdowns for P(MMA-*r*-POEM)

B.1. H_2O_2 Regeneration Studies

Table B.1. XPS peaks for P(MMA-*r*-POEM) comb for cleaning with H_2O_2
Values in parentheses are % area calculations made ignoring the CH peak (since this is influenced by XPS pump oil fouling).

Peak Number	Species	*Pristine Comb*		*Cleaned Comb*	
		Position (eV)	**% Area**	**Position (eV)**	**% Area**
1	COO	289.0	12.0 (19.1)	289.0	14.05 (20.8)
2	CO	286.6	35.4 (*56.3*)	286.6	37.3 (*55.1*)
3	C-COO	285.7	15.4 (24.5)	285.7	16.3 (24.1)
4	CH	285.0	37.2 (--)	285.0	32.35 (--)

Table B.2. XPS peaks in P(MMA-*r*-POEM)/PVDF blend for cleaning with H_2O_2
Values in parentheses are % area calculations made ignoring the CH peak (since this is influenced by XPS pump oil fouling).

Peak	Species	*Pristine Blend*		*Cleaned Blend*		*Annealed Blend*	
		Position	**% Area**	**Position**	**% Area**	**Position**	**% Area**
1	CF_2 (PVDF)	290.8	36.45 (40.6)	290.7	30.0 (35.7)	290.8	30.0 (36.0)
2	COO	289.0	4.4 (4.9)	289.0	7.0 (8.3)	289.0	6.8 (8.1)
3	CO	286.8	10.3 (*11.5*)	286.9	12.3 (*14.6*)	286.9	11.5 (*13.8*)
4	CH_2 (PVDF)	286.3	36.45 (40.6)	286.2	30.0 (35.7)	286.3	30.0 (36.0)
5	C-COO	285.7	2.1 (2.3)	285.7	4.8 (5.7)	285.7	5.1 (6.1)
6	CH	285.0	10.3 (--)	285.0	15.9 (--)	285.0	16.6 (--)

B.2. Chromerge Regeneration Studies

Table B.3. XPS peaks for P(MMA-*r*-POEM) comb for cleaning with Chromerge
Values in parentheses are % area calculations made ignoring the CH peak (since this is influenced by XPS pump oil fouling).

Peak Number	Species	*Pristine Comb*		*Cleaned Comb*	
		Position (eV)	**% Area**	**Position (eV)**	**% Area**
1	COO	289.0	9.3 (18.6)	289.0	17.6 (23.8)
2	CO	286.6	37.1 (*74.0*)	286.8	30.9 (*41.7*)
3	C-COO	285.7	3.7 (7.4)	285.7	25.6 (34.5)
4	CH	285.0	49.9 (--)	285.0	25.9 (--)

Table B.4. XPS peaks for P(MMA-*r*-POEM)/PVDF blend cleaned with Chromerge
Values in parentheses are % area calculations made ignoring the CH peak (since this is influenced by XPS pump oil fouling).

Peak	Species	*Pristine Blend*		*Cleaned Blend*		*Annealed Blend*	
		Position	**% Area**	**Position**	**% Area**	**Position**	**% Area**
1	CF_2 (PVDF)	290.8	26.4 (32.1)	290.7	29.4 (35.2)	290.8	29.7 (38.9)
2	COO	289.0	6.8 (8.3)	289.0	6.8 (8.2)	289.0	4.7 (6.1)
3	CO	286.8	16.6 (*20.2*)	287.0	11.3 (*13.5*)	286.9	10.8 (*14.1*)
4	CH_2 (PVDF)	286.3	26.4 (32.1)	286.2	29.4 (35.2)	286.3	29.7 (38.9)
5	C-COO	285.7	5.9 (7.2)	285.7	6.5 (7.8)	285.7	1.5 (2.0)
6	CH	285.0	17.8 (--)	285.0	16.6 (--)	285.0	23.6 (--)

Appendix C: Supplementary Plots for P(MMA-*r*-POEM)/PVDF Membranes

C.1. Supplementary Plots for Figure 5.5

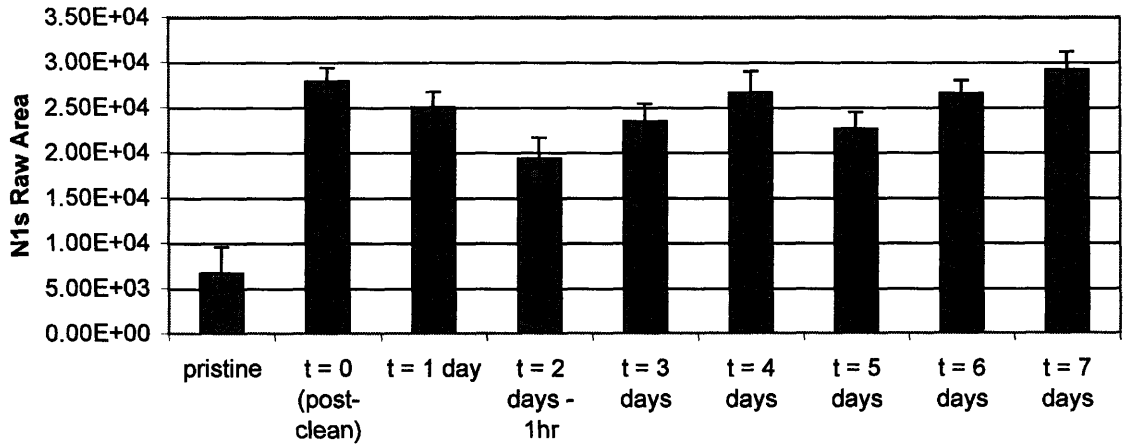

Figure C.1. Surface fouling for the experiment in Figure 5.5
A pristine membrane (F-040324) was cleaned in Chromerge for 30 minutes and subsequently annealed for the times indicated. Each data point is an average of three readings.

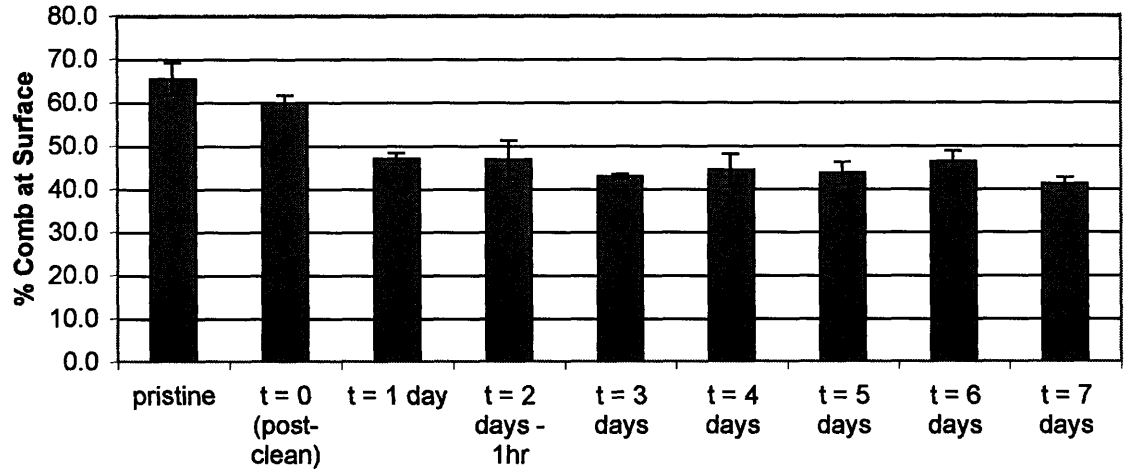

Figure C.2. Comb surface coverage for the experiment in Figure 5.5
The amount of comb is based on the intensity of the COO XPS signal. Each data point is an average of three readings.

C.2. Supplementary Plots for Figure 5.8

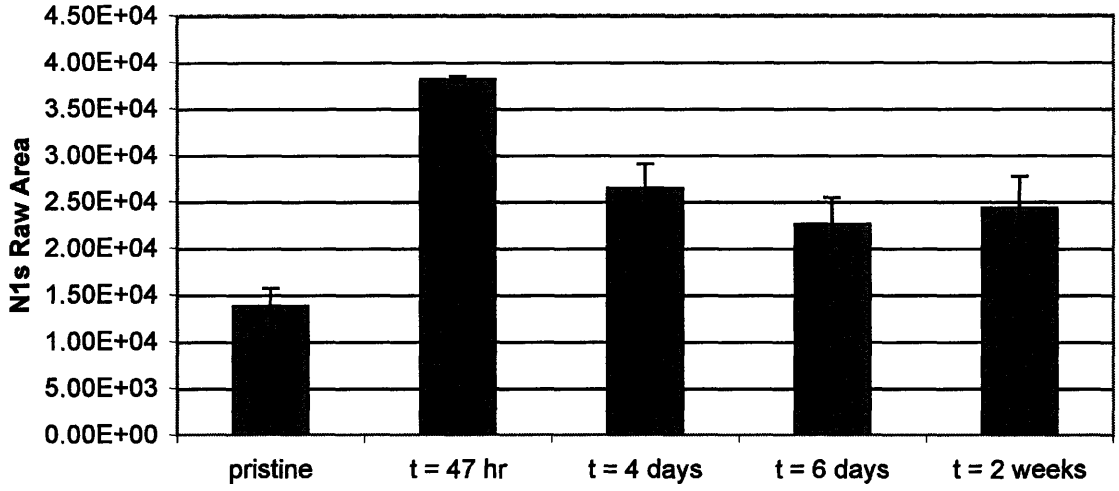

Figure C.3. Surface fouling for the experiment in Figure 5.8
A pristine membrane (F-040310) was cleaned in Chromerge for varying amounts of time. Each data point is an average of three readings.

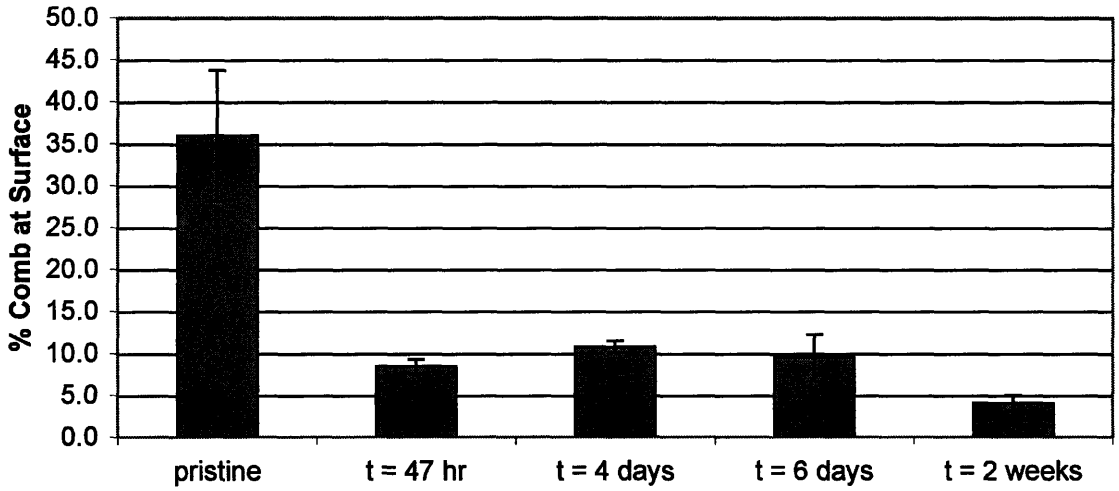

Figure C.4. Comb surface coverage for the experiment in Figure 5.8
The amount of comb is based on the intensity of the COO XPS signal. Each data point is an average of three readings.

C.3. Supplementary Plots for Figure 5.10

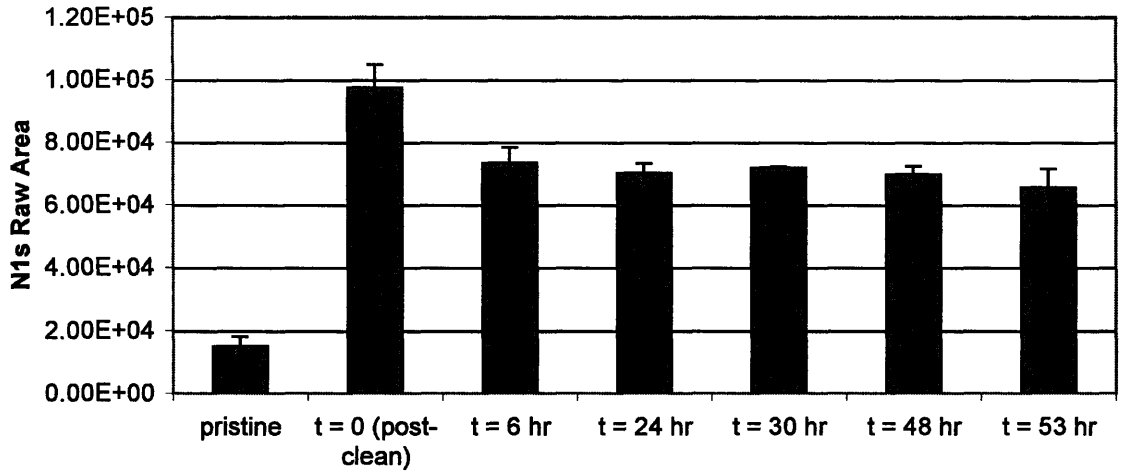

Figure C.5. Surface fouling for the experiment in Figure 5.10
A pristine membrane (F-040324) was cleaned in Chromerge for 24 hours, then annealed for varying lengths of time. Each data point is an average of three readings.

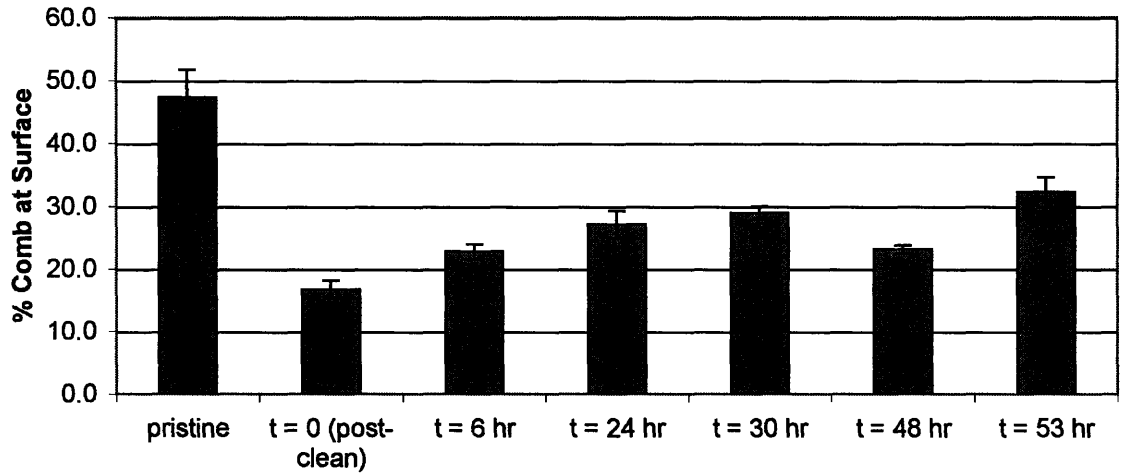

Figure C.6. Comb surface coverage for the experiment in Figure 5.10
The amount of comb is based on the intensity of the COO XPS signal. Each data point is an average of three readings.

C.4. Plots of A_{CO}/A_{COO} for P(MMA-*r*-POEM)/PVDF Membranes

For all plots, each data point is an average of three readings. Values are not given for samples which were found to have no comb/PEO at their surfaces.

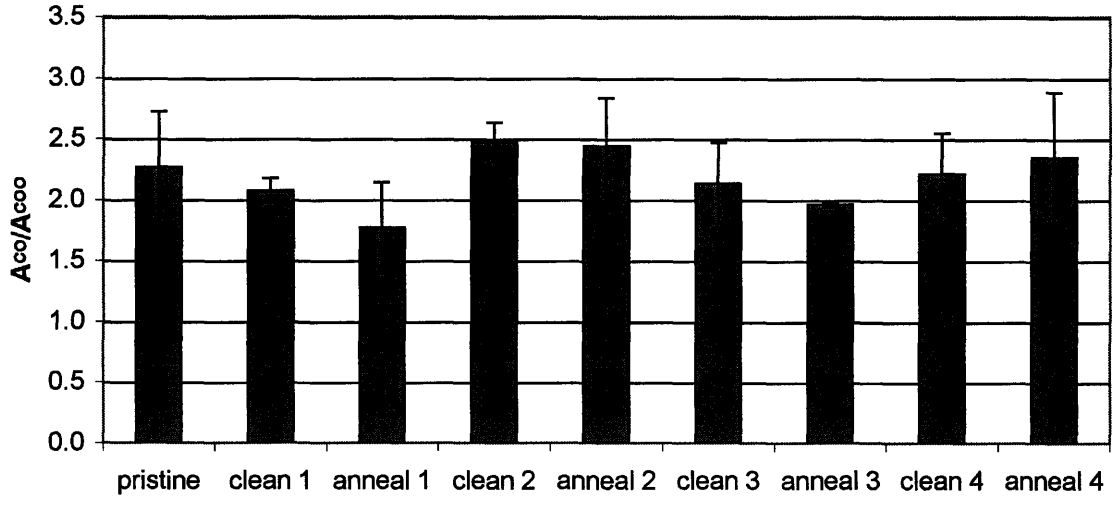

Figure C.7. A_{CO}/A_{COO} values for H_2O_2 regeneration study
Differences between values are not statistically significant.

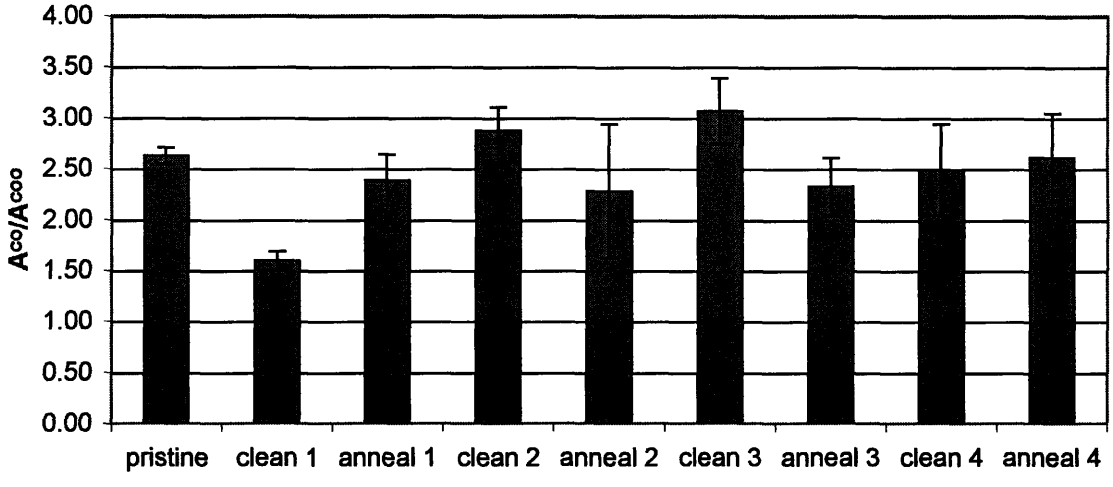

Figure C.8. A_{CO}/A_{COO} values for acid regeneration trial 1
The pristine and clean 1 values are statistically different, as are the clean 1 and anneal 1 values. All others are not statistically different.

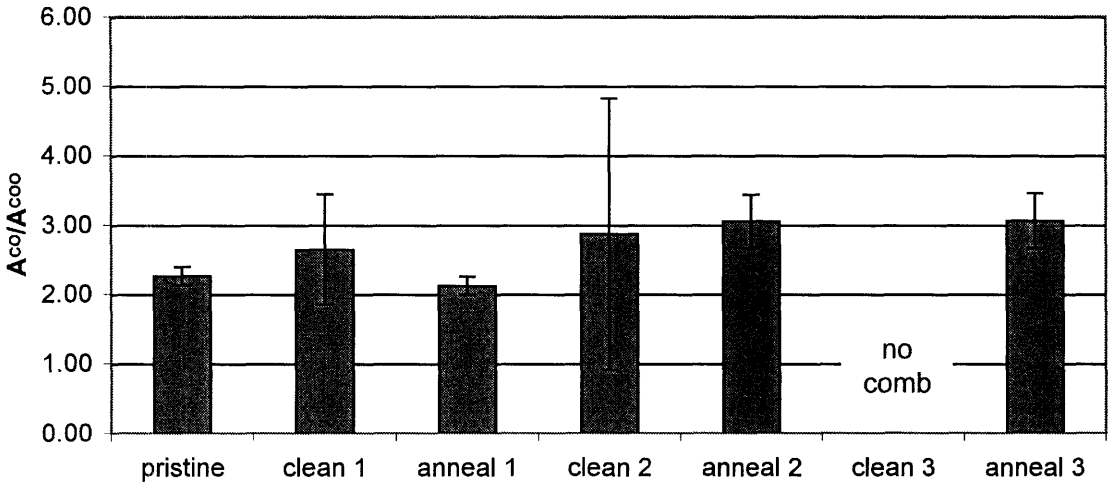

Figure C.9. A_{CO}/A_{COO} values for acid regeneration trial 2
Differences between values are not statistically significant.

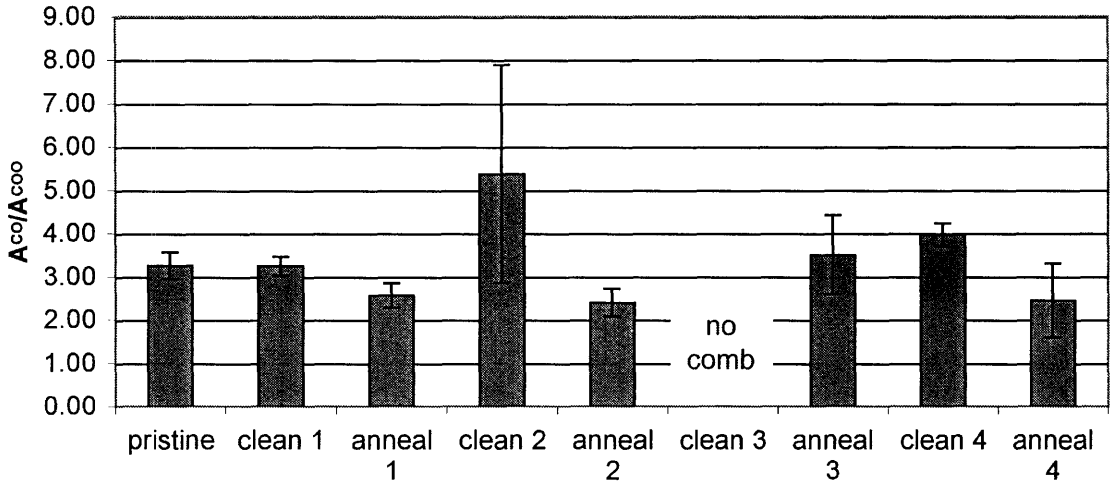

Figure C.10. A_{CO}/A_{COO} values for acid regeneration trial 3
Differences between values are not statistically significant.

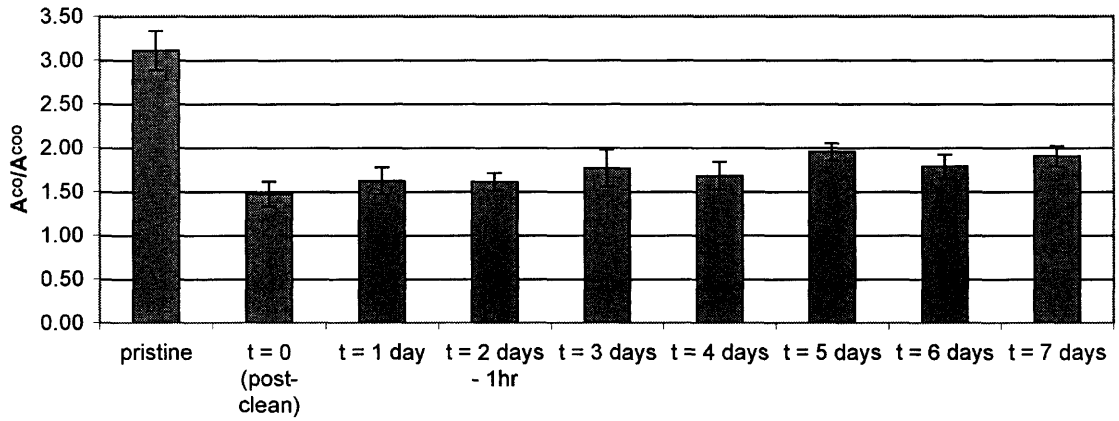

Figure C.11. A_{CO}/A_{COO} values for annealing kinetics study 1
Corresponds to data give in Figure 5.5. The pristine value is statistically different from the remaining values; all others are not statistically different from each other.

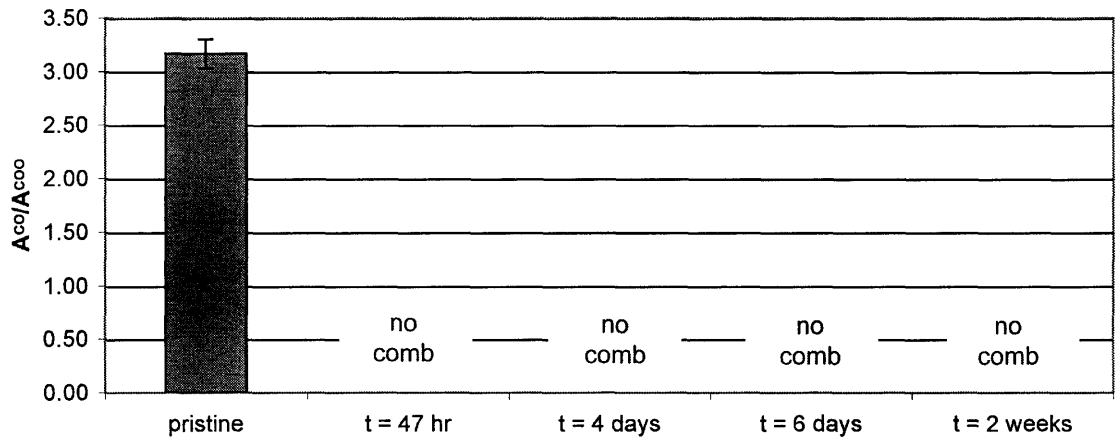

Figure C.12. A_{CO}/A_{COO} values for cleaning kinetics study
Corresponds to data given in Figure 5.8.

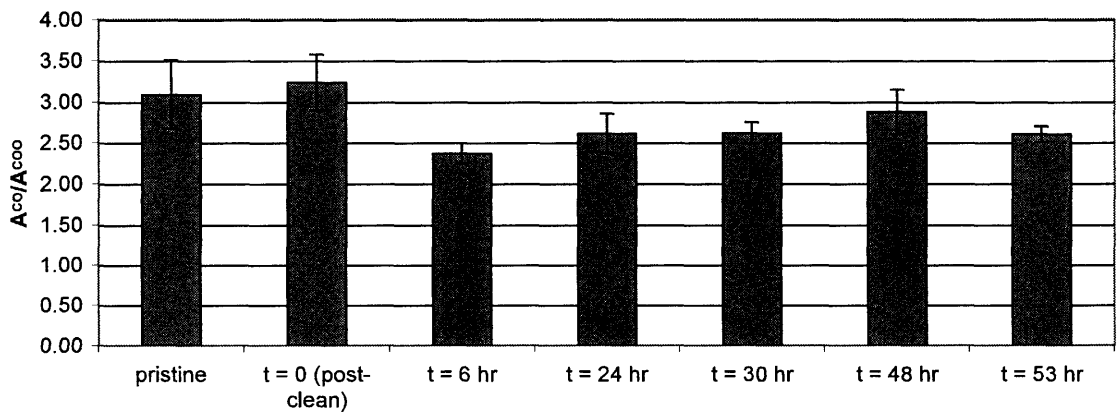

Figure C.13. A_{CO}/A_{COO} values for annealing kinetics study 2
Corresponds to data given in Figure 5.10. Values are not statistically different.

Appendix D: Raw Flux Data for P(MMA-*r*-POEM)/PVDF Membranes

D.1. P(MMA-*r*-POEM) Regeneration Filtration 1

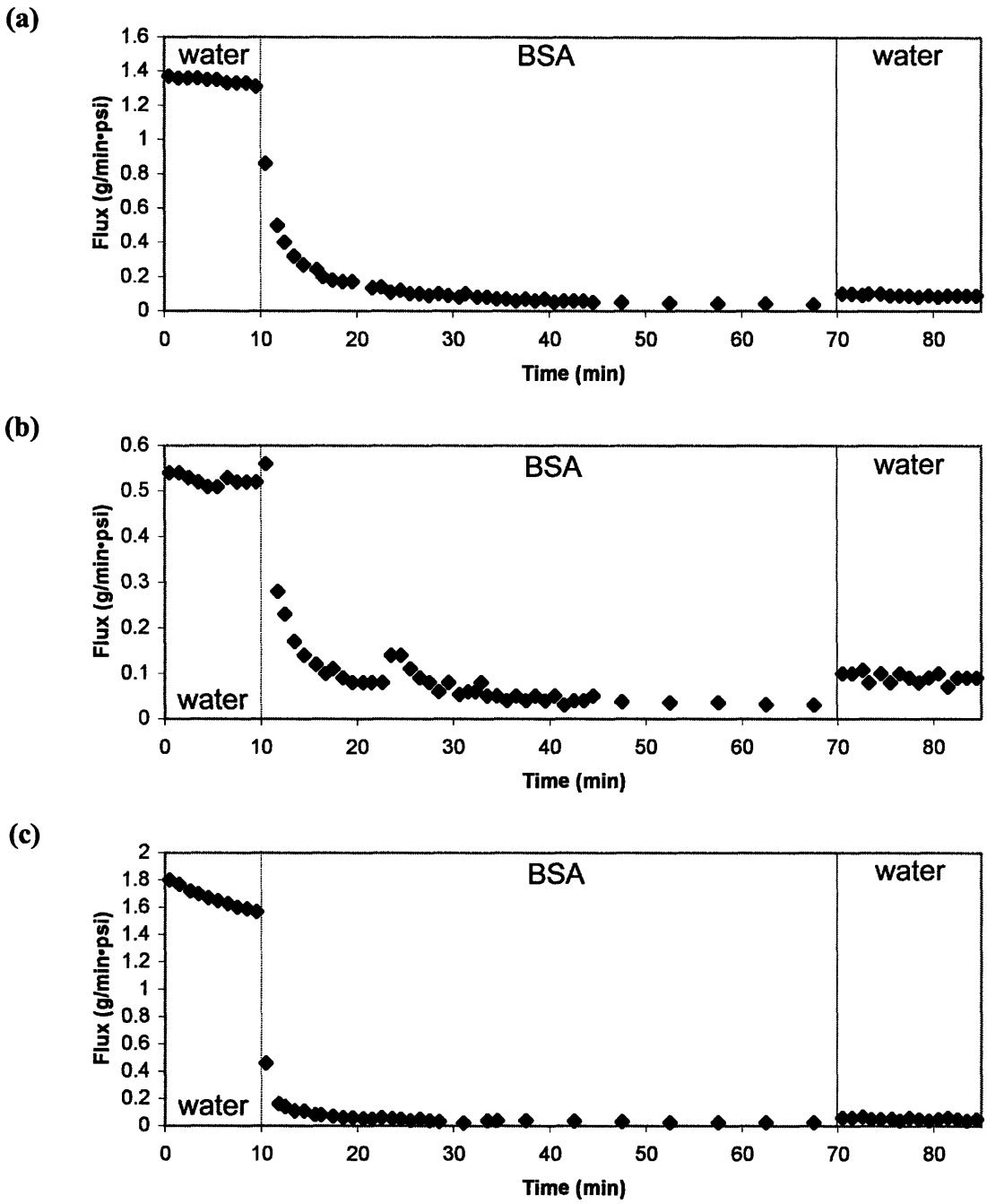

Figure D.1. Raw flux data for Regeneration Filtration 1
All flux plots are for the same membrane disc (from F-040324). (a) The pristine membrane, (b) the membrane (after the trials in (a)) cleaned for 30 min. in Chromerge, (c) the membrane (after (b)) cleaned for 30 min. in Chromerge, and annealed in 90°C water for 18 hr. Fouling solution was 1 mg/mL BSA in PBS. R_{BSA} after 20 minutes of fouling was (a) 0.1, (b) 0.2, (c) 0.3.

D.2. P(MMA-*r*-POEM) Regeneration Filtration 2

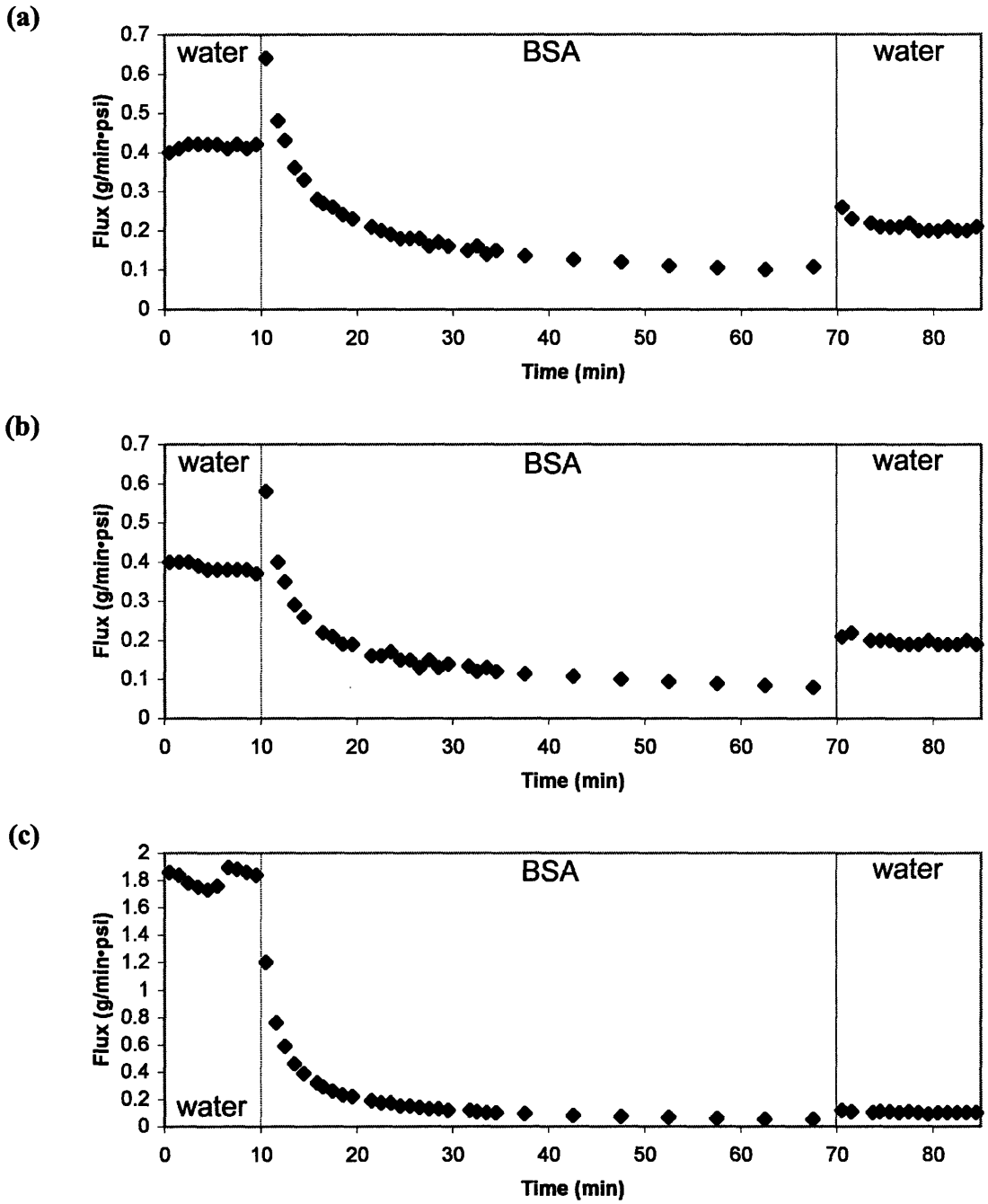

Figure D.2. Raw flux data for Regeneration Filtration 2
All flux plots are for the same piece of membrane (F-040324). (a) The pristine membrane, (b) the membrane (after the flux trials in (a)) cleaned for 30 minutes in Chromerge, (c) the membrane (after (b)) cleaned for 30 minutes in Chromerge, then annealed in 90°C water for 18 hours. The BSA fouling solution was 0.1 mg/mL in PBS. R_{BSA} after 20 minutes of fouling was (a) 0.3, (b) 0.4, (c) 0.4.

D.3. P(MMA-*r*-POEM) Regeneration Filtration 3

(a)

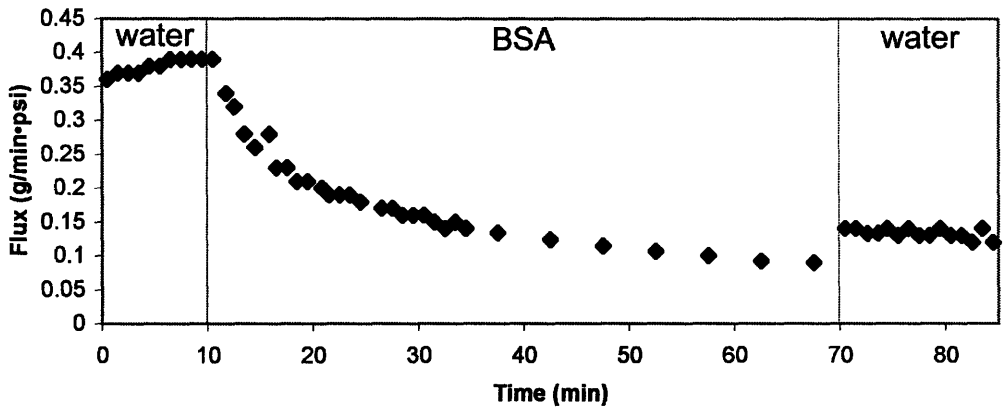

(b)

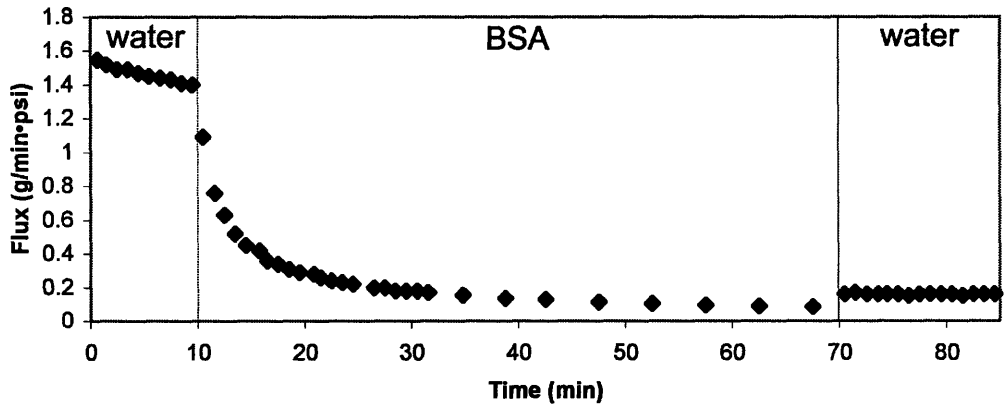

(c)

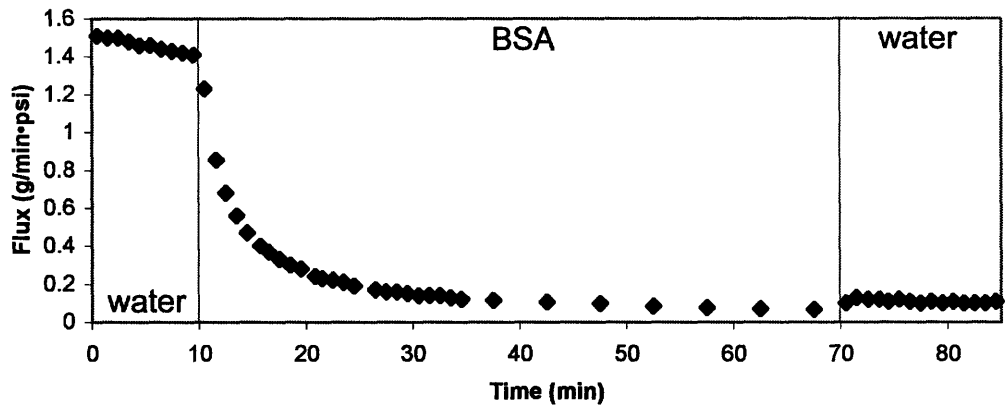

(Figure continued on next page)

(d)

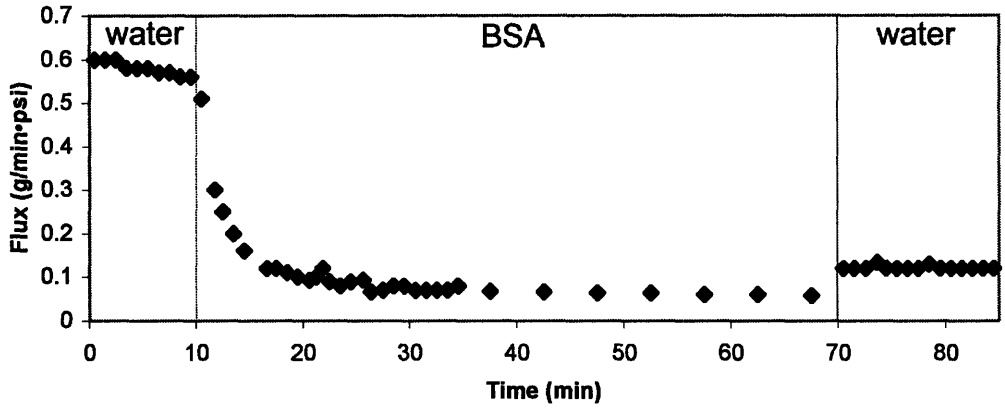

(e)

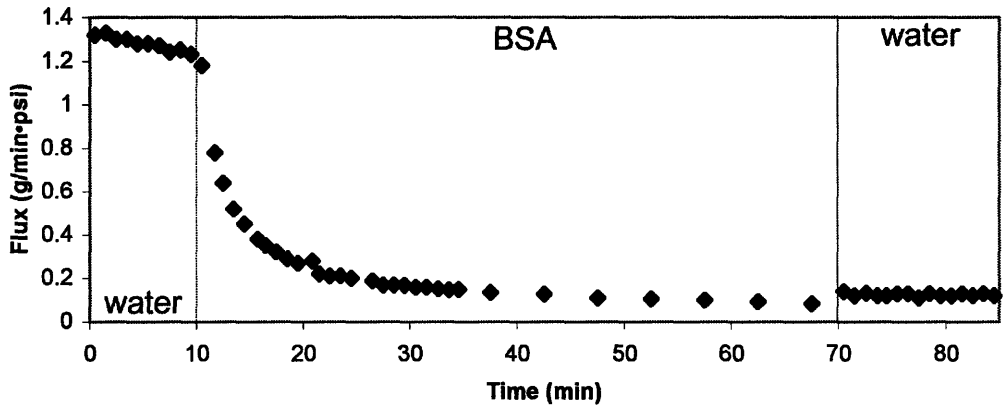

Figure D.3. Raw flux data for Regeneration Filtration 3
All flux plots are for the same piece of membrane (F-040324). (a) The pristine membrane, (b) the membrane (after the flux trials in (a)) cleaned for 30 minutes in Chromerge, (c) the membrane (after (b)) cleaned for 30 minutes in Chromerge, then annealed in 90°C water for 18 hours, (d) the membrane (after (c)), cleaned and annealed as in (c), (e) the membrane (after (d)), cleaned and annealed as in (c). The BSA fouling solution was 0.1 mg/mL in PBS. R_{BSA} after 15 minutes of fouling was (a) 0.5, (b) 0.2, (c) 0.6, (d) 0.0, (e) 0.0.

D.4. P(MMA-*r*-POEM) Regeneration Filtration 4

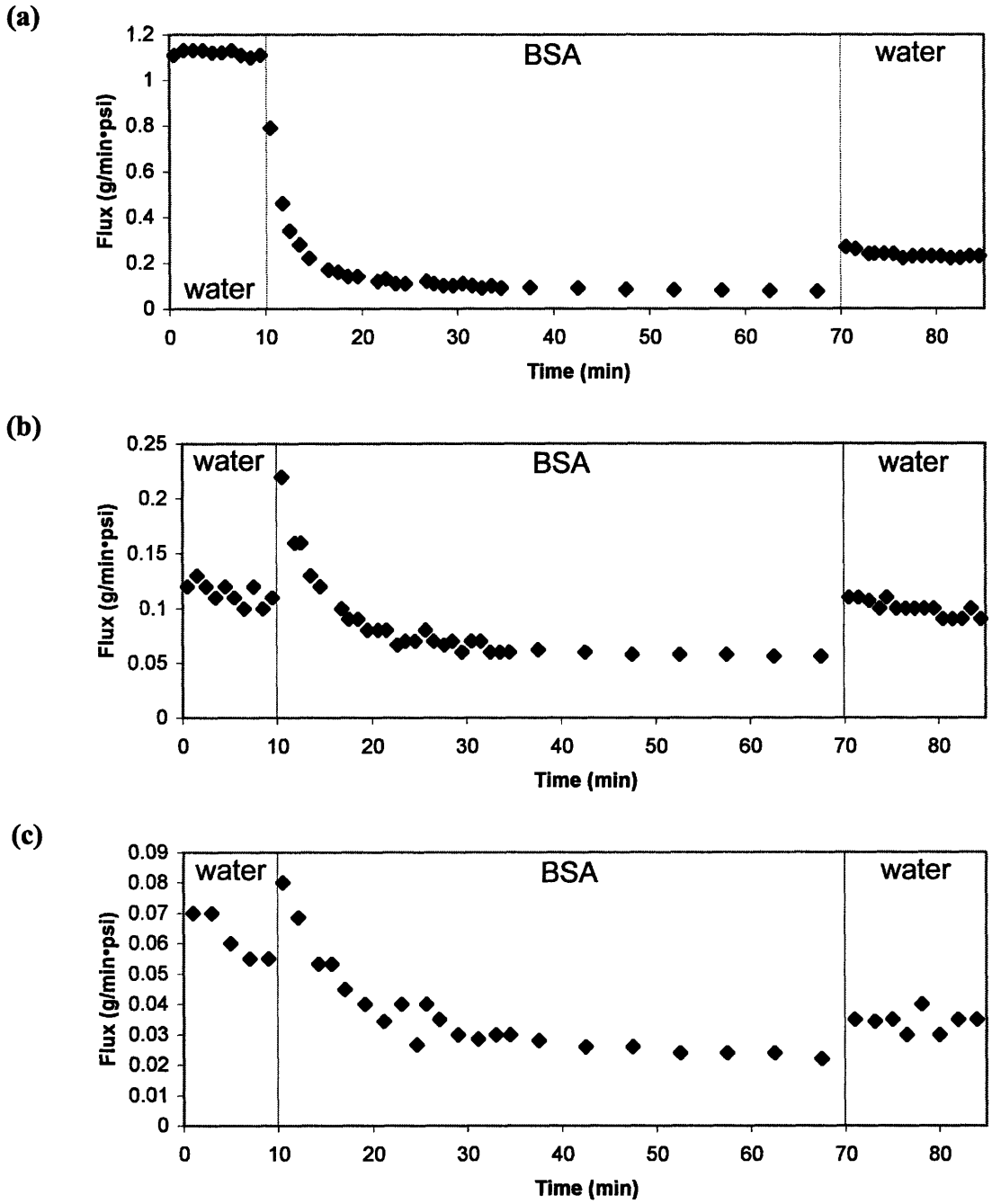

Figure D.4. Raw flux data for Regeneration Filtration 4
All flux plots are for the same piece of membrane (F-040324). (a) The pristine membrane, (b) the membrane (after the flux trials in (a)) cleaned for 18 hours in Chromerge, (c) the membrane (after (b)) cleaned for 30 minutes in Chromerge, then annealed in 90°C water for 18 hours. The BSA fouling solution was 0.1 mg/mL in PBS. R_{BSA} after 15 minutes of fouling was (a) 0.3, (b) 0.0, (c) 0.4.

D.5. PVDF Control

(a)

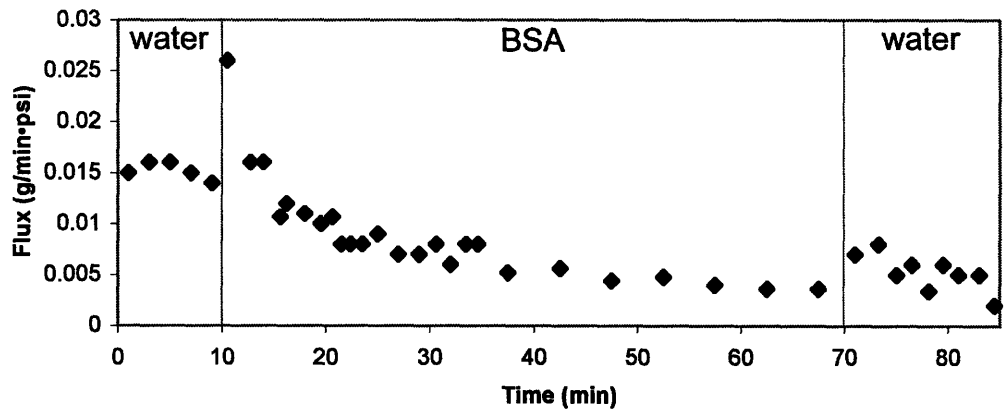

(b)

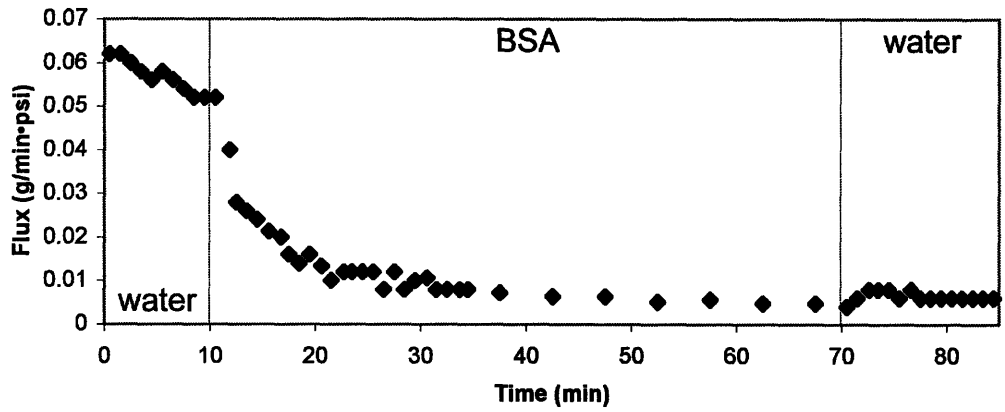

(c)

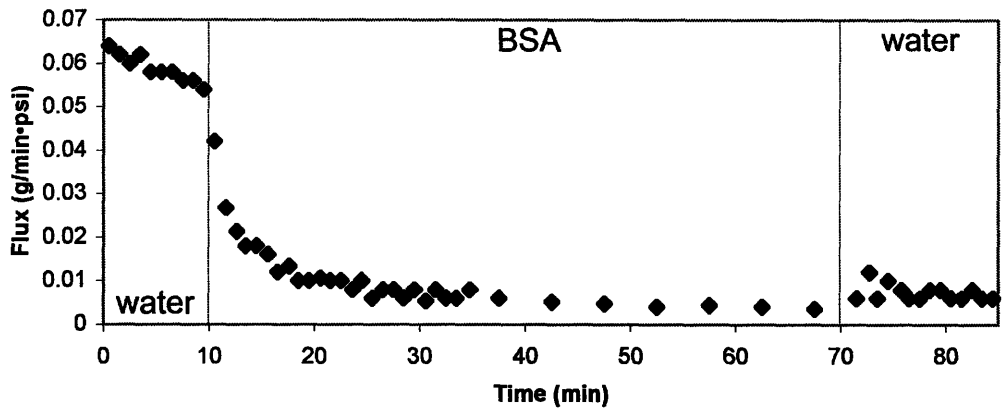

Figure D.5. Raw flux data for PVDF Control
All flux plots are for the same piece of PVDF membrane. (a) The pristine membrane, (b) the membrane (after the flux trials in (a)) cleaned for 30 minutes in Chromerge, (c) the membrane (after (b)) cleaned for 30 minutes in Chromerge, then annealed in 90°C water for 18 hours. The BSA fouling solution was 0.1 mg/mL in PBS. R_{BSA} after 20 minutes of fouling was (a) 0.0, (b) 0.2, (c) 0.2.

Appendix E: NMR and XPS Spectra of P(MA-*r*-POEM)

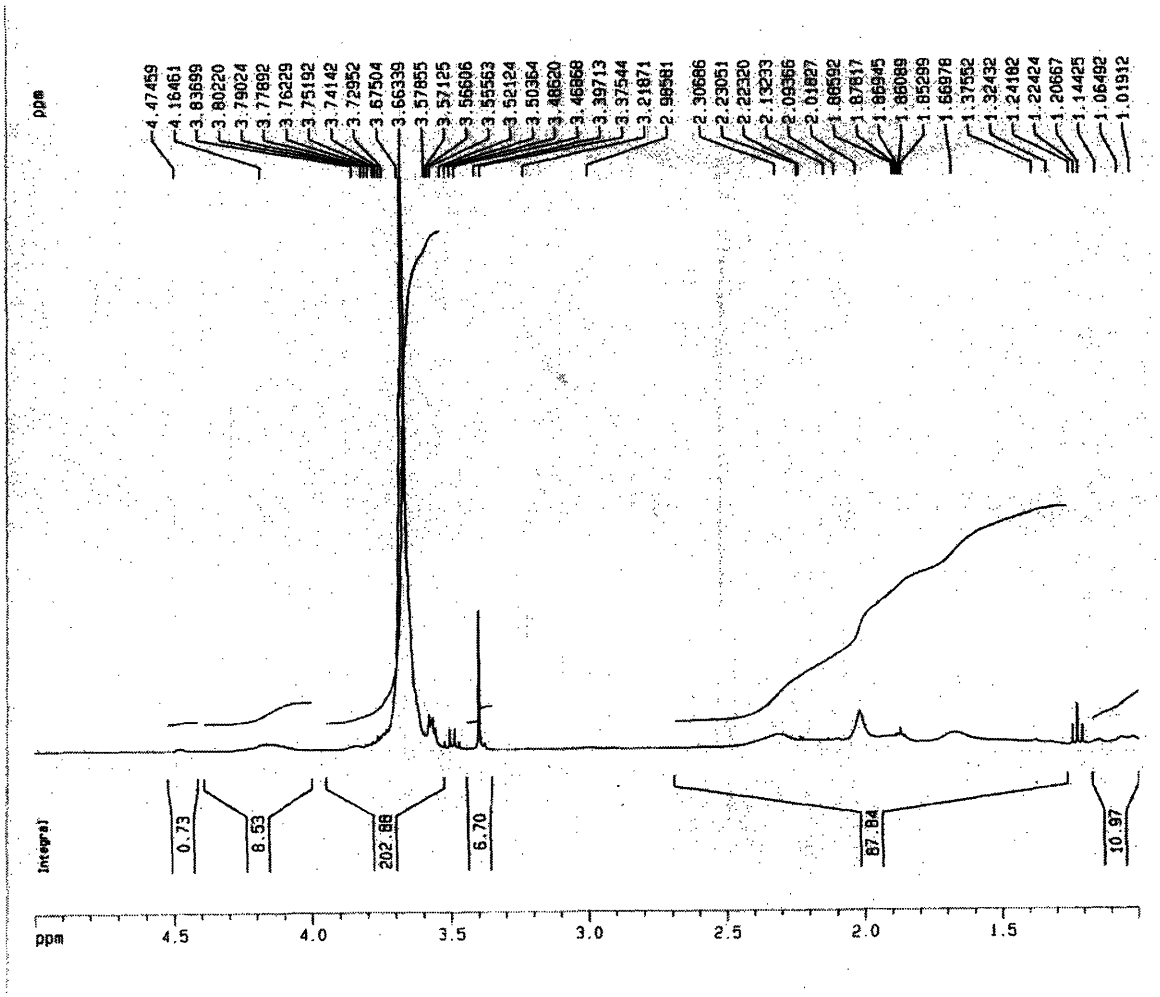

Figure E.1. NMR of the low MW P(MA-*r*-POEM) comb polymer

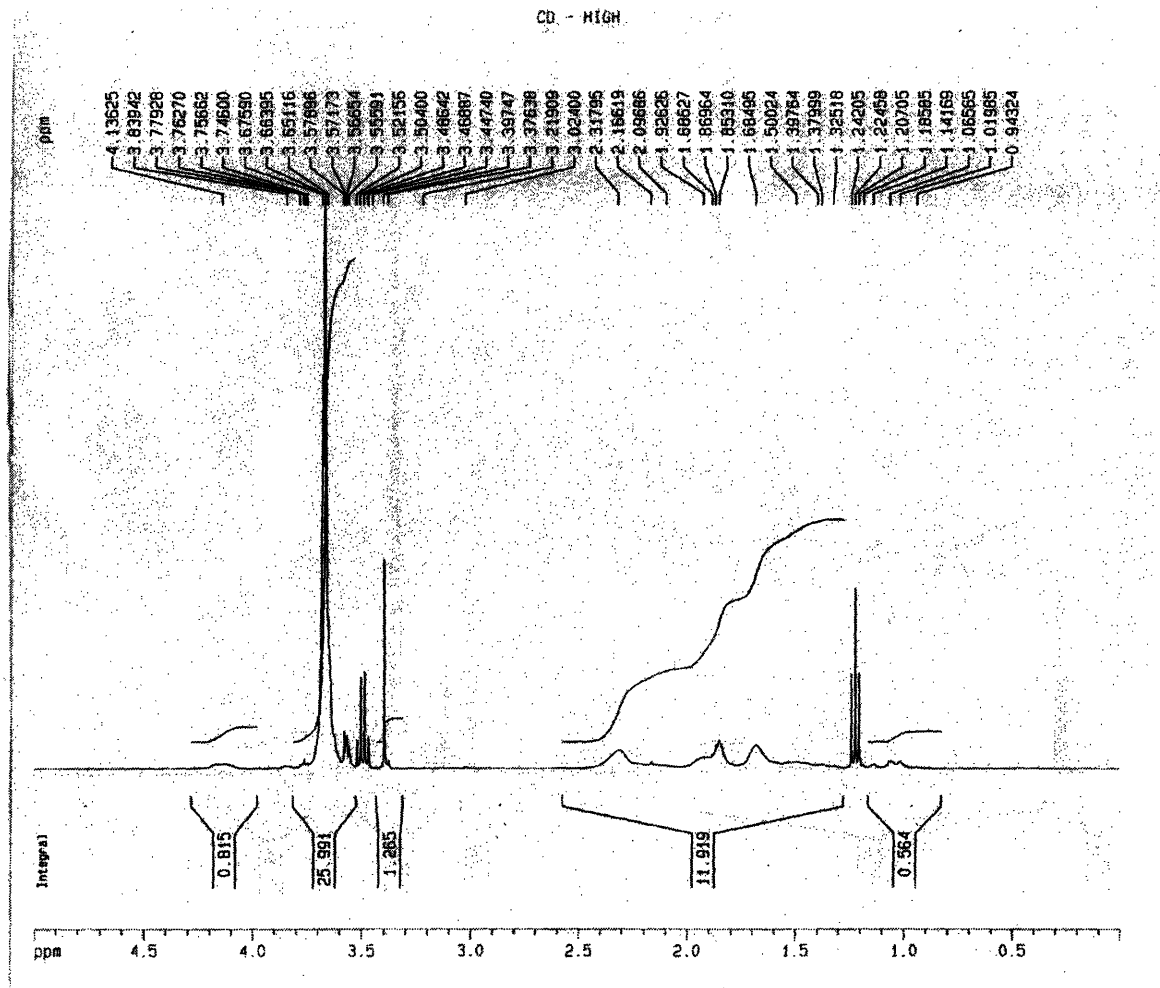

Figure E.2. NMR of the high MW P(MA-*r*-POEM) comb

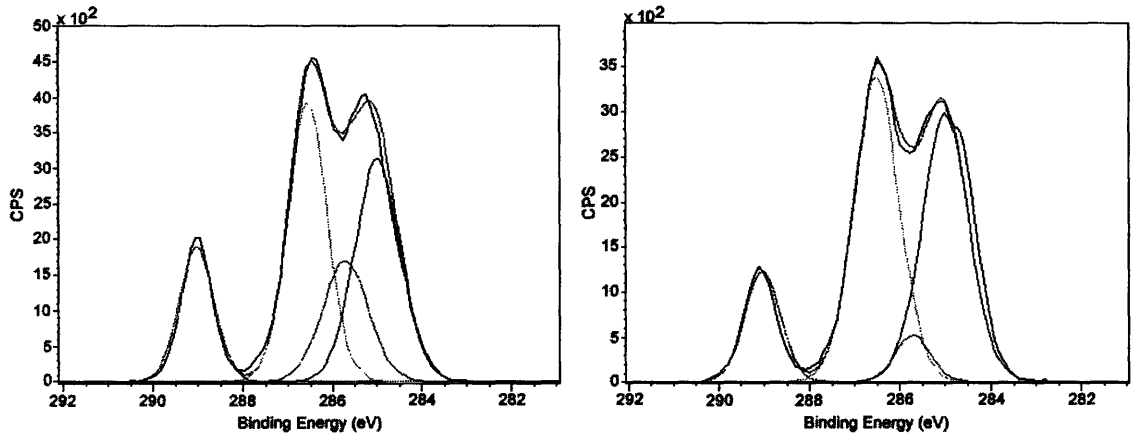

Figure E.3. XPS of Pall P(MA-*r*-POEM) combs
Left: low molecular weight comb, *right:* high molecular weight comb.

Table E.1. Breakdown of peaks in P(MA-*r*-POEM) XPS spectra
Values in parentheses are % Area calculated by ignoring the 285 eV CH peak

Peak Number	Species	*Low MW Comb*		*High MW Comb*	
		Position (eV)	**% Area**	**Position (eV)**	**% Area**
1	COO	289.0	15.7 (23.3)	289.0	12.4 (20.7)
2	CO	286.6	34.6 (51.4)	286.5	44.2 (73.9)
3	C-COO	285.7	17.0 (25.3)	285.7	3.2 (5.4)
4	CH	285.0	32.7 (--)	285.0	40.2 (--)

Appendix F: Oil/Water UV/Vis Concentration Standards

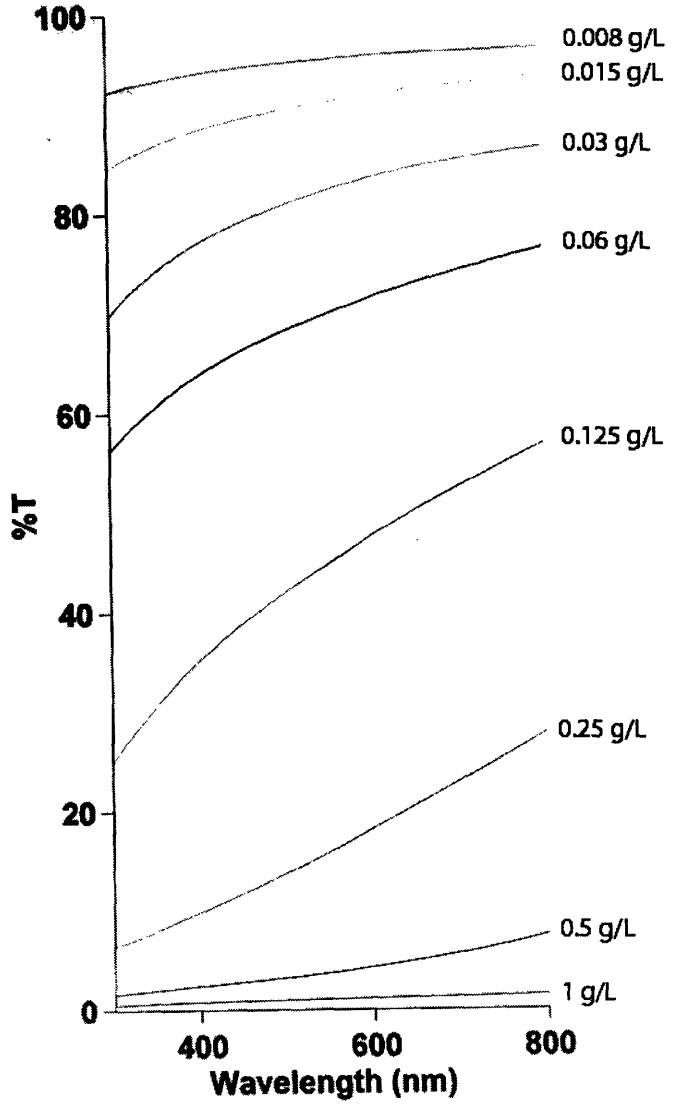

Figure F.1. A plot of oil/water UV/Vis concentration standards
Standards were made by serial dilution of a 1 mg/mL oil/water solution.